

## Distribution Agreement

In presenting this thesis or dissertation as a partial fulfillment of the requirements for an advanced degree from Emory University, I hereby grant to Emory University and its agents the non-exclusive license to archive, make accessible, and display my thesis or dissertation in whole or in part in all forms of media, now or hereafter known, including display on the world wide web. I understand that I may select some access restrictions as part of the online submission of this thesis or dissertation. I retain all ownership rights to the copyright of the thesis or dissertation. I also retain the right to use in future works (such as articles or books) all or part of this thesis or dissertation.

Signature:

---

Robert Moot

---

Date

Novel immunogen-specific variable lymphocyte receptors for creation of chimeric antigen receptors and methods for improved transduction and gene delivery

By

Robert Moot  
Doctor of Philosophy

Graduate Division of Biological and Biomedical Science  
Molecular and Systems Pharmacology

---

Trent Spencer, Ph.D.  
Advisor

---

Christopher Doering, Ph.D.  
Committee Member

---

Brian Petrich, Ph.D.  
Committee Member

---

Lily Yang, Ph.D.  
Committee Member

Accepted:

---

Lisa A. Tedesco Ph.D.  
Dean of the James T. Laney School of Graduate Studies

---

Date

Novel immunogen-specific variable lymphocyte receptors for creation of chimeric antigen receptors and methods for improved transduction and gene delivery

By

Robert Clinton Moot  
B.S. University of Georgia, 2007

Advisor: Trent Spencer, Ph.D.

An abstract of  
A dissertation submitted to the Faculty of the  
James T. Laney School of Graduate Studies of Emory University  
in partial fulfillment of the requirements for the degree of  
Doctor of Philosophy  
in the Graduate Division of Biological and Biomedical Science,  
Molecular and Systems Pharmacology  
2017

## Abstract

Novel immunogen-specific variable lymphocyte receptors for creation of chimeric antigen receptors and methods for improved transduction and gene delivery

By: Robert C Moot

Gene therapy, as an approach to disease treatment, has applications in a wide variety of prospective fields. This methodology is not without limits, however, as there is still a need to improve both the transduction process as well as the impact of the transgene conveyed via the viral vector. The studies herein focus on improving both transduction efficiency and the functionality of a therapeutic transgene.

The application of the transgene improvement focuses on the use of chimeric antigen receptors (CARs). CARs are a type of engineered, recombinant cell surface receptor that can be expressed on an effector cell to allow for directed recognition of a target antigen. One of the limitations of CARs as a cancer therapy is the availability of tumor cell target antigens. Increasing the number and variety of targetable tumor related antigens would improve its application to a wider variety of tumors. As a way to expand the antigen repertoire to which a CAR can be directed, we have implemented the use of the lamprey variable lymphocyte receptor (VLR). The VLR is the primary component of the adaptive immune system of the lamprey and hagfish. Due to its unique structure, the VLR binds antigen in a fundamentally different manner than traditional immunoglobulin-based antibodies. In addition to an alternate binding geometry, the VLR is also less subject to the constraints of self-tolerance. Combined, these two factors may improve the identification and utilization of cancer cell target antigens.

Along with improving the efficacy of CAR therapy, additional research completed herein has focused on improving the efficiency of transduction with viral vectors. We have identified several methods that may improve transduction efficiency. These include pretreatment of target cells with a small molecule selected from a high-throughput screen, increasing the concentration of virus on the target cells through use of a microfluidics device, and the use of an AAV6 vector to transfer a CAR transgene to innate cells. Together, these techniques may increase the impact of gene therapy by increasing the efficiency of viral gene transfer.

Novel immunogen-specific variable lymphocyte receptors for creation of chimeric antigen receptors and methods for improved transduction and gene delivery

By

Robert Clinton Moot  
B.S. University of Georgia, 2007

Advisor: Trent Spencer, Ph.D.

A dissertation submitted to the Faculty of the  
James T. Laney School of Graduate Studies of Emory University  
in partial fulfillment of the requirements for the degree of  
Doctor of Philosophy  
in the Graduate Division of Biological and Biomedical Science,  
Molecular and Systems Pharmacology  
2017

## **Acknowledgements**

I would like to first acknowledge and thank my mentor and boss Trent Spencer. I have known Trent for over 10 years and in this time he has had an incredible impact on my career and personal development. When I first walked into his office over a decade ago, I asked Trent to take a chance on me and through his career guidance, advice, and counseling I believe that I have grown immensely. Throughout my undergraduate, post-bac, and graduate career Trent has remained a trusted advisor and confidant. He has provided encouragement, assistance, and when needed, criticism. Through his leadership and understanding I have improved in my scientific and personal development. I will forever be grateful to Trent for everything he has done for me.

I would also like to thank Chris Doering for his mentorship during the last decade. He has provided consistent and invaluable insight throughout my career. Chris has an incredible amount of knowledge and understanding along with an unbelievable willingness to help. I know that I would not have been able to complete this project without his support.

I would like to thank the remaining members of my committee, Brian Petrich and Lily Yang. Their guidance and advice has been invaluable as I developed my project and worked through my graduate career. I would also like to thank my lab. It is only through your help that I was able to complete my project.

Finally, I would like to thank my parents. They have supported me unconditionally throughout my life. They have both served as role models providing encouragement and guidance. I cannot thank them both enough for everything they have given me. They have experienced both the highs and lows in my life and have provided unwavering support and encouragement.

## **Table of Contents**

**Abstract**

**Acknowledgements**

**Table of Contents**

**List of Figures and Tables**

**List of Abbreviations**

<b>Chapter 1 – Introduction.....</b>	<b>1</b>
1.1 The history of gene therapy .....	2
1.2 Viral vectors in gene therapy .....	7
A. Lentiviral vector background.....	7
B. Engineering lentiviral vectors for gene therapy .....	12
C. Background and structure of AAV vectors.....	14
D. Engineering AAV vectors for gene therapy.....	15
1.3 Immunotherapy background.....	16
A. Cancer Immunotherapy overview .....	19
B. Monoclonal antibodies.....	20
C. Immune checkpoint inhibitors .....	21
D. Chimeric antigen receptors overview .....	22
E. Clinical trials with chimeric antigen receptors .....	24
1.4 Overcoming the limitations in tumor cell targeting .....	25
A. Variable lymphocyte receptors .....	26
<b>Chapter 2 – Development and screening of immunogen specific VLRs against FVIII and the neuroblastoma cell line SK-N-Be(2) .....</b>	<b>33</b>
2.1 Abstract .....	34
2.2 Introduction.....	34
2.3 Materials and Methods.....	39

2.4 Results .....	45
2.5 Discussion .....	64
<b>Chapter 3 – The use of VLRs as the antigen recognition region of chimeric antigen receptors .....</b>	<b>68</b>
3.1 Abstract .....	69
3.2 Introduction .....	69
3.3 Materials and Methods .....	71
3.4 Results .....	75
3.5 Discussion .....	97
3.7 Supplemental Information .....	100
<b>Chapter 4 – Increasing transduction efficiency .....</b>	<b>107</b>
3.1 Abstract .....	108
3.2 Introduction .....	109
3.3 Materials and Methods .....	114
3.4 Results .....	122
3.5 Discussion .....	146
3.7 Supplemental Information .....	152
<b>Chapter 5 –Discussion and future directions .....</b>	<b>153</b>
4.1 Discussion .....	154
4.2 Results and implications .....	155
4.3 Future Directions .....	162
4.4 Conclusions .....	162
<b>References .....</b>	<b>165</b>
<b><u>List of tables and figures</u></b>	
<b>Figure 1.1 The adaptive immune system of jawless vertebrates uses the VLR as the antigen recognition region .....</b>	<b>27</b>

<b>Figure 1.2 Assembly of the VLR gene</b> .....	29
<b>Figure 1.3 Comparison between the scFv based CAR and the VLR based CAR</b> .....	31
<b>Figure 2.1 Overview of VLR generation process</b> .....	36
<b>Figure 2.2 Lamprey injection schedule for FVIII and SK-N-Be(2) cells</b> .....	48
<b>Figure 2.3 Amplification of the entire VLR repertoire from lamprey total cDNA</b> .....	50
<b>Figure 2.4 Confirmation of immunogen binding VLRs in lamprey serum</b> .....	52
<b>Figure 2.5: The yeast expression vector pYSD2</b> .....	55
<b>Figure 2.6: Yeast display screening for anti-FVIII VLRs</b> .....	57
<b>Figure 2.7: Sorting of the anti-SK-N-Be(2) VLRs</b> .....	59
<b>Figure 2.8: Annotation of the VLR sequencing results</b> .....	63
<b>Figure 3.1: Screening VLR CAR constructs</b> .....	77
<b>Figure 3.2: Screening clone 6 anti-SK-N-Be(2) VLR via co-culture assay</b> .....	79
<b>Figure 3.3: Screening clone 8 anti-SK-N-Be(2) VLR in a CAR construct</b> .....	82
<b>Figure 3.4: Schematic of CAR structures containing the BCL or CD5 VLR and the structure of the mature VLR gene</b> .....	85
<b>Figure 3.5: VLR CAR expression and activation of Jurkat cells when co-cultured with cells expressing the target antigen</b> .....	87
<b>Figure 3.6: Cassettes coexpressing GFP and VLR-CARs show a correlation between expression and activation</b> .....	92
<b>Figure 3.7: BCL and CD5 VLR CAR constructs significantly increase the cytotoxic potential of effector cells when cultured with their target cells</b> .....	94
<b>Supplementary Figure S3.1: Activation of clone 8 VLR CAR expressing Jurkat cells</b> .....	100
<b>Supplementary Figure S3.2: Stable expression of the BCL VLR CAR in transduced Jurkat cells</b> .....	101
<b>Supplementary Figure S3.3: Activation as measured by CD69 upregulation in VLR CAR transduced Jurkat cells</b> .....	102

<b>Supplementary Figure S3.4: CD5 VLR CAR expression in Jurkat cells</b> .....	103
<b>Supplementary Figure S3.5: Flow cytometry analysis of Jurkat cells transduced with the eGFP P2A CD5 VLR CAR construct</b> .....	104
<b>Supplementary Figure S3.6: Selection of CD5 VLR CAR expressing NK-92 cells and CD5 expression on a targeted tumor cell line</b> .....	105
<b>Supplementary Figure S3.7: Flow cytometry analysis from co-culture assay of eGFP P2A BCL VLR CAR transduced Jurkat cells with target BCL cells</b> .....	106
<b>Figure 4.1: Schematic of hybrid PS-PDMS device, which can be used for lentiviral transduction</b> .....	117
<b>Figure 4.2: Determination of the effect on the transduction of K562 cells by varying concentrations of rapamycin and PMA, both independently and in combination</b> .....	124
<b>Figure 4.3/Table 1: Comparison of tube-based method of transduction with standard plate based method of transduction</b> .....	126
<b>Figure 4.4/Table 2: Comparison between transduction using an Amicon filter and the standard plate based method of transduction</b> .....	128
<b>Figure 4.5/Table 3: Transduction of cells in a packed column compared to the standard plate based method of transduction</b> .....	130
<b>Figure 4.6: K562 cells transduced in the hybrid PS-PDMS device</b> .....	132
<b>Figure 4.7: Schematic of AAV6 and Lenti GFP transgene, gamma delta T-cell enrichment and transduction with AAV6 GFP</b> .....	135
<b>Figure 4.8 GFP expression and viability in AAV6 GFP and Lenti GFP transduced cell lineages</b> .....	137
<b>Figure 4.9: AAV6 GFP transduction of NK-92 cells</b> .....	139
<b>Figure 4.10: AAV6 transgene expression decreases over time</b> .....	141
<b>Figure 4.11: Schematic of CD5 AAV6 transgene and GFP expression in naïve and transduced NK-92 cells</b> .....	143

<b>Figure 4.12: NK-92 cytotoxicity assay with Jurkat cells .....</b>	<b>145</b>
<b>Supplementary Figure S4.1: Flow cytometry showing binding of CD5 CAR transfected HEK 293 cells to CD5-Fc fusion protein .....</b>	<b>152</b>

### **List of abbreviations**

AAV: Adeno associated virus  
 ALL: Acute lymphoblastic leukemia  
 CA: Capsid  
 CAR: Chimeric antigen receptor  
 CLL: Chronic lymphocytic leukemia  
 CNS: central nervous system  
 CP: connecting peptide  
 cPPT/PPT: (central) polypurine tract  
 CTLA-4: Cytotoxic T-lymphocyte-associated protein 4  
 DAG: diacylglycerol  
 DLBCL: Diffuse large B-cell lymphoma  
 DMEM: Dubelco's modified eagle medium  
 Env: Envelope  
 FACS: fluorescence activated cell sorting  
 FBS: Fetal bovine serum  
 FL: Follicular lymphoma  
 HEK: Human embryonic kidney  
 HER-2: Human epidermal growth factor receptor  
 HIV: Human immunodeficiency virus  
 HRP: horse radish peroxide  
 HSPC: hematopoietic stem and progenitor cell  
 hUBC: human ubiquitin C  
 IL-2: interleukin-2  
 LRR: Leucine rich repeat  
 LRRCT: C-terminal leucine rich repeat  
 LRRNT: N-terminal leucine rich repeat  
 LRRV: variable leucine rich repeat  
 LRRVe: end leucine rich repeat  
 LTR: Long terminal repeat  
 MA: Matrix  
 MCL: Mantle cell lymphoma  
 MHC: Major histocompatibility complex  
 MLV: Murine leukemia virus  
 MOI: multiplicity of infection

NC: Nucleocapsid  
NK: Natural killer  
OTC Ornithine transcarbamylase  
PAGE: Polyacrylamide gel electrophoresis  
PBS: Primer binding site  
PCR: Polymerase chain reaction  
PD-1: Programmed cell death protein-1  
PDMS: Polydimethylsiloxane  
PKC: phosphokinase C  
PMA: phorbol 12-myristate 13-acetate  
Pol: Polymerase  
PS: Polystyrene  
qPCR: quantitative polymerase chain reaction  
RAG: Recombination activating gene  
RBC: Red blood cell  
scFv: Single chain variable fragment  
SIN: Self inactivating  
SP: Signal peptide  
TAR: Trans activation response element  
TU: transducing units  
VSV-G: Vesicular stomatitis virus G-protein  
WBC: White blood cell  
X-SCID: X-linked severe combined immunodeficiency

## **Chapter 1**

### **Introduction**

### **1.1 The history of gene therapy**

Before gene therapy based studies ever reached human trials, Frederick Griffith established in 1928 the concept of the transforming principle. In this proposal, he describes a method for transformation of a pneumococcal type from non-virulent into a virulent type. In this experiment non-virulent type R bacteria were mixed with type S virulent bacteria that had been heat-inactivated and injected mice with the resulting mixture. The result of this injection was the development of pneumonia in the injected mice, leading to the conclusion that the virulence had been transferred by some method between the two bacterial strains. After isolating colonies of the S form from the mice, Griffith was able to establish that the R form had converted to the S form and adopted its virulent nature. Further experiments based off this observation revealed that something in the extract of the bacterial cells was responsible for the observed transformation. Later, Avery and McCarty revealed the material responsible for this transformation to be DNA [1].

Following the establishment of the transforming principle and the wide acceptance of DNA as the primary unit of genetic inheritance, Joshua Lederberg introduced the notion of transduction in 1958. The experiments that set this discovery in motion were also done on bacteria and involved separating two types of bacteria by a glass filter. On one side were drug-resistant strains of Salmonella and on the other side was wild-type Salmonella. This experiment revealed that the genes for drug resistance could be transferred between the two bacteria despite the bacterial cells being unable to pass through the filter. From this observation, Lederberg concluded that something present in the filtrate was carrying the necessary genes for drug resistance. Later discoveries determined that instead of naked DNA, the transfer of genetic information was mediated via a bacteriophage [2]. This initial discovery, paved the way for the future development of viral vectors as a method of gene transfer.

The next major step in the advancement of gene therapy came from a laboratory studying gene transfer and modification in which a researcher, Waclaw Szybalski, was able to show the transfer of a biochemical trait. This was accomplished using cells requiring DHFR for nucleic acid synthesis. In the absence of DHFR, these cells would resort to a secondary pathway to synthesize nucleic acids. When DHFR is inhibited in cells, only the cells capable of synthesis through the alternate pathway can survive. DNA isolated from the cells capable of DNA synthesis through the alternate pathway was isolated and transformed into naïve cells. In this experiment, Szybalski showed the possibility of gene transfer and correction of genetic insufficiency [2, 3].

In 1961, another step was made in furthering the prospect of therapeutic gene transfer. A researcher named Howard Temin noted that specific gene variants could be transferred via viral infection. The experiment used to elucidate this idea was conducted in chickens infected with the Rous sarcoma virus. The cells of the infected chickens showed gene mutations that were stably expressed in the host cell after viral infection. This observation indicated that genetic information could be transferred not only from DNA to RNA but also the other way around. This observation later led to the discovery and characterization of RNA-dependent DNA polymerases [4]. The lasting impact on the field of gene therapy, however, was the notion that genes could be transmitted via viral vectors and stably integrated and expressed in a host cell[2]. Building on this discovery, and a previous study using the tobacco mosaic virus as a vector to transfer information into viral RNA, Rogers, et al. attempted to use the Shope papilloma virus to transfer the gene for arginase into two patients with a urea cycle disorder. Although the trial proved unsuccessful, it helped to progress the idea of using viral vectors to transfer therapeutic DNA into patients [2, 5].

The first successful human gene transfer experiments took place in 1989 when Steven Rosenberg and colleagues introduced a gene coding for resistance to neomycin into tumor infiltrating lymphocytes (TILs), which were then transfused back into the patient as a treatment for

metastatic melanoma [6]. This treatment was performed based upon the understanding of TILs as a promising therapeutic that on its own had been successful in causing disease regression in certain patients. As a method to determine the longevity and distribution of TILs following injection into patients, TILs were isolated from metastatic melanoma patients and transduced with a retrovirus encoding the neomycin phosphotransferase gene (*neo*) [6, 7]. These cells were then re-infused back into the patients. The presence of the *neo* protein allows the cells to inactivate neomycin and can be used as a means of selection and identification of the gene modified cells. With the results of this study, Rosenberg was then able to proceed with a TIL based treatment for metastatic melanoma in two patients. The results showed moderate success as there was no tumor growth observed at the injection site [1, 8].

After Steven Rosenberg completed the first human gene therapy, the development of further therapeutics for treatment of human disease saw several advancements that paved the way for modern gene therapy approaches. In 1990, Michael Blaese began the first gene therapy trial that used a gene of therapeutic value to the patient. In this trial, Blaese and colleagues treated two patients with adenosine deaminase deficiency. This was a promising target as it is a monogenic disease that causes a deadly immunodeficiency. To treat these patients, white blood cells were isolated from the patients and gene modified with a functional copy of the gene for adenosine deaminase. The results of this trial showed mixed success in which one of the two patients responded positively to the treatment [9]. Two years later, a second gene therapy trial sought to treat adenosine deaminase deficiency. In this trial, the gene for adenosine deaminase was introduced ex vivo via two separate retroviral vectors into bone marrow cells isolated from two patients. The results, assessed two years post-treatment, indicated long-term survival of T and B lymphocytes, marrow cells, and granulocytes that were expressing the functional adenosine deaminase gene [10]. From these trials as well as several others, gene therapy emerged as a popular research topic and public interest in the technology began to grow.

The first major setback in the field of gene therapy came with the death of a patient name Jesse Gelsinger in a trial conducted at the University of Pennsylvania to treat a partial deficiency of ornithine transcarbamylase (OTC). OTC is a liver enzyme that is necessary for removal of excess nitrogen. Although Jesse Gelsinger was deficient in production of the enzyme, his disease was generally well controlled, allowing him to live a mostly normal life. After initiation of the trial, Jesse's health rapidly deteriorated, eventually leading to his death. The results of this trial were highly publicized and Jesse Gelsinger's death came to symbolize the negative influence of financial interests in human subjects research and swayed the public views on gene therapy to a dangerous and potentially deadly intervention. This trial has widely been viewed as a cautionary tale in which at several different points, it proceeded despite safety concerns. The trial was structured as a Phase I clinical trial that was intended to only assess the safety of the therapy rather than provide actual therapeutic benefit. The limited benefits of the trial were eventually revealed to have never been fully communicated to Jesse and his family. When it was initiated, Jesse's ammonia levels fell outside the safety limit established in the protocol. Despite this, the researchers proceeded. Four days following the initiation of the trial, Jesse Gelsinger was dead. In hearings following his death, the extensive connections of several researches conducting the trial to the biotech company Genovo were revealed. The primary researcher, James Wilson, held shares in the company that were valued at \$13.5M, and stood to gain significantly from a positive outcome in the trial. Other issues that arose in the trial were several failures to reveal both potential side effects that had been uncovered in mice in monkeys indicating liver inflammation as a side effect of administration of high vector dose. Additionally, none of the connections of the researcher running the trial to the biotech company that stood to gain from its success were revealed to Jesse or his parents. The failure of this trial represented a difficult milestone in the development of gene therapy as a promising therapeutic, and it would take several more years as well as successful trials to gain back public trust [1, 11].

Another significant setback in development of gene therapy as a potential therapeutic occurred in the year 2000 when 11 children were treated for X-linked severe combined immunodeficiency (X-SCID). The trial used a Moloney murine leukemia viral vector (MLV), a retroviral vector that, due to its integration profile, led to the development of leukemia in many of the children receiving the treatment. This observation led to concerns of insertional mutagenesis as a potential major side effect of gene therapy. Insertional mutagenesis occurs when the viral vector integrates into an area of the host genome and as a result of the integration, impacts normal gene control or expression. The primary cited reason for the impact on gene regulation comes from the integration of the viral transgene and subsequent upregulation of cellular proto-oncogenes through promoter insertion, promoter activation, or gene transcript truncation. The most common method reported in gene therapy trials is enhancer-mediated activation of genes near the viral insertion site [12]. This concern regarding the potential genotoxicity of retroviral vectors led to a shift in development of viral vectors to focus more on lentiviral vectors as a means of introducing a transgene. In further trials for X-linked adrenoleukodystrophy (X-ALD) with lentiviral vectors, analysis of insertion sites indicated a large number of distinct insertion sites that suggested a polyclonal population of lentiviral transduced hematopoietic stem cells were maintained over time. The analysis also indicated the insertions were spread primarily in gene coding regions, without an apparent preference for transcription start sites. Continued observations in these patients revealed there was no clonal expansion in any patient treated [13].

There have been several more recent developments in the progress of gene therapy as a therapeutic. In 2003, China approved a gene therapy treatment called Gendicine. This was the first approval from any country for a gene therapy product. Gendicine is an adenoviral vector that was approved for the treatment of head and neck squamous cell carcinoma and functioned by introducing the wild-type p53 gene [14]. Another development came in 2004 when Ark

Therapeutics Group was granted GMP Certification in the EU to begin manufacturing supplies for the gene-based therapeutic Cerepro. Cerepro is based on an adenoviral vector that encodes the gene for Herpes simplex virus thymidine kinase. This was developed as a therapeutic intended to treat malignant brain tumors. The therapy worked by introducing the thymidine kinase, a pro-drug that activates Ganciclovir to Ganciclovir-monophosphate that is then converted to a toxic metabolite Ganciclovir-triphosphate. Ganciclovir –triphosphate is cytotoxic and can prevent DNA replication [1, 15].

The next major step came when the EMA recommended the EU approve the drug Glybera, marketed by uniQure, for treatment of lipoprotein lipase deficiency. Glybera is an AAV based therapy that delivers the defective protein, lipoprotein lipase, to muscle tissue. When originally developed, Glybera was anticipated to cost approximately \$1.6M per patient. Although the drug showed promise in trials, as of 2016, only one patient has been treated [16].

To this point, over 2300 gene therapy clinical trials have been conducted. A majority of these trials have focused on monogenic diseases or cancer. Their success continues to grow as developments are consistently improving the use of viral vectors as well as the technology for improving the effectiveness of the treatment.

## **1.2 Viral vectors in gene therapy**

### **A. Lentiviral viral vector background**

Lentivirus is a type of retrovirus and is in a family of single stranded RNA viruses that are approximately 80-120 nm in diameter. In the core of these viral particles, are the enzymes: reverse transcriptase, integrase, and protease, along with two copies of positive strand RNA. Surrounding these proteins and the viral RNA is a layer of protein formed by the capsid protein.

Outside this layer, matrix proteins comprise another layer that allows for interaction with another layer derived from cellular lipid bilayer. Embedded in this layer are the envelope proteins, which are responsible for interactions with specific cellular receptors [17].

Retroviruses have previously been divided based upon the organization of their genome into either simple or complex. Simple retroviruses contain at most only one coding region in addition to that of the proteins gag, pro, pol, and env. They do not contain genes for other proteins that may influence RNA synthesis and processing. They are also characterized by a simple pattern of mRNA splicing with most producing only one spliced mRNA. Examples of these viruses are ASLV, mammalian C-type viruses, and the B and D type viruses. Complex retroviruses include the lentiviruses, spumaviruses, and HTLV-BLV group. These viruses have many splice donor sites and can produce complex mRNAs which gives rise to a larger diversity of gene products [18]. Of the retroviruses, one of the best studied is HIV, the virus responsible for acquired immune deficiency syndrome. HIV has also been a popular viral vector used in many gene therapy trials to introduce a transgene into target cells based upon its ability to transduce non-dividing cells.

The genome of the HIV virus encodes three main genes: gag, pol, and env. The HIV gag gene stands for group specific antigen. Gag is initially translated as a multidomain polyprotein that, after cleavage by the viral protease, produces the 6 core structural proteins of HIV. The other proteins contained within the gag polyprotein are MA, CA, SP1, NC, SP2, and p6. The matrix protein (MA), which comprises the N-terminal region of the gag protein, functions to target the gag protein to the plasma membrane. The p24 capsid protein (CA) is a protein fused to the C-terminal region of the matrix protein in the unprocessed gag polyprotein. After processing, this protein becomes the viral capsid. Another protein formed from the gag polyprotein is spacer peptide 1, or SP1. This protein exists between the p24 capsid protein and the nucleocapsid

protein. Cleavage of this protein allows the p24 capsid to form into the viral capsid. Other proteins formed from the gag polyprotein are NC or nucleocapsid protein, spacer peptide 2 (SP2), and p6, which are involved in recruitment of cellular proteins that function to initiate virus budding from the plasma membrane. The gag protein is translated in the cytoplasm and forms the large viral assembly when it reaches the plasma membrane where it binds to and begins assembly of the viron [19].

The pol gene region codes for the enzymes that accompany the single stranded RNA in the viral core. These include protease, reverse transcriptase, and integrase. These three enzymes coded for in the pol gene region are initially constructed as a gag-pol precursor that is produced by frameshifting near the gag 3' end. Among pol enzymes, reverse transcriptase is responsible for converting the viral single stranded RNA to the DNA that will eventually be incorporated into the host cell genomic DNA and replicated with the host cell. Reverse transcriptase works as follows: a cellular tRNA binds to the primer binding site (PBS) and functions to prime DNA synthesis. The PBS is a structured RNA element found near the 5' end of the RNA in the untranslated leader region. After the RNA has been primed, complementary DNA is extended through the 5' region of the RNA, including the U5 and R regions. This process generates an intermediate, termed minus-strand strong-stop DNA. Following the generation of this intermediate, RNase H, a region of the reverse transcriptase enzyme, cleaves the 5' RNA end, removing the U5 and R region and exposing the single stranded DNA. The tRNA primer is then shifted to the 3' end of the RNA molecule in a strand transfer mediated by the single stranded DNA. This process allows the minus-strand DNA synthesis to continue from the duplicate R sequence on either the same or a different molecule. DNA synthesis is continued along the RNA sequence, while simultaneously RNase H degrades the viral RNA. During the degradation of the template strand, a specific region remains intact. This region is called the polypurine tract (PPT). Another polypurine tract called the central polypurine tract (cPPT) exists in HIV in addition to the PPT. The PPT is located in the

U3 region while the cPPT is located centrally in the genome. These polypurine tracts function as primers that allows for synthesis of the plus-strand DNA. RNase H can eventually remove the PPT from the plus-strand DNA following synthesis of several nucleotides. Synthesis of plus-strand DNA is continued along the RNA template until it encounters the tRNA, which blocks further synthesis. The tRNA is subsequently removed by the RNase H. A second strand transfer then takes place in which the plus single-stranded DNA is annealed to the 3' end of the full-length minus-strand DNA. This is accomplished via base pairing of the corresponding PBS sequences. Extension along the minus-strand DNA produces a full length double stranded DNA molecule that is flanked on either side by identical long terminal repeats (LTRs) [20].

The remaining two enzymes encoded in the pol gene include protease and integrase. Protease is responsible for gag-pol cleavage as well as maturation of the viral particle. Integrase is involved in catalyzing integration of the viral DNA into the genome of the host cell. This is accomplished in two steps. In the 3' end processing, two nucleotides are deleted from the 3' end of the initially blunt viral DNA. This exposes the dinucleotides at both 3' ends of the viral DNA. The next reaction is a strand transfer in which the exposed 3' hydroxyls at the ends of the viral DNA disrupt two phosphodiester bonds in the host genomic DNA. Formation of an integration intermediate is next repaired by the cells own enzymes resulting in the ligation of the viral DNA into the host cell genome [21].

The third primary gene encoded in the HIV genome is env, which is responsible for production of the viral envelope. These proteins are heavily glycosylated and are the only viral protein exposed on the virus surface [22]. Because of this, it is these env proteins that determine HIV tropism, the cell types infected by the virus. In HIV, the env gene codes for a precursor protein, gp160. The gp160 protein is processed to form a non-covalently bound homotrimer that is then cleaved into gp120 and gp41 that persists as a fusion protein. Within this fusion protein, gp120 contains the

region capable of binding the CD4 receptor on T-cells as well as the seven transmembrane chemokine receptors that function as co-receptors in HIV binding [23].

The above genes and their encoded proteins are referred to as the viral structural proteins and comprise the majority of the HIV genome. The remaining HIV viral proteins are classified into two classes, the essential regulatory elements and the accessory regulatory proteins. The essential regulatory elements include the genes *tat* and *rev*. *Tat* stands for transactivator of HIV gene expression and encodes the proteins responsible for binding the TAR RNA element and activating the initiation of transcription as well as elongation of the HIV DNA using the promoter present in the LTR of the integrated viral DNA [24]. The other essential regulator element is *rev*. *Rev* is a 19kDa phosphoprotein that, along with *tat*, is found primarily in the nucleus of the infected cell. *Rev* binds the *rev* response element (RRE) and stimulates export from the nucleus of the viral mRNA. In the absence of *rev*, viral mRNA is retained in the nucleus. *Rev* has also been shown to contribute to the stability of the mRNA.

The accessory regulatory proteins are encoded by the genes: *VIF*, *VPR*, *VPU*, and *NEF*. *VIF* stands for viral infectivity factor and is involved in improving the infectivity of the virus [25]. *VPR*, or viral protein R, is a protein which, when incorporated in the viral particle, cooperates with an element of the *gag* precursor and is believed to target the import into the nucleus of the preintegration complex, as well as several other processes. *VPU* stands for viral protein U and functions to degrade CD4 in the host cell endoplasmic reticulum as well as improve the release of viral particles from the host cell plasma membrane. *VPU* is expressed along with *env* as a bicistronic mRNA and is unique to HIV-1, not occurring in HIV-2 or any SIV strain. The final protein, *NEF*, is a primarily cytoplasmic that associates with the host cell plasma membrane. It has been shown to be critical to HIV progression in vivo [26].

## **B. Engineering lentiviral vectors for gene therapy**

Lentivirus is one of the primary viral vectors that have been most explored for its potential applications to gene therapy. The benefits lentivirus provides are that it can transduce quiescent cells and can be engineered into replication incompetent virus. The process for producing a lentiviral vector encoding a predetermined transgene involves transfection of a producer cell line with an expression plasmid. Along with the gene of interest, this expression plasmid must also contain the two viral LTRs, along with regulatory elements such as cPPT and RRE sequences. The cells most commonly used as a producer cell line are human embryonic kidney cells (HEK-293). The remaining genes, gag, pol and env, necessary for HIV production, are provided in trans via co-transfection with the expression plasmid into the producer cell line. These genes can be contained in either two or three plasmids. The accessory genes, vif, vpr, vpu, and nef, have been shown in studies to be unnecessary for viral production or infection of the lentivector and are not included in the plasmids used for transfection [17].

One of the primary considerations that arose early in the development of lentivirus as the viral vector of choice in gene therapy studies was the tropism of the virus. The tropism of a virus determines which cellular receptors are recognized and subsequently, which cells can be infected. The tropism is determined based upon the type of glycoprotein in the viral envelope. The tropism of wild-type HIV primarily allows for recognition and infection of cells displaying the CD4 T-cell receptor. The limited expression of this receptor on cell types other than T-cells limits the potential applications of wild-type HIV as a viral vector [22]. To overcome this limitation, lentiviral vectors are pseudotyped to allow for infection of a broader range of cell types [27]. The most common approach to pseudotyping lentiviral vectors involves the use of glycoprotein G of the vesicular stomatitis virus (VSV-G). VSV-G pseudotyped virus expresses VSV envelope glycoprotein G which recognizes the LDL receptor on a host cells [28]. Because this receptor is nearly ubiquitously expressed, pseudotyping with VSV-G allows the lentiviral vectors to infect a

wide range of cell types [29]. Another benefit that is realized through the pseudotyping of lentivirus is that it allows for production of higher titer virus. This is because expression of the VSV-G in the HIV envelope increases particle stability [17]. Overall, the developments in pseudotyping lentiviral vectors have led to generation of viruses that are widely infectious as well as more stable than their wild-type counterparts.

Another of the critical developments early in the generation of lentiviral vectors to make them suitable for gene delivery in humans focused on the need to remove the replicative capacity of the wild-type virus. To eliminate the possibility of viral replication after transduction of the host target cells, self-inactivating (SIN) lentiviral vectors were developed [30]. Creating a SIN vector is accomplished through deletion of a nucleotide segment in the U3 region of the viral 3' LTR that contains the TATA box. This deletion prevents viral replication while maintaining viral titer and transgene expression. The reason this process is successful in eliminating replicative capacity is that during reverse transcription, the viral 3' LTR is copied to the 5' end of the vector genome. The defect, which inactivates the promoter, then functions to prevent initiation of translation of the viral DNA [31].

Having produced a lentiviral vector that was broadly pseudotyped as well as replication incompetent obviated many of the concerns surrounding the safety and efficacy of lentiviral vectors and increased their utility from a gene therapy standpoint. Further engineering then focused on improving several processes to further improve performance and safety. Among these is the inclusion of the cPPT sequence in the expression vector which functioned to improve viral nuclear import [32]. Another prominent development that improved the safety of lentiviral vectors was replacing the U3 portion of the 5' LTR with a CMV promoter. This modification allowed for Tat-independent transcription of the viral genome [31].

In summary, a majority of the developments of lentiviral vectors for gene therapy focused heavily on improving both safety and functionality of the virus. The increased pursuit of lentiviral vectors as a gene therapy vector was, in part, a result of the data indicating an increased risk for insertional mutagenesis in gamma-retroviral vectors and, as such, the integration profile of lentiviral vectors was heavily researched. To date, many of these concerns of genotoxicity have been assuaged by recent studies indicating that lentiviral vectors do not preferentially integrate near proto-oncogenes like gamma-retroviral vectors. Other developments that served to establish lentiviral vectors as a viable option in gene therapy trials were the pseudotyping with VSV-G, generation of SIN vectors, and the development of methods to increase the titer of viral preparations [17].

### **C. Background and structure of AAV vectors**

Another virus that is used extensively in gene therapy along with lentivirus is Adeno-associated virus (AAV). AAV is a non-enveloped single stranded DNA virus around 4.7 kilobases (Kb) long that belongs to the parvovirus family [33]. It is not associated with any human disease despite greater than 70% of humans testing seropositive for AAV [34]. Discovered in 1965 by Bob Atchison, M. David Hoggan, and Wallace Rowe, AAV was originally found as a contaminant in an adenovirus preparation. It was from this discovery that AAV was named, as its presence seemed to correlate with adenovirus infection. Currently there have been 13 different serotypes identified and many more recombinant species described [35].

The AAV viral genome contains two 145 base pair inverted terminal repeats (ITRs) that flank three open reading frames, Rep, Cap, and aap, which together code for nine total proteins under control of three promoters [36]. The four proteins encoded by the Rep gene are involved in replication and packaging. These proteins include Rep78, Rep68, Rep52, and Rep40. The proteins arising from the Cap gene form the outer capsid shell. This capsid shell is arranged in an

icosahedral structure that is 25 nm in diameter. This arrangement of the capsid makes the structure very stable, providing resistance to brief exposure to heat, low pH, and certain proteases [36]. This capsid is also implicated as a primary determinant in cell binding and internalization. There are believed to be 60 proteins that arrange to form the viral coat with the capsid proteins in the molar ratio of 1:1:10, VP1:VP2:VP3. The *aap* gene codes for the assembly activating protein, a nuclear protein believed to be involved in capsid assembly. This is accomplished via an alternative reading frame that overlaps partially with the *cap* gene [37]. The ITRs, flanking these genes, operate as self-priming hairpins that serve as the origins for DNA replication as well as function in packaging of the AAV genome [38].

The ITRs, along with the capsid also direct the AAV serotype and determine the infectivity in different tissue types. Early work into AAV biology focused on AAV2. As a result, a majority of the AAV vectors contain ITRs from the AAV2 serotype. Another consideration in the use of AAV as a gene therapy vector is the variant of capsid used. Differences in sugar binding that result from capsid sequence variations can influence the cell type that is most readily transduced. The different AAV serotypes each have subtle differences that determine the effectiveness with which they transduce a particular cell type. Along with the main interactions mediated by cell surface carbohydrates, secondary receptors also influence cell and tissue specificity between the AAV serotypes. AAV6, used herein, has been shown to be the most effective serotype for transduction of hematopoietic stem and progenitor cells (HSPC) [39].

#### **D. Engineering AAV vectors for gene therapy**

AAV was first investigated as a potential vector for delivery of a therapeutic transgene in the 1980s. The pioneering work that allowed for AAV to be used in the context of gene therapy was accomplished by providing a method to circumvent the need for co-infection with adenovirus. This was done by transfection of the AAV plasmid clone into human cells that were infected with

adenovirus. Through this development, researchers were able to remove the AAV viral genes and replace them with a predetermined DNA sequence. To produce functional AAV from producer cells, the rAAV genome would then be complemented with plasmids containing the Rep and Cap genes. Following these initial developments, it was discovered that the entire coding region between the two ITRs could be removed while still maintaining the capacity for replication in packaging if the remaining genes were provided in trans. The Rep and Cap genes, provided in trans would not have the ITRs present and the virus produced would therefore not have the ability to package wild-type virus. This method is now the standard in the field for AAV production [36, 40].

The inability of AAV to integrate into genomic DNA is one reason that it is an attractive vector for gene therapy. This arises from the previously described development where expression of the Rep proteins is removed, allowing the transgene contained between the ITRs to form a circular concatemer that can exist in the nucleus of the transduced cell in episomal form. As the episomal DNA has not integrated into the target cell genome, cellular division results in the dilution of these episomes and subsequent loss in expression of the transgene encoded proteins. This property of AAV makes it ideal for situations where control over the length of transgene expression is desired. As AAV expression is diluted out during cell division, this method for transgene delivery offers an opportunity to effectively control the length of time a particular transgene is expressed. This offers several benefits over integrating viruses, as there are situations where transient expression of a transgene may be preferable to stable expression, such as when the side effects of the transgene expression prove undesirable. In this situation, limiting the time for which the transgene is expressed may prove advantageous.

### **1.3 Immunotherapy background**

Along with gene therapy and many times as a result of gene therapy research, immunotherapy has expanded and improved considerably over the years. The field began with the intuition that the immune system may play a more significant role in the initiation and progression of disease than was, at the time, fully understood. Initial efforts treating the immune response as a target that could potentially be manipulated to provide a health benefit began in the 1800s. While progress was at times slow, immunotherapy has since developed into a promising therapeutic with applications relevant in a variety of indications.

The initial observation that triggered a deeper interest in the interplay of the immune system with disease focused primarily on the role of the immune response to cancer development. The first documented progress in, what would eventually become the field of immunotherapy, began with a series of reports suggesting that in an event where some cancer patients developed an infection, their cancer would occasionally enter remission. These reports eventually piqued the interest of a doctor, William B. Coley. As a young doctor specializing in cancer treatment, Coley was interested in the mechanism that allowed patients to overcome a cancer considered at the time to be untreatable. In his personal experience, Coley had documented a case wherein a patient displayed a remission in their cancer after infection with *Streptococcus pyogenes* [41]. From this observation, Coley began the development of an approach that he would continue over the course of his career. His hypothesis was, that by kick-starting the immune system through bacterial infection, he might provide a method for improving remission rates in cancer patients. Further testing of his theory provided Coley enough evidence that some infections could result in a small increase in remission rates of cancer patients that he decided to continue his research. Coley continued investigation into his treatment and eventually established a technique where he would infect cancer patients with an attenuated bacterial stock, later to become known as Coley's toxin. Over the course of his career, Coley infected hundreds of patients with these bacterial cultures and, despite the crude nature of his approach, was able to show slight benefit to the intervention,

with a ~10% improvement in cure rate [42]. Building upon Coley's initial observation and subsequent treatment, continued development and research into the immune response to disease began to take shape.

The next important milestone in the progress of immunotherapy was the concept of a magic bullet, introduced by Paul Ehrlich. At its foundation, this concept proposes the idea that a treatment may be developed that could allow for a certain disease causing entity to be specifically targeted while leaving the rest of the body unaffected. Although the idea of a magic bullet has yet to be fully realized, certain advances, guided by this initial concept, have generated several promising therapeutics. One meaningful innovation that moved progress closer to realization of the magic bullet was the development of monoclonal antibodies and their potential application to disease management. The basis for monoclonal antibody technology began with the discovery and characterization of the B-cell receptor. This understanding allowed for more detailed investigation into the role of immunoglobulin in the immune response to infection. Subsequent contributions in the field revealed the ability of antibodies raised against a pre-specified antigen to effectively discriminate their binding partner amongst a heterogeneous population of potential targets. The resulting research, fueled by what was seen as a mechanism to target treatment to a specific cell type, provided even further understanding into antibody structure and function as well as their potential as a therapeutic. The rapid progress resulting from these advancements in antibody technology eventually hit a delay when the challenge of purifying a single antibody clone developed. This problem arose as a result of an inadequate replicative ability and limited life span of the isolated primary B-cells used to produce the desired antibody. This problem was eventually overcome through the development of hybridoma technology. Hybridomas are produced through the fusion of an antibody producing B-cells with an immortalized melanoma cell line. The result being a method wherein the antibody producing fusion cells could be cultured

and expanded indefinitely, allowing for secretion of a significant quantity of a single antibody clone.

### **A. Cancer immunotherapy overview**

Immunotherapy as a cancer treatment approach has expanded in its scope and application in recent years to provide promising and effective treatment for a variety of different cancer types. The underlying basis of immunotherapy is to deliver a type of treatment that makes use of the body's own natural immunity as a means of eliminating the tumor. In healthy individuals, the typical immune response is initiated through a complex series of events that enable identification of a tumor cell by the host immune system. Tumor antigens are presented by the MHC complex of the nascent tumor cell. Via this presentation, the host immune system is able to identify and initiate an immune response to the tumor cell. This immune response is responsible for much of the tumor suppressive properties of the immune system. As a cancer progresses, the tumor can act to create an immunosuppressive environment which functions to dampen the immune response. The objective of an immunotherapy intervention is to deprive the immune system of this inhibition and return the ability of tumor cell recognition and killing. By using the natural defenses of the patient, immunotherapy is able to provide a targeted and specific method for tumor cell killing.

One powerful approach to circumvent immune suppression is the chimeric antigen receptor (CAR). Other potential interventions include checkpoint inhibition [44], cell therapy, and monoclonal antibody therapy. Many of these approaches may also be provided as a therapy used in combination with CAR based therapy to achieve an even greater success rate. The underlying mechanism remains that the treatment is intended as a means to reinvigorate the immune response to a tumor. Through these methods, there has been much success realized in the field of cancer

treatment and both life expectancy and quality of life post treatment has improved significantly in only the past several decades.

Although the beginnings of immunotherapy emerged much earlier, modern cancer immunotherapy began to take shape in the 1980s when Steven Rosenberg introduced immune cell therapy as a cancer therapeutic. From this concept, the field has expanded to encompass several different treatment approaches, all, however, using the immune system as the primary driver of anti-tumor response.

### **B. Monoclonal antibodies**

A monoclonal antibody, as mentioned previously, is the secreted immunoglobulin produced by a single B-cell clone fused to a myeloma cell. In decades following initial development, this technology was further refined to provide the basis for several powerful cancer treatments. As a result of their pioneering impact on targeted therapy, the Nobel Prize for medicine was awarded to Georges Köhler and César Milstein for their creation of the hybridomas that allowed for monoclonal antibody production.

Along with the introduction of monoclonal antibodies, the notion that the cell surface was a complex and differentiated structure was integral to the progress of monoclonal antibodies for disease treatment. The concept of cell surface differentiation antigens was originally proposed by Lloyd Old and Ted Boyse as a way of defining subsets of mouse leukocytes based upon their function and lineage [45]. From this discovery, cell surface antigens that defined different cell types were documented. This led directly to the development of the cluster of differentiation classification of cell surface antigens. The idea that certain cell types could be uniquely identified based upon structures present on their cell surface opened the possibility of raising antibodies that would bind specifically to a cell type while excluding other cells in the body.

With the development of monoclonal antibodies, the idea that tumor cells could be targeted was also being explored. Antibody treatment for cancer began with the approval of rituximab by the FDA in 1997. Rituximab is an anti-CD20 monoclonal antibody that bound preferentially to B-cells displaying the CD20 ligand. There are now greater than 10 monoclonal antibodies approved by the FDA for treatment of cancer. There are also different classes of monoclonal antibodies that exert specific anti-tumor effects. Naked monoclonal antibodies do not rely on a drug conjugate to kill the tumor cells. Some of these antibodies work by tagging the cells they bind to for recognition by the immune system. An example of one of these is alemtuzumab, which is used in the treatment of chronic lymphocytic leukemia (CLL). It works by binding to CD52 on lymphocytes and directing the body's cytotoxic response to kill these cells. Another type of antibody in this class that can act through a different mechanism is trastuzumab. In patients that overexpress the HER-2 protein, trastuzumab acts by binding the receptor and preventing its activation by growth factors. In a normal cell, HER-2 acts to promote cell growth and division. In a cancer cell, the protein is overexpressed which allows these cells to rapidly proliferate, leading to the development of cancer. Treatment with trastuzumab blocks the signaling through this receptor by growth factors, decreasing the growth and proliferation signals [46].

### **C. Immune checkpoint inhibitors**

Immune checkpoint inhibitors have shown promise in recent years as a cancer treatment. Checkpoint inhibitors rely on the notion that the tumor can induce tolerance in T-cells resulting in a blunting of the immune response to tumor growth. This is accomplished through the production of ligands that bind to T-cells and activate their inhibitory pathways. The success of immune checkpoint inhibitors relies on blocking this signaling in T-cells as a way to free them from the immune suppression that prevents them from attacking the tumor cells. In a typical T-cell response, the T-cell is exposed to an MHC presenting an antigen that is recognized as non-self.

During this activation, there are also inhibitory receptors such as CTLA-4, PD-1, Lag-3, Tim-3, Tigit, and Vista that function to limit the amount of immune stimulation received after the T-cells are activated. As each of the ligands to these receptors can function to inhibit T-cell activity, production by tumor cells would prevent a proper immune response to tumor cell growth. The two ligands that have been used most successfully to block this inhibitory action by the tumor are CTLA-4 ligand and PD-1 ligand. CTLA-4 stands for cytotoxic T lymphocyte associated protein 4. It is a member of the immunoglobulin superfamily and shares many similarities with CD28, a co-stimulatory molecule that functions in T-cell activation. They both have similar protein sequences and CTLA-4 can bind to CD80 and CD86, the same ligand as CD28, although with higher avidity. Because both CD28 and CTLA-4 bind the same receptors, there is competitive binding between the two. CTLA-4 binding inhibits T-cell action while CD28 promotes T-cell activation [47]. The other ligand of interest in cancer treatment via immune checkpoint inhibitors is PD-1 ligand. PD-1 stands for programmed cell death ligand 1. The PD-1 receptor is also a member of the immunoglobulin superfamily and is more broadly expressed as well as expressed over a longer time frame than CTLA-4. The PD-1 receptor is found on activated T-cells, B-cells, and NK cells. The ligand for PD-1 can be expressed by both immune cells as well as tumor cells and when bound to the receptor, it transmits an inhibitory signal to the cell. This is accomplished by clustering with the T-cell receptors post-ligand binding and recruiting phosphatase SHP2. Recruitment of SHP2 results in dephosphorylation of several of the molecules involved in T-cell receptor signaling, the result of which is suppression of T-cell receptor signaling [47].

#### **D. Chimeric antigen receptors overview**

Chimeric antigen receptors provide a means of redirecting effector cell reactivity toward a preselected antigen. This is accomplished through the use of specific engineering of the receptor using an antigen recognition region that is joined to a series of signaling molecules. Using this approach, cytotoxic effector cells can be created that can recognize a predetermined antigen in a

MHC independent manner. In most applications, the effector cell is a cytotoxic T-cell that is able to selectively kill target cells through interactions mediated by the CAR.

Since their foundation in the late 1980s, chimeric antigen receptors have seen many renditions aimed at refining and improving their activity [48, 49]. The CAR, itself has undergone several iterations of its structure that have enabled the cell bearing this receptor to more effectively sustain growth and division as well as react to binding of the target antigen. The common structure of a chimeric antigen receptor is comprised of an antigen recognition region, a transmembrane domain, and an intracellular signaling domain. First generation CARs were a combination of the CD3- $\zeta$  internal signaling domain and one of either CD4[50] or CD8[51, 52] co-stimulatory domains. These receptors were linked to the CD3-  $\zeta$  domain which signal through phosphatidylinositol and tyrosine kinase pathways[53]. In these first generation CARs, the linking of a receptor region to an internal signaling domain allowed for T-cell activation but also impaired cell survival due to a failure to maintain survival signaling once the cells were activated. The result of this was death of the CAR-modified cells. To improve on this design, the second generation CARs included an intracellular signaling domain in the CAR design. The inclusion of this component helped to improve survival of the cell by increasing the signaling through co-stimulatory domains necessary in T-cell activation. The third generation CARs includes other components such as 4-1BB and Ox40, intended to further aid in cell survival and activation. Other additions have been made to the receptor including additional co-stimulator domains as well as stand-alone ligands aimed at improving signaling strength.

#### **E. Clinical trials with chimeric antigen receptors**

The most promising developments in CAR technology have been in CAR T-cells directed against the CD19 cell surface antigen. The CAR T-cells developed against CD19 have been used clinically to treat cancer in which the CD19 antigen is expressed on the tumor cell surface. These

include, B-ALL, CLL, follicular lymphoma (FL), diffuse large B-cell lymphoma (DLBCL), and mantle-cell lymphoma (MCL) [54].

CAR T-cell therapy for B-ALL has proven effective in the clinic and has been pursued by several institutions, each using a different CAR design. Memorial Sloan Kettering Cancer Center initiated a study using a CD28 and CD3-zeta CAR to treat 32 adults with relapsed/recurring B-ALL, achieving a 91% complete response. University of Pennsylvania and Children's Hospital of Philadelphia have developed a CAR comprised of a 4-1BB sequence, also paired with the CD3-zeta internal signaling domain. Their trial for B-ALL led to a 90% complete response in treated patients. The National Cancer Institute has moved forward with a CAR similar to Memorial Sloan Kettering, which involves a CD28 co-stimulatory molecule and a CD3-zeta internal signaling domain. In this trial of 20 children and young adults, they achieved complete response in 70% of the patients. Fred Hutchinson Cancer Center initiated a trial that treated 20 adults with B-ALL using a 4-BB/CD3-zeta CAR and reached 83% complete response. Through these trials, the most commonly observed toxicities were cytokine release syndrome and B-cell aplasia.

CARs have also been used to treat low-grad B-cell malignancies such as chronic lymphocytic leukemia (CLL). Many of these trials have been met with varied clinical response. One of such trials was performed at Memorial Sloan Kettering Cancer Center, where a CAR comprised of CD28 and CD3-zeta, and directed against CD19 was used to treat CLL along with B-ALL. This study resulted in 3 of the 4 patients treated experiencing either a reduction in the lymphadenopathy or stable disease. Another trial completed by the National Cancer Institute also used a CD28/CD3-zeta CAR directed against CD19 to treat CLL and resulted in one patient with complete response, two with partial response, and one with stable disease.

Aside from CD19, other potential CAR targets have been investigated. Anti-CD22 CARs have been developed to treat follicular lymphoma, non-Hodgkin lymphoma, diffuse large B-cell

lymphoma, and B-ALL. ROR1 has been investigated as a target to treated chronic lymphocytic leukemia and small lymphocytic lymphoma. Anti-CD30 CARs have been used in the treatment of Hodgkin lymphoma, and non-Hodgkin lymphoma. CARs directed against BCMA and CD138 have been used to treat multiple myeloma. Additionally, CD123, CD33, and LeY have been used as CAR targets in the treatment of acute myeloid leukemia [54].

Although many of these trials have shown success in the clinic, there are still limitations in the cancers that can be targeted via CAR technology. Much of the focus of the research herein is on the antigen recognition region of the CAR. The most common source of antigen recognition region is the single chain variable fragment (scFv), which is the variable heavy and variable light chain of an antibody that have been linked by a short peptide linker. The development and success of CARs is tied intricately to the ability of the researcher to identify a suitable target antigen that would successfully allow for identification and elimination of the tumor cell while minimizing the risk of side effects. The risks this sort of intervention poses to the patient receiving treatment can often be significant and must be balanced with the necessity of reducing tumor burden. To be an effective tumor cell target, a selected antigen needs to be present on the population of tumor cells and simultaneously absent from cell necessary for survival. As cancer has proven both a heterogeneous and adaptable disease, effectively selecting a target has been a primary limitation in the progress of immunotherapy as a whole. The risks of targeting an inappropriate antigen have been severe and life threatening in past trials that have used CAR therapy [55]. Because of this, selecting an appropriate target is critical to obtaining success with CAR technology [54].

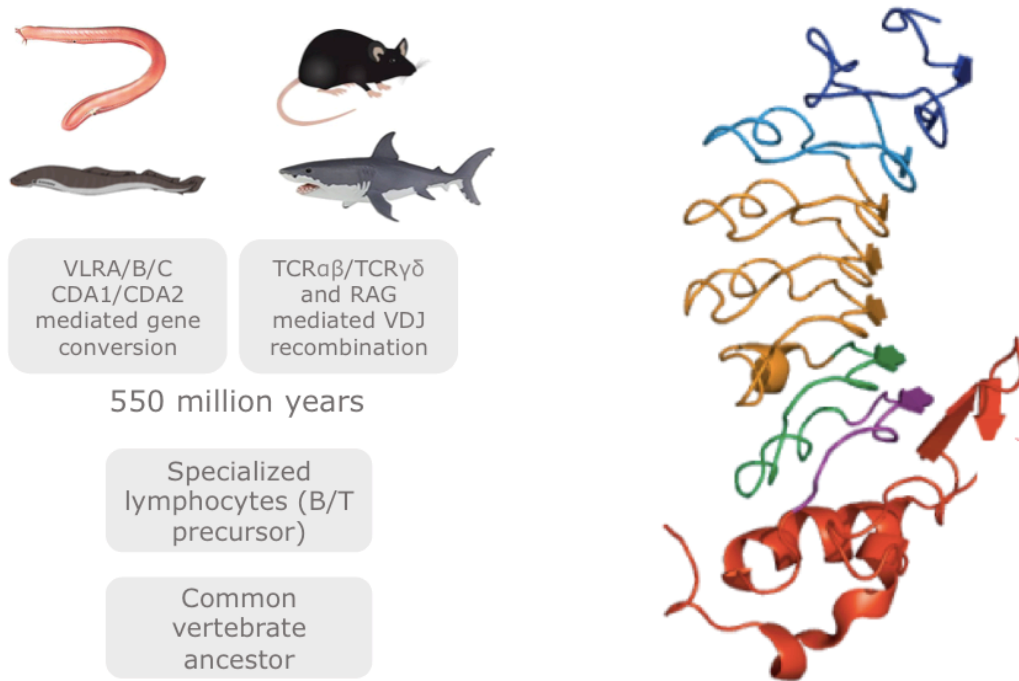
#### **1.4 Overcoming the limitations in tumor cell targeting**

Chimeric antigen receptors (CARs) provide a means to redirect immune effector cells to recognize and target a pre-specified antigen in an MHC-unrestricted manner. If this antigen is

displayed on a tumor cell, the CAR effector cell can mediate a cytotoxic response resulting the death of the tumor cell [56-59]. Although CAR therapy has moved forward rapidly in its development and application, there are still limitations that have hampered progress of the technology. One of the primary limitations is the unavailability of appropriate tumor cell target antigens. Currently, there are only a limited number cellular antigens that have been targeted in the clinic [55, 60-66]. In addition to the limitations imposed by limited tumor cell targets, there have also been issues in CAR trials with either CARs acting off-target where they recognizing an antigen or protein similar to the desired target, or on-target but with off-tumor effects, where the target antigen is recognized on other, non-tumor cells [55, 60-66]. To improve the development of CAR technology, a method to expand the tumor cell antigen repertoire would be necessary. An alternative method to the typical scFv has been proposed herein that uses the adaptive immune system of the sea lamprey as a way to increasing the repertoire of potential antigens that can be targeted using a CAR complex [67-70].

#### **A. Variable lymphocyte receptors**

The VLR is the primary component of the lamprey and hagfish adaptive immune system. VLRs serve a similar purpose as immunoglobulin in the mammalian adaptive immune system but have a fundamentally different structure. Despite these differences in the structure of their immune receptors, the lamprey adaptive immune system is equally as competent as that of immunoglobulin based immune system and VLRs recognize as diverse an assortment of antigens as conventional antibodies [67-70]. The lamprey immune cells rely on a process to generate receptor diversity wherein LRR cassettes are spliced into an incomplete VLR gene in predetermined positions with a mature VLR gene having the structure LRRNT, LRR1, LRRVe, CP, and LRRCT. Because the incomplete germ line VLR gene is flanked by hundreds of LRR repeats that can splice into each of these positions, sequential assembly of the VLR gene using random splicing of the cassettes results in generation of a unique VLR as the cell matures.

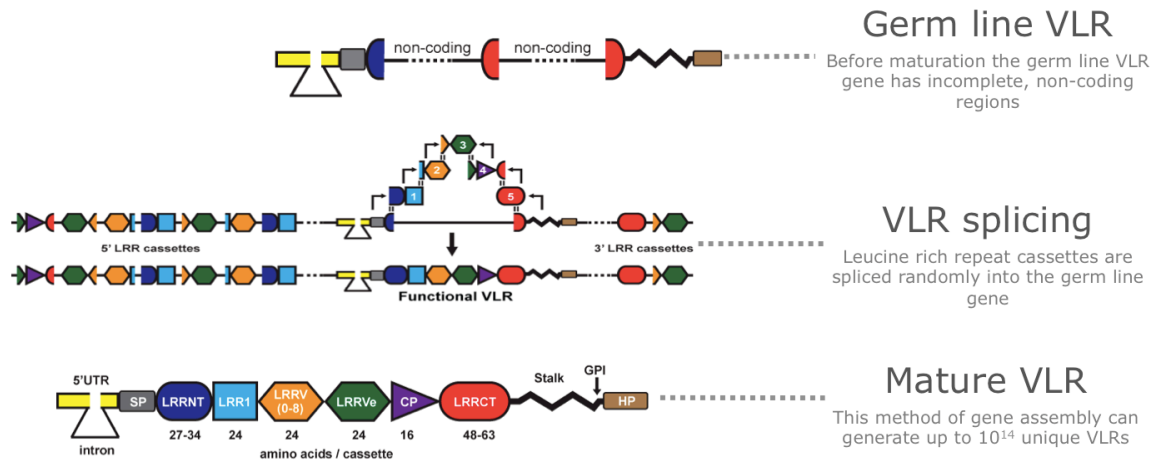
**Figure 1**

Velikovsky CA. Structure of a lamprey variable lymphocyte receptor in complex with a protein antigen. *Nat Struct Mol Biol.* 2009 Jul;16(7):725-30

**Figure 1 The adaptive immune system of jawless vertebrates uses the VLR as the antigen recognition region.** The only two extant species of jawless vertebrates, the lamprey and hagfish use the VLR to recognize and bind antigen. These two species diverged ~550 MYA from the common vertebrate lineage. Because of this evolutionary distance, their immune system has receptors distinct from that of all other vertebrates.

Another feature of the VLR generation process that allows for production of a diverse array of VLRs is the ability to splice anywhere between 0-8 LRR cassettes into the LRRVe position of the VLR gene. The result of this is that the size of the VLR gene increases by  $\sim 220 \text{ \AA}^2$  for every LRR added. Overall this process of VLR generation results in a potential to generate up to  $10^{14}$  unique VLR genes [67-70]. To take advantage of this process, antigen specific VLRs can be produced via immunization of the lamprey with a target antigen. In the experiments detailed herein, both a soluble protein and a tumor cell line have been shown to be capable of initiating an immune response in the lamprey and subsequent production of antigen specific VLRs following immunization. A method to refine the complete assortment of VLRs to identify antigen binding VLRs has also been developed. In this method, the whole VLR library is cloned into a yeast display vector and transformed into naïve yeast. Sorting these yeast to select binders of the antigen of interest results in a pool of VLRs shown to bind a specific antigen [71, 72].

Figure 2

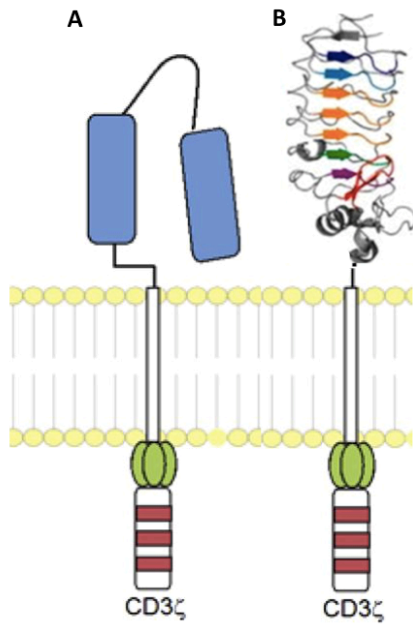


Herrin BR. And Cooper MD., *Alternative adaptive immunity in jawless vertebrates. J Immunol.*

2010 Aug 1;185(3):1367-74

**Figure 2 Assembly of the VLR gene.** The VLR is assembled in a piecemeal manner through combinatorial addition of LRR cassettes that flank the germ line VLR gene. The LRR cassettes are guided into regions based upon conserved sequences present on both the germ line VLR gene and on the ends of the LRR cassettes.

The primary interest in developing antigen specific VLRs is in identification and binding of antigens or antigen epitopes that have not been previously targeted. This is possible due to the many differences between VLRs and immunoglobulin-based antibodies described above. There are two main reasons VLRs are believed to provide a method for targeting previously undefined antigens. The first is based on the structural differences between the VLR and conventional antibodies. The VLR is known to be crescent shaped with  $\beta$ -strands found on the convex portion of the structure. It is these  $\beta$ -strands that are believed to be the primary contributors to antigen binding [67-70, 73-77]. Previous studies have shown that due to this unique structure, VLRs tend to contact different epitopes than conventional antibodies. This tendency was also observed in VLRs and antibodies raised against the same antigen. VLRs can also contain between 0 and 8 LRRs in the LRRVe region resulting in a considerable variation in size. This variability in the overall size of the receptor has also been shown to allow certain epitopes to be contacted by the VLR that would not typically be accessible to antibodies [73]. The second reason VLRs may be able to recognize antigens that conventional antibodies cannot is that due to the lamprey's evolutionary distance, antigens that may be invisible to other animal models used in antibody generation would be recognized by the VLR. Together, these differences in the lamprey and VLR may allow for targeting of antigens or antigen epitopes that would otherwise be inaccessible.

**Figure 3**

*Image adapted from Maude, S.L., et al., CD19-targeted chimeric antigen receptor T-cell therapy for acute lymphoblastic leukemia. Blood 2015 125:4017-4023*

**Figure 3 Comparison between the scFv based CAR and the VLR based CAR.** A. The variable heavy and variable light chains that comprise the scFv are depicted in blue. This attaches to the CD28 transmembrane region that is then linked to the CD3 $\zeta$  internal signaling domain. B. The VLR replaces the scFv as the antigen recognition region of the CAR. Other components of the CAR remain unchanged.

In addition to providing evidence that antigen specific VLRs can be generated through lamprey immunization, we have also shown that these VLRs can be used to replace the scFv as the antigen recognition region of a CAR. Together, these data provide a method that may increase receptor diversity and potentially increase the number of tumor cell target antigens available in CAR therapy. The benefit of using VLRs in CARs would be the potential to increase the number of tumor types that could be targeted via CAR therapy. Additionally, two methods to improve the gene transfer efficiency have been identified. One approach has indicated improvements in lentiviral transduction while the other has provided an AAV based method for transfer of a CAR transgene.

## **Chapter 2**

**Development and screening of immunogen specific VLRs against Factor VIII and the neuroblastoma cell line SK-N-Be(2)**

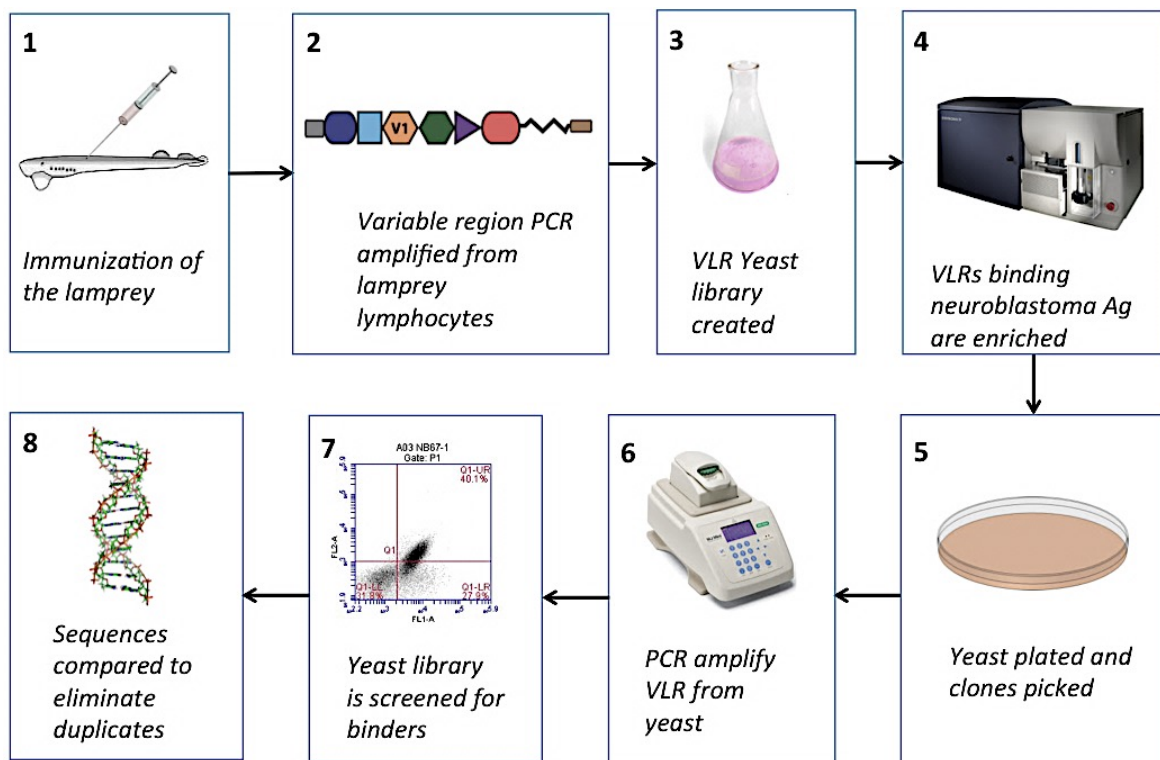
**Abstract**

VLRs are the functional component of the lamprey adaptive immune system. They differ significantly in structure compared to the Ig-based antibodies of jawed vertebrates, but are analogous in function and have been shown to be capable of recognizing and binding as wide and diverse an array of antigens as conventional antibodies [67-69, 76, 78]. The difference in structure is due to the divergence of lampreys and hagfish from the common vertebrate lineage ~450 million years ago, leading to two distinct but equally adaptable immune systems. Because VLRs provide a unique method of antigen recognition, generation of VLRs against certain antigens may provide several benefits not realized with typical immunoglobulin based antibodies. The results herein demonstrate that VLRs can be effectively generated against both a purified protein as well as a cancer cell line. The protein selected was factor VIII and lampreys immunized with varying amounts of the FVIII protein all demonstrated a response to immunization through production of FVIII binding VLRs in the plasma. A similar process was used to generate VLRs against the neuroblastoma cell line SK-N-Be(2). Two candidate VLRs were selected following a high-throughput screen and subsequent refining of the VLR library for binders against the SK-N-Be(2) cell line. Overall, the success of this process has provided evidence that antigen specific VLRs can be generated against both a soluble protein and a tumor cell line via lamprey immunization.

**2.1 Introduction**

The unique process of VLR generation produces a receptor equally capable of binding antigen as immunoglobulin based antibodies, however, the process by which these VLRs are generated varies from that of T-cell and B-cell receptor generation. While antibodies are produced by a Recombination-activating gene (RAG)-dependent recombination process, VLRs are RAG independent and formed by a rearrangement of the germ line gene. Although, lampreys seem to lack lymph nodes and a thymus, they do contain lymphoid and myeloid cells found in the blood

and tissues. Lamprey lymphocytes are comprised of both T-like cells and B-like cells that produce VLR-A and VLR-B, respectively. A third cell type, somewhat analogous to the  $\delta\gamma$  T-cell lineage produces VLR-C [78, 79]. Our work herein has focused exclusively with VLR-B produced from the lamprey B-like cells. In these cells, VLRs are generated through assembly of leucine-rich repeat (LRR) cassettes, forming the mature VLR gene. The diversity in the VLR structure comes from the process of gene assembly in which a series of LRR cassettes flanking the incomplete VLR gene are spliced into the several distinct locations in this gene in a variable manner [67-69, 76, 78]. Each LRR element is incorporated only once, with the exception of the LRRV elements. These segments can vary in number from 0 to 8 LRRs in the mature gene. Each additional LRR introduced increases the surface area by  $\sim 220 \text{ \AA}^2$  [67-69, 76, 78]. The result of this process is a complete VLR-B gene capable of binding antigen. Antigen specific VLRs can be obtained from immunizing lampreys with a target antigen or cell type (i.e., immunogen). Immunized lampreys are then screened for serum antigen-reactive VLR positivity prior to lymphocyte harvesting and cDNA library generation. Due to the conserved nature of the terminal VLR gene sequences, it is possible to amplify the entire VLR cDNA repertoire in a single reaction, which can be then cloned into a surface display expression system for high-throughput screening and candidate VLR discovery [71, 72]. This system allows for both positive selection of immunogen reactive VLRs as well as negative screening for detection of off-target reactivity (e.g., homologous proteins) and on-target, off-tumor reactivity (e.g., normal tissue or cells). An overview of this process is depicted in Figure 1.

**Figure 1**

**Figure 1: Overview of the VLR generation process** Lampreys are immunized with a selected immunogen in three injections spanning 6 weeks. Following immunization, the entire VLR repertoire can be amplified from cDNA obtained from the RNA in the lamprey lymphocytes. Cloning the VLR library into a yeast surface display system allows for enrichment of antigen binding VLRS. This enriched population is then plated to select for individual yeast colonies, which can be grown up and screened for binding against the selected immunogen. After specific colonies have been identified, the VLR can be amplified out of the yeast and sequenced.

Candidate VLRs that meet the screening criteria then can be engineered in place of the scFv on first, second or third generation CAR scaffolds, with the VLR replacing the scFv as the antigen binding region. The primary impetus for developing VLRs as a replacement for the scFv of traditional CARs is that the VLR has been shown to bind antigen in a manner distinct from that of Ig-based antibodies. This difference in binding is due to the structural differences found between VLRs and the traditional monoclonal antibodies from which scFvs are derived. Based on crystal structures, VLRs are known to have an overall crescent shape with  $\beta$ -strands and a C-terminal loop found on the convex portion of the structure [67-70, 74, 76]. These regions have been shown to function as the antigen binding portion of the VLR and are able to expand in size with the incorporation of additional LRRV cassettes. Because of this difference in structure, VLRs generated against the same antigen may bind to dissimilar and distinct epitopes and at different affinities compared with conventional antibodies [73-76]. This variation in binding sets VLRs apart from Ig-based antibodies as a method for directing CAR T-cells to previously unavailable antigen epitopes.

Lampreys have been previously demonstrated to be capable of generating VLRs against several different types of immunized antigens. The usefulness of this approach is to provide an alternative to conventional antibodies. VLRs may be valuable in several different applications where an alternative to conventional antibodies would be beneficial. This is due to the properties of VLRs, described previously, that allow them to bind to epitopes generally inaccessible to Ig-based antibodies. Additionally, due to the evolutionary distance from the common vertebrate lineage, lamprey are not expected to be as constrained by the limits of self-tolerance as would be more conventional mammalian models. One potential protein to which the technology for generating VLRs may be useful is factor VIII (FVIII). FVIII is a protein that serves as a co-factor in the clotting cascade that allows for clot formation following vascular injury. It is a commonly researched protein due to its role in hemophilia A, where its absence or decreased presence leads

to the development of a bleeding disorder. Hemophilia A is currently the most common inheritable deficiency in coagulation. Individuals with severe hemophilia A can experience frequent hemorrhaging which can lead to chronic and debilitating arthropathy, hematomas of the subcutaneous connective tissue of muscle, and internal bleeding [80]. The use of antibodies directed against FVIII is critical in the investigation of hemophilia A treatment and a VLR-based method that may target potentially unavailable epitopes on the FVIII molecule and provide benefits to the ongoing research efforts. To generate these VLRs, an immunization schedule for injection of purified FVIII into lampreys was established. The resulting data indicates the potential for anti-FVIII VLR generation.

To further demonstrate the usefulness of the VLR in a broad range of applications, a neuroblastoma tumor cell line SK-N-Be(2) was selected for immunization into lampreys. The SK-N-Be(2) cell line was selected as a target due to its availability as a representative tumor cell line. It was established in the 1970s from the bone marrow of a male donor under 18 who had been diagnosed with disseminated neuroblastoma [81]. Neuroblastoma provides a useful cancer type for investigation, as it is an aggressive cancer with a limited cure rate. It is a tumor derived from the primitive cells of the sympathetic nervous system known as the neural crest cells. It forms as a solid cancer arising most frequently in children and is known to be the most common extra-cranial neoplasm occurring during childhood [82]. There is a reported incidence rate of approximately 650 cases yearly and this accounts for close to 15% of all pediatric cancer related deaths. Of the patients diagnosed with neuroblastoma, approximately 40% will be classified as high-risk for whom the 5-year survival rate is only 30% [83]. The current therapies in place include high-dose chemotherapy with autologous stem cell rescue, and immunotherapy. These treatments, however, have been shown to provide benefit to only around 10-20% of patients [84]. As with many cancers, the need to balance the negative side effects with the benefits of treatment limits the efficacy of many therapies. Despite the modest increase in median survival achieved

through the current methods, there are still important limitations in the success of these techniques due mainly to the difficulty in specifically targeting tumor cells while also maintaining viability in the non-cancerous cells throughout the treatment process. Immunotherapy based treatment of neuroblastoma would benefit greatly from further identification of targetable antigens on the tumor cells. As an alternative antigen receptor, the VLR may provide a means of identifying and targeting CARs to the neuroblastoma tumor cells.

The goal of this project is the development and implementation of a protocol that would produce gene modified effector cells expressing a CAR specific for a neuroblastoma tumor antigen. In previous studies, anti-tumor CARs have been composed of a single chain antibody variable fragment (scFv) that has specificity for a tumor associate antigen. To generate a VLR, the neuroblastoma cell line SK-N-Be(2), previously described, will be used to immunize the sea lamprey at varying cell numbers in order to elicit an immune response. The resulting VLRs produced can be amplified from the lamprey RNA and screened for specificity against tumor antigens. The proposed project will add innovation to the current method of CAR design through use of lampreys as the source of the antigen receptor. As described previously, the VLR may provide a method to direct CAR expressing effector cells against previously unavailable antigens. Generation of anti-SK-N-Be(2) VLRs that can function as the antigen recognition region of a CAR would confirm the efficacy of the VLR generation process.

## **2.2 Materials and methods**

### **Lamprey immunization with FVIII**

Three lampreys were immunized on a pre-specified injection schedule with purified recombinant FVIII protein. The recombinant FVIII protein used for injection is B-domain deleted with murine derived A1 and A3 regions and human derived A2, C1, and C3 regions. The injection schedule, depicted in Figure 1A has 12 lampreys divided into three groups. The lampreys were anesthetized

by immersion in 0.5g/L of ethyl-3 aminobenzoate, methanesulfonic acid salt in buffered water for 30 minutes. The three lampreys in cohort 1 received injections of 100 $\mu$ L of 70% PBS. The three lampreys in cohort 2 were injected with 100 $\mu$ L of 4 $\mu$ g FVIII in 70% PBS. Cohort 3 received 20 $\mu$ g FVIII in 70% PBS. Cohort 4 was injected with 100 $\mu$ L of 50 $\mu$ g FVIII in 70% PBS. The injections were performed at 2-week intervals with the entire injection schedule spanning 6 weeks.

### **Lamprey immunization with SK-N-Be(2) cells**

12 total lampreys were divided into 4 groups containing 3 lampreys each. Following administration of anesthetic by immersion in 0.5g/L of ethyl-3 aminobenzoate, methanesulfonic acid salt in buffered water for 30 minutes, the first group received an injection of  $1 \times 10^5$  total SK-N-Be(2) cells in a total volume of 50 $\mu$ L. The second group received an injection of  $2 \times 10^5$  total SK-N-Be(2) cells in a total volume of 50 $\mu$ L. The third group received an injection of  $5 \times 10^5$  total SK-N-Be(2) cells in a total volume of 50 $\mu$ L. The final group received an injection of 50 $\mu$ L of 70% PBS. These injections were repeated at two week intervals for a total of three injections as depicted in Figure 2B.

### **Sacrifice of the lampreys and blood collection**

2 weeks following the final injection, the lampreys were sacrificed by submersion in buffered water containing 5g/L ethyl-3 aminobenzoate, methanesulfonic acid salt for 30 minutes. Following sacrifice, lampreys were injected with 50 $\mu$ L of 3mM EDTA. Lampreys were then gripped with a hemostat by the mouth and bifurcated immediately above the cloaca using surgical scissors. Blood was evacuated from the lamprey into a 15mL conical tube containing 10 $\mu$ L 3mM EDTA.

### **RNA isolation and creation of cDNA library**

Lamprey white blood cells (WBCs) were isolated from the whole blood via centrifugation of the lamprey blood for 30 minutes at 400 x g in 55% Percoll. Lymphocytes were extracted from the Percoll gradient following centrifugation. Following extraction, lymphocytes were counted and washed in 70% PBS. An RNeasy kit was used to extract RNA from the lamprey lymphocytes (Qiagen 74104). RNA was converted to cDNA using a first strand synthesis kit (Invitrogen: 11904-018).

### **Amplification of VLR from cDNA**

Amplification of the VLR was performed using two-step, nested PCR. The first step used primers designed to amplify the entire VLR gene. Primer sequence are, Fwd: 5'-TGGGCATTTTCGAGGGGCTAG-3', Rev: 5'-GCATGTCCCTCGCAGTGTTC-3'. The second step used primers designed to bind the constant regions flanking the VLR gene. Primer, Fwd: 5'-AAAAAAGGCCACCGGGGCCGCATGTCC-3', Rev: 5'-AAAAAAGGCCCCAGAGGCCCTGGGCATTTTCGAGGGGCT-3'. Amplification with the primers listed above adds the unique restriction sites BamHI and NheI. Screening of the PCR amplicons indicated amplified VLRs ranging in size from ~600bp to ~800bp (Figure 2). The PCR was conducted as follows: KOD hot start DNA polymerase (Novagen<sup>®</sup>) and Zymolase (Zymo Research), were combined with the primers listed above and incubated for 30 minutes at 37°C allowing the Zymolase to break down the yeast cell wall. Following Zymolase incubation, PCR was performed as follows: initial denaturation: 95°C for 3 min followed by denaturation: 95°C for 30 seconds, annealing: 55°C for 30 seconds, extension 72°C for 1 minute. The previous 3 steps were repeated for 30 cycles. The final extension was performed at 72°C for 10 minutes.

### **ELISA for anti-FVIII VLRs**

To perform the ELISA to detect anti-FVIII VLRs in the immunized lamprey plasma, 96-well 1/2 area high binding ELISA plates (Corning 3690) were coated with lamprey plasma dilutions.

Samples were plated starting with: 67% PBS only, then naïve plasma, then serial dilutions of injected lamprey plasma at 1:1, 1:10, 1:100 performed in triplicate. The dilutions were all done in 67% PBS in a total volume of 25 $\mu$ L. The plates were covered and incubated for 2h at 37°C. The plates were then washed two times with wash buffer using an electronic plate washer. Following the wash step, the plates were blocked by adding 160 $\mu$ l of blocking buffer to each well of the plate and incubating for two hours at room temperature. The FVIII protein was diluted, and 25 $\mu$ l of 1.5  $\mu$ g/ml FVIII was added to the plate that and incubated at 37°C for 1 hour. The plate was then washed in wash buffer using a plate washer and the biotinylated antibody, 4(21)C, was added to the FVIII at concentration, 6 $\mu$ g/mL in 25 $\mu$ L blocking buffer. The plate was then incubated at room temperature for 1 hour and washed two times in wash buffer. Following the wash, Streptavidin HRP was diluted 1:1000 in blocking buffer and 40 $\mu$ L was added per well. Following a wash, the plate was developed by mixing 1:1 TMB substrate reagents and adding 40 $\mu$ L to each well. The plate was allowed to develop for 30 minutes then stopped with 40 $\mu$ L 2M H<sub>2</sub>SO<sub>4</sub> to stop the reaction. The plate was read on a plate reader at 450 nm using the endpoint protocol.

### **Screening of lamprey plasma for anti-SK-N-Be(2) VLRs**

To screen the lamprey plasma for the presence of anti-SK-N-Be(2) VLRs, a flow cytometry based method was used. After collection and separation of lamprey blood via Percoll centrifugation, the plasma was collected and diluted, 1:10 and 100 $\mu$ L was added to  $1 \times 10^6$  SK-N-Be(2) cells. The cells were incubated at 37°C for 15 minutes then washed in PBS and resuspended in 100 $\mu$ L PBS with 1% BSA. The cells were then stained with anti-VLR antibody for an additional 15 minutes. Following the incubation and a wash step, the cells were analyzed via flow cytometry for the presence of VLR bound to SK-N-Be(2) cells.

### **Cloning the polyclonal VLR library into the yeast expression plasmid and transformation into yeast**

Both the yeast display vector depicted in Figure 5 and the polyclonal VLR population were cut with BamHI and NheI. The VLR insert was ligated into the vector using quick ligase, the result being a polyclonal population of VLRs ligated into the yeast display vector. To transform this vector into yeast, the yeast strain *S. cerevisiae* was cultured overnight at 30°C in YPD media. Following incubation, the yeast were diluted 1:5 and cultured for 3 hours to initiate log phase growth. The yeast cells were then washed once with dH<sub>2</sub>O and resuspended in 1M sorbitol to a concentration of 10<sup>9</sup> cell mL<sup>-1</sup>. Two hundred μL of yeast along with 1 μg of the digested yeast display vector, pYSD2, and 2 μg of the amplified VLR PCR product were mixed then electroporated at 2.5 kV using a Micropulser™ electroporator (Bio-Rad). The total number of transformants was estimated to be 1.1 × 10<sup>6</sup> VLRB clones [85].

### **Screening the FVIII VLRs**

Following creation of the yeast display vector, the anti-FVIII VLR yeast library was plated on yeast growth plates containing YSD media. The yeast colonies were allowed to grow at 30°C for 48 hours. Following the incubation, 42 colonies were selected from the plate and grown up in SDCAA media overnight on a shaker at 30°C. To begin log phase growth, each yeast clone was diluted 1:5 in SDCAA media and incubated on a shaker at 30°C for 3 hours. Following the incubation, to induce expression of the VLR on the yeast cell surface, the yeast were spun down at 400 x g for 15 minutes and resuspended in 5mL of SGCAA media. The yeast were then incubated overnight at 30°C on a shaker. After the incubation, yeast clones 1-21 and 21-42 were combined. To screen for VLRs binding to FVIII, purified recombinant FVIII protein used for lamprey immunization was biotinylated using EZ-link NHS-LC-LC-biotin (Thermo 21343) according to manufacturers instructions. Following biotinylation 100μL of the biotinylated FVIII was added to each yeast culture and incubated for 30 minutes at 30°C. The yeast were then

washed 2 times in ice cold PBS then stained with an anti-HA antibody. Flow cytometry was performed to determine binding to biotinylated FVIII.

#### **Sorting of yeast surface displayed VLR library and plating for individual colony growth**

To enrich for the SK-N-Be(2) binding VLRs, the yeast surface display library was cultured overnight in SDCAA media at 30°C. After incubation, the yeast were spun at 400 x g for 10 minutes and washed once in dH<sub>2</sub>O. The yeast were then resuspended in 5 mL of SGCAA to induce VLR expression and incubated overnight at 30°C. Following the incubation, the yeast were diluted 1:5 in 5mL of SGCAA and cultured for 3 hours at 30°C to induce log phase growth. After the incubation, the yeast were washed once in H<sub>2</sub>O and counted using a hemocytometer. From this population, 1x10<sup>8</sup> yeast were transferred to a polystyrene tube for flow sorting. Running concurrently with the incubations, biotinylated SK-N-Be(2) lysate was prepared. This was performed by removing 1x10<sup>7</sup> SK-N-Be(2) cells from a culture and following manufacturers directions for labeling with biotin (Thermo 21343). Following labeling, the cells were washed then resuspended in 1mL of RIPA buffer (Sigma R0278) and incubated on ice for 5 minutes to lyse the cells. After lysis, the lysate was spun at 10,000 x g to remove cell debris and then transferred to a new tube. To stain the yeast library, 500µL of the biotinylated SK-N-Be(2) cell lysate was transferred to the tube containing 1x10<sup>8</sup> yeast cells and incubated for 30 minutes at RT on a rotating mixer. Following incubation, the cells were washed once in dH<sub>2</sub>O and stained with anti-VLR antibody. Yeast displaying SK-N-Be(2) binding VLRs were enriched via flow sorting on double positives for anti-biotin and anti-VLR antibodies.

#### **Selection and screening of VLR clones**

Following the VLR enrichment via flow cytometry sorting, the yeast population was cultured in SDCAA media overnight then washed once with dH<sub>2</sub>O and spread onto a SDCAA agar plate. The plate was incubated for 48 hours at 30°C to allow for colony growth. After incubation, 50 yeast

colonies were selected from the plate and grown in SDCAA media overnight for further screening.

### **Screening the selected VLR clones**

With 50 yeast colonies selected, the corresponding VLRs were further screened for binding to SK-N-Be(2) cells lysate. This was accomplished using the same procedure as followed for enriching the polyclonal VLR population. Briefly, each yeast colony was brought to log phase growth then  $1 \times 10^8$  yeast cells were transferred to a polystyrene tube. Biotinylated SK-N-Be(2) cell lysate was added to the tube and incubated for 30 minutes at RT. Following incubation, the yeast were stained with anti-biotin antibody. Analysis via flow cytometry indicated yeast colonies binding to the target cell lysate. The colonies with the highest percentage of binders to the cell lysate were moved to the next round of screening. From this process, 20 clones were selected for further analysis using the same method. After the process was complete, 10 clones remained for further testing.

### **Sequencing the VLRs clones**

The 10 VLR clones selected for further analysis were sequenced from the yeast using a PCR based method. This process was conducted with an initial step of a 30 minute incubation with Zymolase to break down the yeast cell wall. Following that step, PCR was carried out as described previously. Primers were used that bound the constant region flanking the VLR, Fwd: 5'-TGGGCATTTTCGAGGGGCTAG-3', Rev: 5'-GGCCCCAGAGGCCCTGGGC-3'. Following amplification from the yeast, the amplicons were sent for sequencing using the primer: 5'-GGCCACCGGGGCCGCATGTCC. The results of this sequencing were annotated to ensure accuracy by comparing the sequenced constant regions to the anticipated VLR constant regions.

## **2.3 Results**

### **Overview of VLR generation process**

Figure 1 provides an overview of the process by which antigen specific VLRs are generated and screened for specificity. This initial step is injection of the lampreys with the antigen of interest (Figure 2A,B). This process was refined previously to allow for successful production of antigen specific VLRs in the immunized lampreys [74, 86]. Following completion of the injection schedule, the VLR region is amplified from the lamprey lymphocytes and used to create a VLR yeast library. Enrichment of this library for binders to the antigen of interest results in a refined polyclonal library that can be plated on yeast growth plates to allow for individual colony selection. Another round of PCR amplification performed on yeast grown from these colonies allows for isolation of the clonal VLR, which can be sent for sequencing. The individual colonies are then further screened for binders to the antigen of interest using the same method described above. This information, combined with the sequencing data can be used to eliminate duplicate VLRs and identify VLR sequences for further testing.

### **Recombinant FVIII and SK-N-Be(2) cells were injected into lampreys to elicit an immune response and subsequent production of VLRs binding the immunized antigen.**

The recombinant FVIII used in this study was injected following a schedule previously established [74] and depicted in Figure 2A. Briefly, the lampreys were divided into control and experimental groups that received either injection of 70% PBS or FVIII at the concentrations 4 $\mu$ g, 20 $\mu$ g, or 100 $\mu$ g. These concentrations were established based upon a previous series of immunizations wherein 100 $\mu$ g was found to be the maximum concentration of FVIII that was not toxic to the lampreys. In this previous immunization, 3 of the 4 lampreys injected with either 150 $\mu$ g or 200 $\mu$ g died following either the second or third immunization. The injection of SK-N-Be(2) cells was completed in a similar protocol to that of FVIII with the concentrations based on work previously completed in the lab of Max Cooper. The cells were administered at doses of 1x10<sup>6</sup>, 2x10<sup>6</sup>, or 5x10<sup>6</sup> as depicted in Figure 2B. The purpose of the injection schedule is to allow

for generation of a maximum immune response following each injection with the result being the production of a large population of antigen-binding VLRs that can be obtained from each lamprey. Due to the fact that the lampreys used in these experiments are outbred, a necessity based upon the lamprey's unique lifecycle, the immune response of the individual lampreys will vary considerably with each lamprey within each cohort as well as between the cohorts potentially responding differentially to immunization. The result of this variability is that it becomes difficult to predict the response of any particular lamprey. A lamprey in the cohort receiving the lowest dose may initiate a greater and more successful immune response than a lamprey in the high dose cohort. Similarly, lampreys that have received that same dose may respond with a considerably different immune response.

Figure 2A

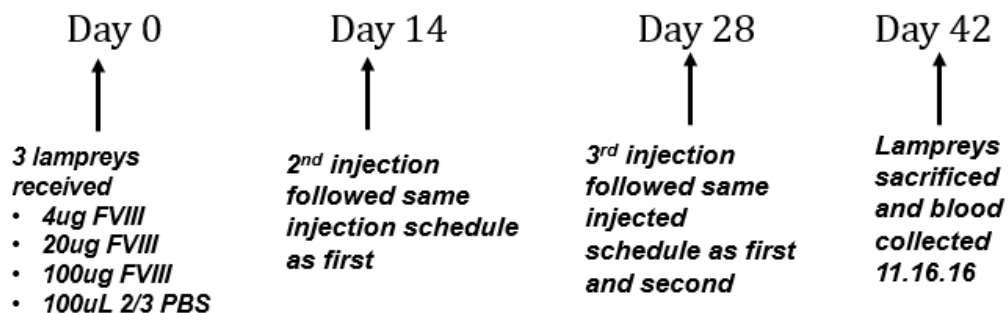
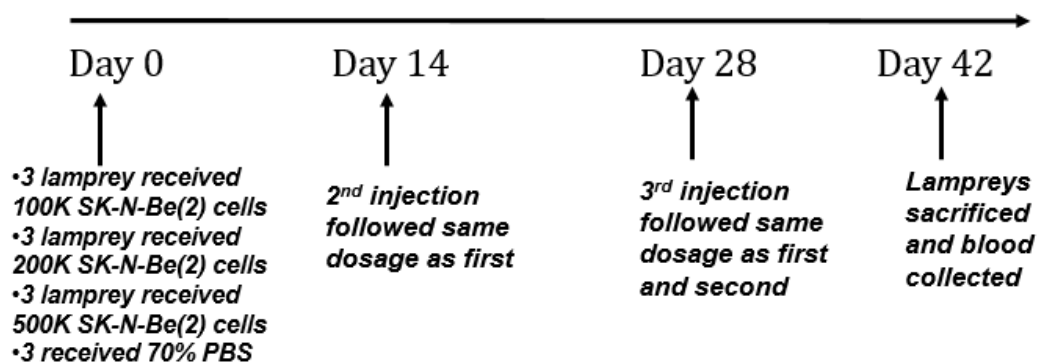


Figure 2B

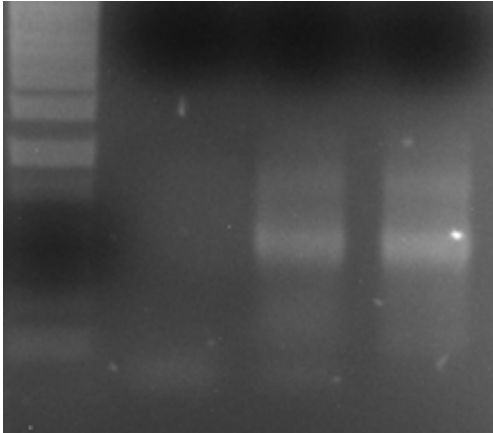
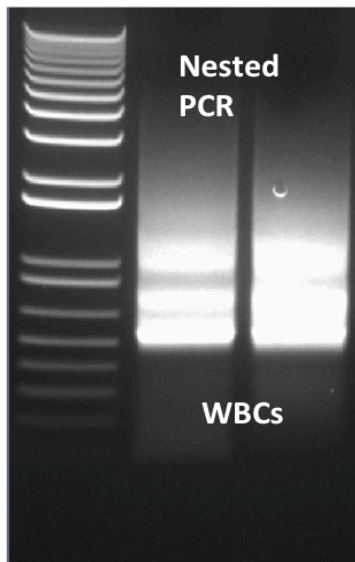


**Figure 2: Lamprey injection schedule for FVIII and SK-N-Be(2) cells.** A. The lamprey injection schedule for immunization with recombinant FVIII. 12 lampreys were divided into three cohorts that received 4 $\mu$ g, 20 $\mu$ g, 100 $\mu$ g, or 70% PBS. The injections were repeated every two weeks for a total of three injections. Two weeks following the conclusion of the injection schedule, the lampreys were sacrificed.

### **Amplification of the VLR library from the lamprey lymphocytes**

Once the immunization schedule was completed in the lampreys, the complete repertoire of VLRs generated in these lampreys needed to be isolated. One of the issues that arose initially was in the method by which the lamprey lymphocytes are isolated from the rest of the blood cells. Because lamprey red blood cells (RBCs) have a nucleus, traditional methods of lysing the RBCs would be ineffective in lysing lamprey RBCs. Initially, it was assumed that the RNA extraction from the lamprey lymphocytes could be performed without needing to lyse the RBCs. The results from these initial tests indicated that the presence of RBCs significantly decreased the RNA yield obtained from in the isolation. Due to this reduced yield, amplification of the VLR library was unsuccessful and another series of immunizations with three new cohorts of lampreys was needed. With these new cohorts, it was determined that a method for specifically extracting the lymphocytes was needed. The method that eventually proved successful was layering the total lamprey blood onto a Percoll solution followed by centrifugation at 400 x g. This method successfully separated the RBCs, WBCs, and plasma and allowed for collection of the lamprey lymphocytes as well as plasma while leaving behind the RBCs.

Having resolved the issues with lymphocyte isolation, RNA could then be extracted from the lamprey lymphocytes and converted to cDNA. From this point, and in order to demonstrate the successful isolation of the polyclonal VLR library from the lamprey lymphocytes, PCR was performed using primers directed to the constant regions flanking the VLR in order to amplify the VLR gene. The results obtained via gel electrophoresis of the PCR amplicons indicate a successful amplification of the VLR population as evidenced by the presence of a large band stretching from ~600 bps to ~800 bps. The size variation in this band is accounted for by the variability in the LRR(V) region of the VLR gene. Because anywhere between 0 and 8 LRR cassettes can be incorporated into the VLR during the maturation of the lymphocyte, the resulting VLRs vary in length. The results of this amplification are depicted in Figure 3A and 3B.

**Figure 3A****Figure 3B**

**Figure 3. Amplification of entire VLR repertoire from lamprey total cDNA** Amplification of the lamprey VLR is accomplished using primers specific for the constant regions flanking the VLRs. A. Image of a agarose gel separating the lamprey VLRs obtained through amplification of the lamprey cDNA of three different lampreys. In lane 1 are the VLR amplified from the lamprey injected with  $1 \times 10^5$  total SK-N-Be(2) cells. Lane 2 is the lamprey injected with  $2 \times 10^5$  total SK-N-Be(2) cells. Lane 3 is from the lamprey injected with  $5 \times 10^5$  total SK-N-Be(2) cells.

**VLRs binding to recombinant FVIII were produced in immunized lampreys and expressed in the lamprey plasma**

An ELISA assay designed to detect anti-FVIII VLRs showed a dose response in the plasma derived from immunized lampreys. In the lamprey injected with the lowest concentration of FVIII, the ELISA indicated a lower concentration of FVIII binding VLRs. The results imply that by increasing the concentration of FVIII injected into the lampreys, a higher concentration of anti-FVIII antibodies can be obtained. Overall, the results from this ELISA demonstrate that the lamprey immunization with FVIII produced anti-FVIII VLRs that could be screened for in the lamprey plasma.

**VLRs binding to the SK-N-Be(2) cell line were produced in immunized lampreys and expressed in the lamprey plasma**

The results of the flow assay performed on SK-N-Be(2) cells incubated with plasma from immunized lampreys indicate the presence immunogen specific VLRs. These results, shown in Figure 4B show that the SK-N-Be(2) cell line is bound by soluble VLRs in the lamprey plasma. The first panel of the figure shows the naïve lamprey plasma while the following three panels show the three lamprey that were injected with varying cell numbers of SK-N-Be(2) cells. The lamprey in the second panel received  $1 \times 10^5$  SK-N-Be(2) cells, the lamprey in the third panel received  $2 \times 10^5$  SK-N-Be(2) cells, and the lamprey in the final panel received  $5 \times 10^5$  SK-N-Be(2) cells. The binding of VLRs in the lamprey plasma is indicated by the shift in the population along the x-axis of the histogram, indicating the cells have bound to VLR and are thus staining positive with the anti-VLR antibody.

Figure 4A

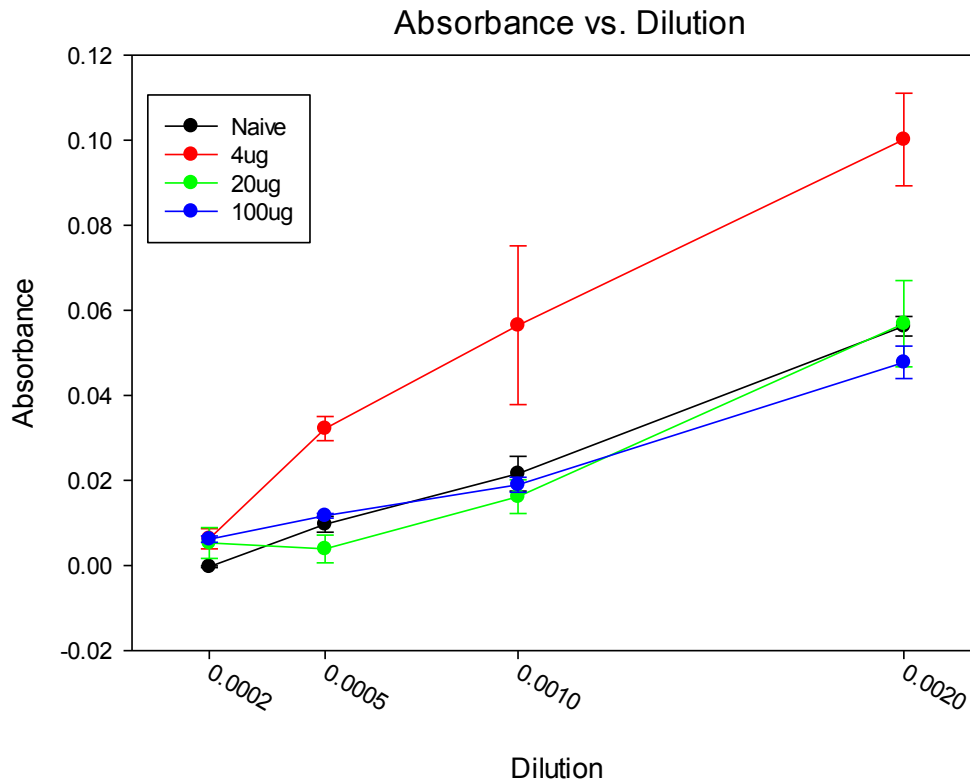
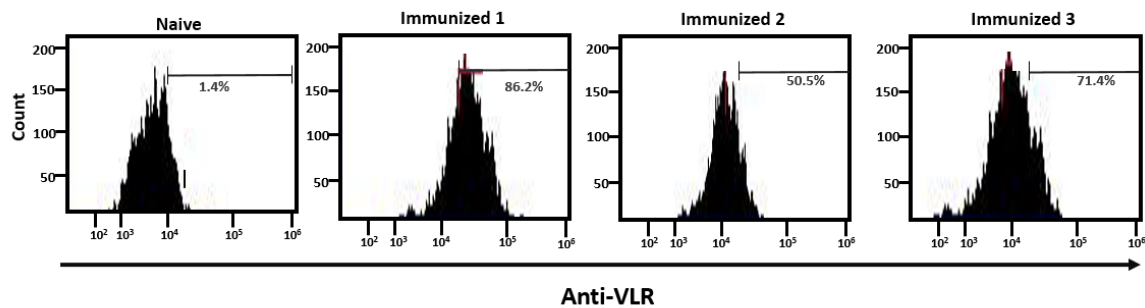


Figure 4B



**Figure 4. Confirmation of immunogen-binding VLRs in lamprey serum.** A. The ELISA developed in figure 4A shows the presence of anti-FVIII antibodies in the plasma of lampreys immunized with FVIII. Each line represents a cohort of three lampreys that were injected with FVIII at either 4 $\mu$ g, 20 $\mu$ g, or 100 $\mu$ g. B. The flow diagram shows the presence of anti-SK-N-Be(2) VLRs in the immunized lamprey plasma. In this assay, SK-N-Be(2) cells will be bound by

immunogen-specific VLRs in the plasma if the immunization has been successful. Positive binding of the soluble immunogen specific VLRs to the target SK-N-Be(2) cells was indicated via labeling with anti-VLR antibody and analysis by flow cytometry. The three lampreys assayed all showed varying levels of immune response as evidenced by the shift in the population along the x-axis.

### **Cloning into the yeast surface display plasmid**

In order to express the VLR library in a yeast display model, the VLR is cloned into an expression vector (Figure 5) that when expressed in the yeast cell results in a fusion protein of the VLR with the yeast flocculation protein. This allows for display of the VLR on the yeast cell surface. The purpose of this step is to provide a method for high-throughput analysis of the polyclonal VLR population. Because the VLR fusion protein is under control of a galactose inducible promoter, it will not be expressed until the yeast are cultured in galactose containing media. This prevents expression of the VLR from hindering growth of the transformed yeast and dilution of the VLR containing yeast due to preferential division of the non-transformed yeast cells. When the yeast library is cultured in galactose containing media and the VLR fusion protein is expressed, the yeast can be analyzed in a high-efficiency manner using flow cytometry. Other components in this construct include the CYC1 terminator which has been shown to increase the half-life of mRNA as well as improve gene expression control [87], the TEF-1 alpha gene promoter, and the CEN6/ARS4 centromere, which is both necessary and sufficient for accurate chromosomal segregation [88]. In order to allow cloning of the amplified VLRs into this vector, an SfiI restriction site was added. Collectively, these components allow for effective cloning of the VLR library into this vector and expression of the VLR on the yeast cell surface following transformation.

Figure 5

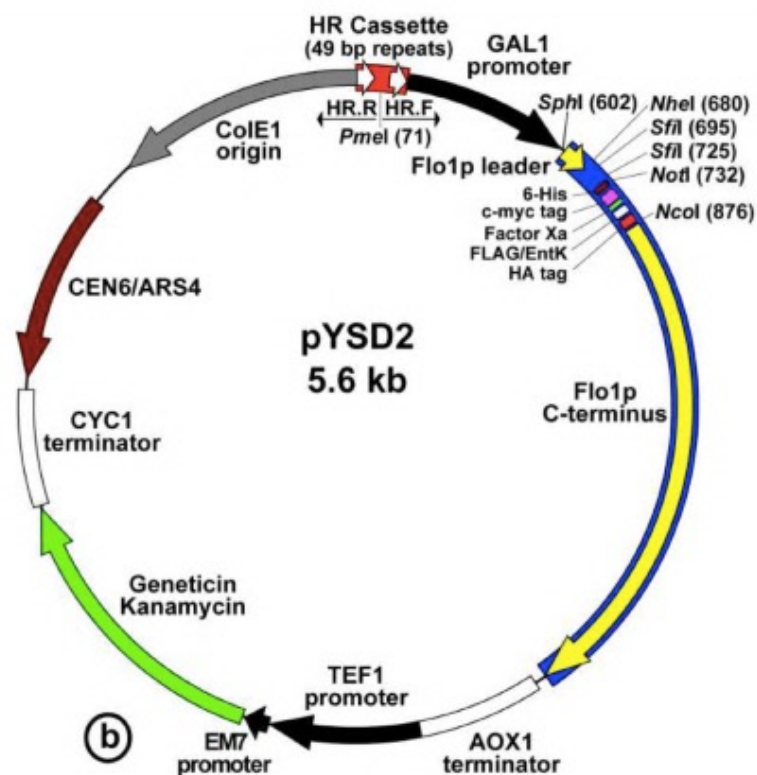


**Figure 5. The yeast expression vector pYSD2** Cloning the polyclonal VLR library into this yeast expression vector leads to the production of a fusion protein between the VLR and the C-terminal region of the yeast flocculation protein 1p. The Flo1p C-terminus serves as the yeast fusion protein that allows for the VLR to be displayed on the cell surface. The Geneticin and Kanamycin genes provide antibiotic based selection of positively transduced yeast cells. The GAL1 promoter allows for inducible expression of the yeast/Flow1p fusion peptide in the yeast cell. The CEN6/ARS4 is a centromere. The CYC1 terminator is present to increase in mRNA half-life. ColE1 stands for Colicin E1 origin of replication. The AOX1 terminator decreases the occurrence of false-positive clones from a secondary recombination event [89].

**Screening the anti-FVIII yeast display against biotinylated FVIII**

Cloning the anti-FVIII VLRs into the yeast display system provides an effective method to screen selected colonies against biotinylated FVIII to determine positive binding of VLRs in the polyclonal population. In the results shown in Figure 6, yeast colonies selected from a plate were combined to allow for a more efficient method of screening multiple colonies. In these results, 42 colonies were picked from a plate and combined in two different cultures of 21 clones each. Because the FVIII yeast display did not undergo enrichment via flow sorting, it is expected that the overall percentage of FVIII specific VLRs would be lower than if the enrichment had taken place prior to plating for individual colonies. The modest shift of the population in Figure 6B,C compared to Figure 6A indicates binding of the yeast displayed VLR to the biotinylated lysate incubated with each yeast culture. In these results the binding is compared to the naïve yeast that was treated identically to the transformed yeast. Overall, these results indicate there are likely anti-FVIII VLRs in the yeast colonies selected and that the method established herein can be used to successfully generate immunogen-specific VLRs.

Figure 6

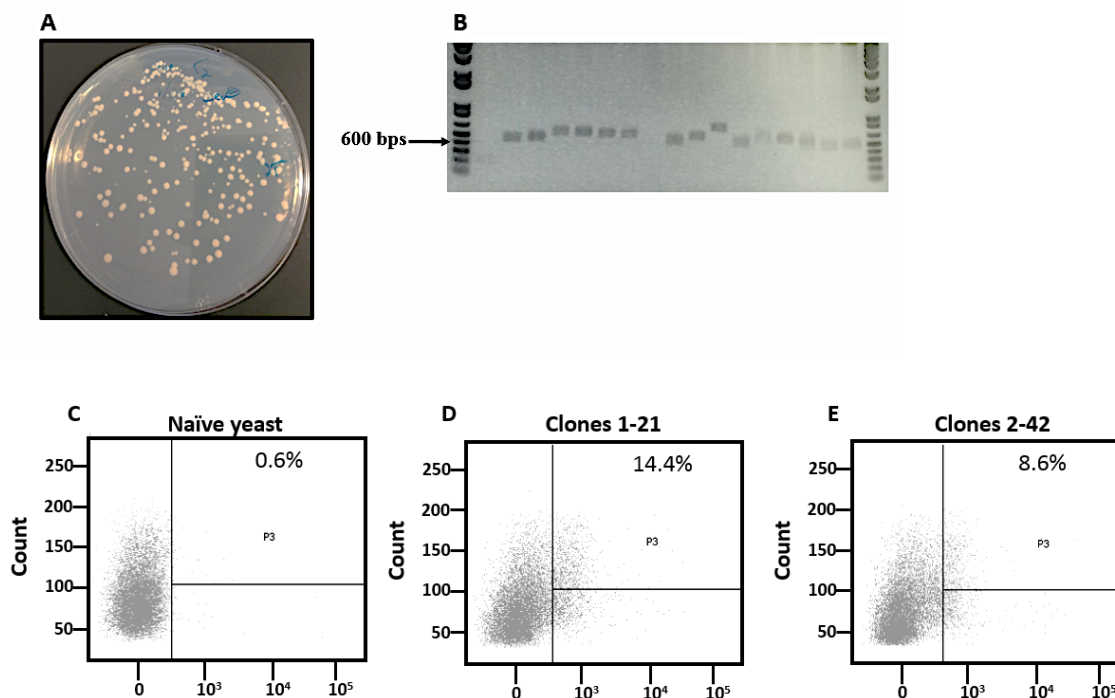


**Figure 6 Yeast display screening for anti-FVIII VLRs.** The VLR library amplified from FVIII immunized lampreys was cloned into a yeast expression vector (Figure 5) and transformed into naïve yeast. A. The transformed yeast was plated onto agar plates and 42 clones were selected and allowed to grow overnight in 5mL SDCAA media. B. PCR was used to confirm the presence of the VLR in the grown up yeast colonies. Depicted are the first 17 colonies of the 42 that were selected. Clones in which a VLR did not amplify were discarded and a new colony was picked. D. The first 21 clones selected from the transformed yeast were combined and screened for binding to biotinylated FVIII. E. This process was repeated by combining clones 21-42 and screening for binding to biotinylated FVIII. A. Naïve yeast that was also incubated with biotinylated FVIII and stained with anti-HA tag was included as a control. The results of the flow cytometry indicate positive binding of yeast colonies to the biotinylated FVIII in the two cultures containing transformed yeast but not the naïve culture.

### **Enrichment of SK-N-Be(2) binding VLRs**

Having established a successful method for immunogen specific VLR generation with both a purified protein and a cell line, the concentration of the next series of experiments focused exclusively on the screening and selection of anti-SK-N-Be(2) VLRs. To accomplish this, the yeast display library needed to be enriched for VLRs binding the SK-N-Be(2) cells line. The method for enriching the yeast, the results of which are shown in Figure 7, allows for yeast that are displaying a VLR to bind to the biotinylated SK-N-Be(2) lysate to be sorted. The process is accomplished by incubating the yeast displaying the polyclonal VLR library with biotinylated SK-N-Be(2) cell lysate and subsequent staining with anti-biotin and anti-VLR antibodies. Sorting via flow cytometry depicted in Figure 7B indicates the population of yeast that were sorted from the total transformed yeast population. Figure 7A shows the same process performed with VLRs from a naïve lamprey. The result of this process in the immunized lampreys is an enriched population of VLRs that have a confirmed ability to bind to the target cell lysate. Further refining of this process is conducted on individual yeast colonies using the same method of incubation with biotinylated SK-N-Be(2) cell lysate. The flow cytometry analysis from this process is displayed in Figure 7C. In these individual colonies, a positive binder to the desired antigen is shown as an increase in the population double positive for anti-biotin anti-VLR staining. The process of refining the yeast colonies to identify positive binders resulted in the selection of 10 clones from the original 20 that were assayed. The 10 clones identified as the strongest binders to SK-N-Be(2) cell lysate are indicated via arrows in Figure 7D.

Figure 7A

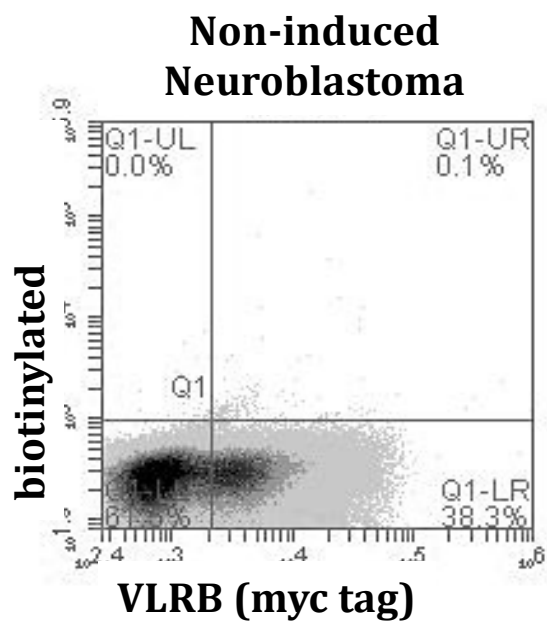


Figure 7B

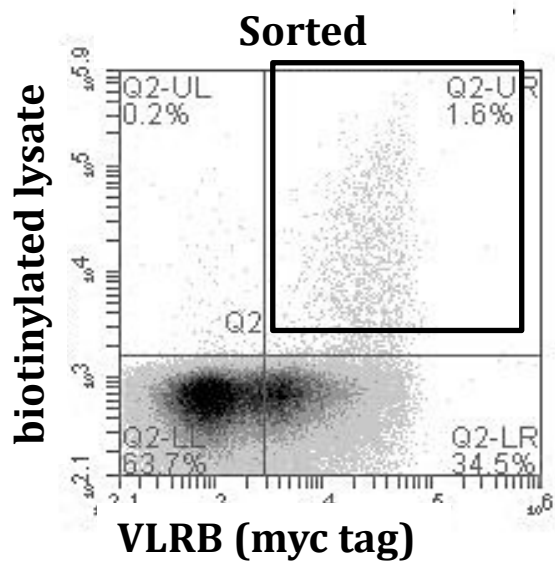


Figure 7C.

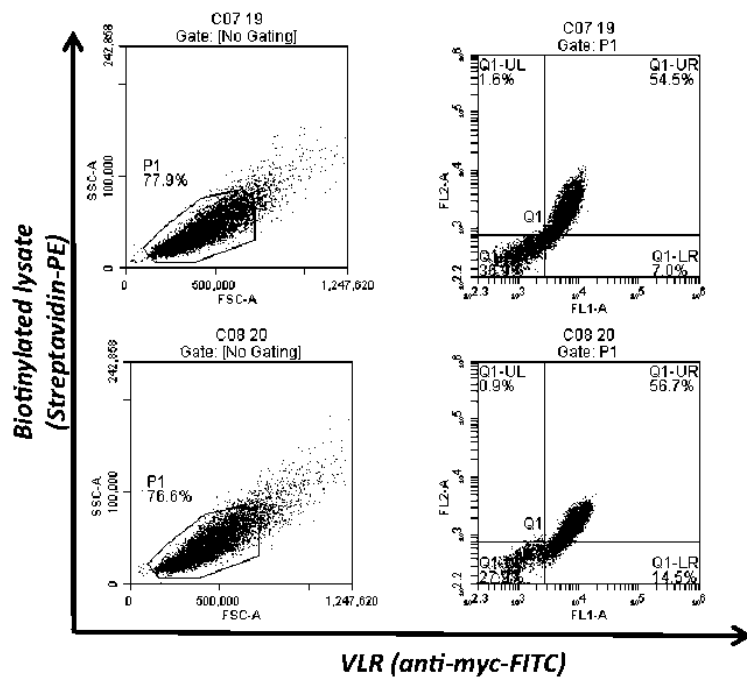
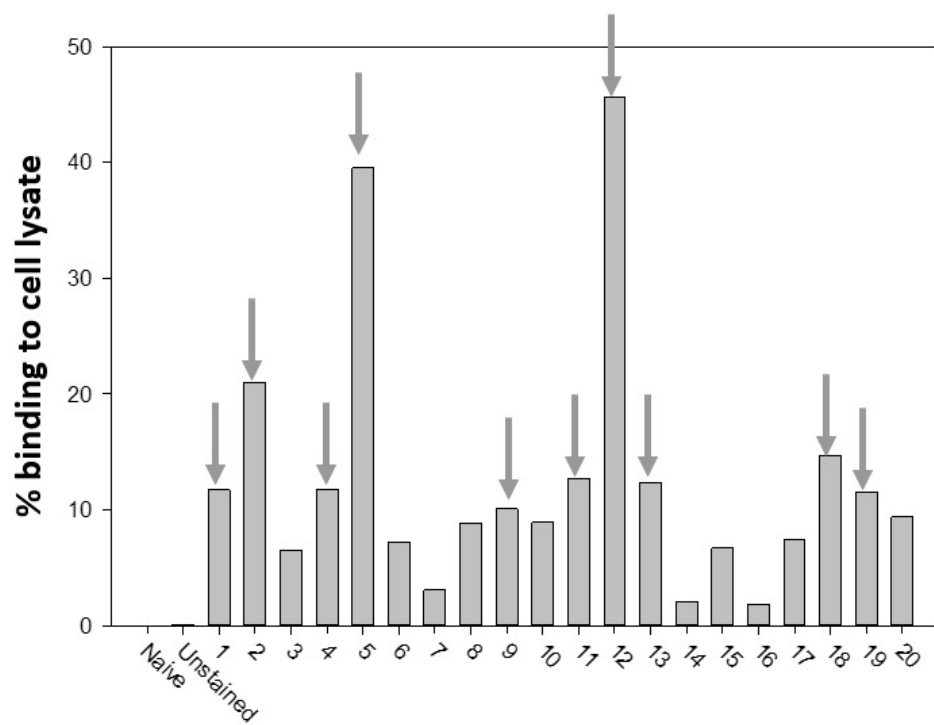


Figure 7D



**Figure 7. Sorting of the anti-SK-N-Be(2) VLRs** A. VLR transformed non-induced yeast library cultured with biotinylated SK-N-Be(2) cell lysate and stained with anti-biotin and anti-VLR antibodies. B. VLR transformed induced yeast cultured with biotinylated SK-N-Be(2) cell lysate and stained with anti-biotin and anti-VLR antibodies. The box indicates the yeast colonies binding the SK-N-Be(2) lysate. This population was sorted from the remaining population of yeast to enrich for binders to the SK-N-Be(2) cell line. C. The primary flow data used to select colonies for further screening. The monoclonal yeast populations obtained from plating the enriched yeast population from figure 7A were grown up and further screened against biotinylated SK-N-Be(2) cell lysate and stained with anti-biotin and anti-VLR antibodies. D. The process for screening individual colonies was repeated over 20 clones. This data is depicted in the graph with clones selected for further analysis indicated via an arrow.

**Sequencing of selected VLRs and annotation of results**

Following the selection of the top 10 VLR clones that bound the biotinylated SK-N-Be(2) lysate with the highest affinity, the VLRs were amplified from the yeast using primers directed against the VLR constant region. This allowed for amplification of only the VLR gene. Sequencing was conducted using a second downstream primer directed against the constant region of the VLR. Annotation of the results allowed for confirmation of the accuracy of the VLR sequences obtained from the sequencing run. This analysis was accomplished by comparing the known constant and conserved regions of the VLR sequence with the results obtained via sequencing. If the constant and conserved regions from the VLR did not correspond to the anticipated constant and conserved regions in the sequence, the process was repeated until the sequence obtained was determined to be accurate. The results of this annotation are depicted in Figure 8.

Figure 8

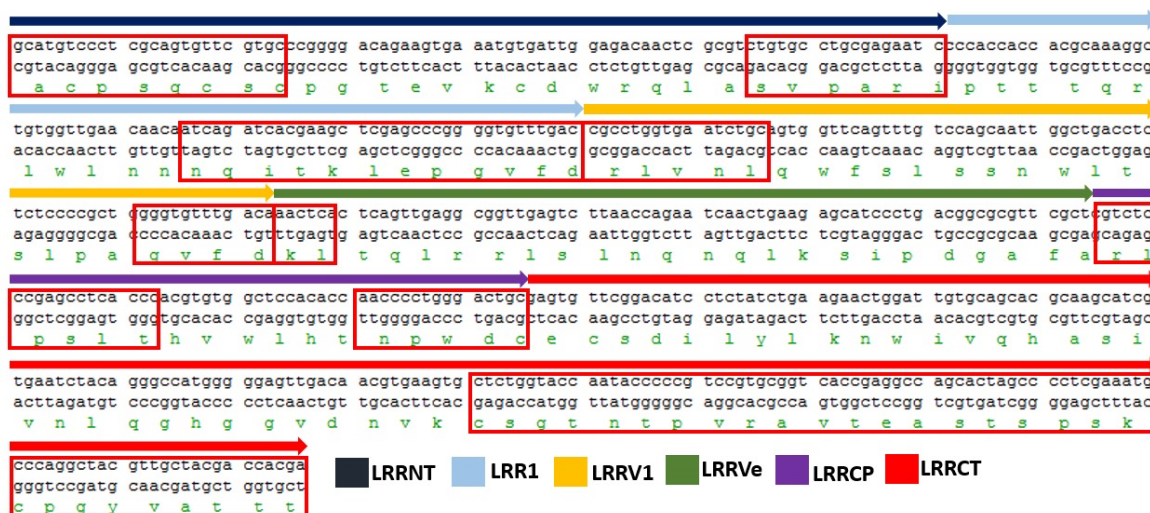


**Figure 8. Annotation of the VLR sequencing results** The complete VLR sequence obtained from PCR amplification of the VLR gene from the yeast display is depicted. Constant and conserved regions are boxed. The 6 regions of the VLR are indicated via shaded arrows. The arrangement is LRRNT, LRR1, LRRV1, LRRVe, LRRCP, and LRRCT.

## 2.4 Discussion

VLRs represent an alternative to immunoglobulin based adaptive immune response. As a receptor that can achieve binding avidities equal to that of its antibody counterpart, VLRs may hold many opportunities to expand the number of antigens that can be targeted through immune receptor engineering. Development of VLR technology involves the generation of antigen specific receptors through immunization of the lamprey and subsequent refining of the VLR pool to identify appropriate binding candidates. This process, outlined herein, has led to the identification of VLRs suggested to bind to the FVIII protein as well as VLRs shown to bind the neuroblastoma cell line SK-N-Be(2).

The VLRs generated against FVIII may prove to be relevant in research involving hemophilia A, as hemophilia A is a bleeding disorder that results from a defect in gene encoding the clotting cofactor FVIII. A valuable tool in the research into FVIII involves the use of anti-FVIII antibodies. These antibodies are useful in several research approaches including identification of FVIII in solution, inhibition of FVIII function, and purification of FVIII. There has been little previous development of the VLR as an alternative to antibodies for binding soluble proteins and, to date, none have been raised against the FVIII protein. The results, herein, indicate a process by which an anti-FVIII VLRs may be generated through lamprey immunization as well as the process by which the polyclonal pool of VLRs may be refined to identify binding partners to the FVIII molecule. The results indicate a positive immune response in the lamprey as well as the presence of FVIII in the lamprey plasma. Future progress should focus on the extraction of the VLR library and expression of the anti-FVIII VLRs in this a yeast display plasmid vector for production of an anti-FVIII VLR yeast library. Expression in the yeast strain would allow for the production of a VLR and yeast flocculation fusion protein displayed on the yeast cell surface. This yeast library could then be screened for binding to biotinylated FVIII molecules to enrich the population for FVIII binding VLRs through flow cytometry sorting. As the initial steps have been

accomplished and the method for screening and enriching an anti-FVIII VLR has been established, this project shows promise for the future refining and identification of anti-FVIII VLRs.

One of the major limitations to the progress of CAR therapy is the availability of cancer cell target antigens. A majority of current CAR trials have focused on a limited number of cell targets. The CAR trials that have been most successful have primarily targeted the cell surface antigen CD19. CD19 is present on all circulating mature B-cells and has provided a promising target in the treatment of B-cell non-Hodgkin lymphoma (NHL), acute lymphoblastic leukemia (ALL), and chronic lymphocytic leukemia (CLL) [90]. Although these trials have been successful in treating the respective cancer, CAR technology is still limited to targeting only a handful of cancer cell antigens [90]. Moving progress forward would require the identification of other potential targets that could be leveraged to improve the precision and applicability of CAR therapy. VLRs may provide a potential alternative to traditional immunoglobulin based antibodies. As mentioned previously, they can be generated with avidities equal to that of immunoglobulin as well as provide a potentially untapped method of antigen recognition [76]. One of the benefits provided by VLRs over antibodies is that VLRs have been previously shown to have a distinct binding profile to their target antigen. In studies seeking to identify the antigen epitopes contacted by antibodies and VLRs generated against the same antigen, VLRs bound separate epitopes that were not engaged by the antibody. The results also indicated that while antibodies typically bound flat, planar epitopes, VLRs were unrestricted by this preference [73]. Additionally, VLRs may broaden the antigen repertoire by binding antigens that would be unavailable to antibodies through the constraints of self-tolerance that are present when generating antibodies using a more typical mammal model. In this way, VLRs may expand the antigen-binding repertoire of the CAR and increase the potential for tumor cell targeting.

In the results presented herein, lampreys immunized with the neuroblastoma cell line SK-N-Be(2) showed an immune response and successful generation of VLRs directed against this target cell line. This process outlines a method by which lampreys can be successfully immunized with a cancer cell line to produce an immune response resulting in generation of antigen specific VLRs. With the validity of this process confirmed, the potential for VLR generation against a tumor cell line is established. The application of this method for VLR generation through lamprey immunization and subsequent enrichment for potential binders can then be used in future studies to identify VLRs specific to a larger assortment of tumor cells. Additionally, these receptors hold additional potential in CAR immunotherapy as they may replace the scFv on the CAR construct.

To move these studies forward, it would be necessary to identify the binding partners for the generated VLRs. For the anti-FVIII VLR, this would mean analyzing the FVIII domain to which the selected VLRs bind as well as determining their impact on FVIII function following binding. For the neuroblastoma cell line SK-N-Be(2), identifying the binding partner for both of the clones selected would allow for comparison with previously identified neuroblastoma antigens as well as determination of potential cross-reactivity with other cell types. If this process resulted in the generation of a VLR binding a unique antigen against which antibodies have yet to be developed, this could result in a method to potentially improve CAR therapy for treatment of neuroblastoma. Additional future developments could also focus on further identification of SK-N-Be(2) binding VLRs from the already established library, which can then be validated through the process outlined above and moved into a screening process. Overall, the data presented herein represent a promising step toward generation of VLRs to both a soluble protein as well as a cancer cell line, both of which hold potential relevance for future development in their respective fields.

Overall, these data suggest a method for lamprey immunization and identification of binding VLRs to a pre-specified antigen. The relevance of this approach is that the identified VLRs may

augment the potential pool of targetable antigens. For therapeutic proteins such as FVIII, this may allow for identification and production of VLRs that complement the contribution of antibodies to ongoing research. The immunization of lampreys with a tumor cell line such as SK-N-Be(2) provides a validated method for generating VLRs against a tumor cell line. The implication of this result is that these VLRs may be used to improve the ability to target tumor cells through identification of antigens or antigen epitopes previously unavailable to antibodies. The processes developed herein have successfully met milestones that improve the likelihood of their eventual success and potential applications in future research.

### Chapter 3

#### **The use of VLRs as the antigen recognition region of chimeric antigen receptors**

This research was published in *Molecular Therapy Oncolytics*.

Moot R<sup>1</sup>, Raikar SS<sup>2</sup>, Fleischer L<sup>1</sup>, Querrey M<sup>2</sup>, Tylawsky DE<sup>2</sup>, Nakahara H<sup>3</sup>, Doering CB<sup>4</sup>, Spencer HT<sup>4</sup>.

Genetic engineering of chimeric antigen receptors using lamprey derived variable lymphocyte receptors.

*Molecular Therapy Oncolytics*, 2016. **3**: p. 16026

1: Department of Molecular and Systems Pharmacology, Graduate Division of Biological and Biomedical Sciences, Emory University School of Medicine, Atlanta, Georgia, USA.

2: Department of Pediatrics, Aflac Cancer and Blood Disorders Center, Emory University School of Medicine, Atlanta, Georgia, USA.

3: Department of Pathology and Laboratory Medicine, Emory University School of Medicine, Atlanta, Georgia, USA.

4: Department of Molecular and Systems Pharmacology, Graduate Division of Biological and Biomedical Sciences, Emory University School of Medicine, Atlanta, Georgia, USA; Department of Pediatrics, Aflac Cancer and Blood Disorders Center, Emory University School of Medicine, Atlanta, Georgia, USA.

**Abstract**

CARs are used to redirect effector cell specificity to selected cell surface antigens. Using CARs, antitumor activity can be initiated in patients with no prior tumor specific immunity. Although CARs have shown promising clinical results, the technology remains limited by the availability of specific cognate cell target antigens. To increase the repertoire of targetable tumor cell antigens we utilized the immune system of the sea lamprey to generate directed variable lymphocyte receptors (VLRs). VLRs serve as membrane bound and soluble immune effectors analogous but not homologous to immunoglobulin. They have a fundamentally different structure than immunoglobulin (Ig)-based antibodies while still demonstrating high degrees of specificity and affinity. To test the functionality of VLRs as the antigen recognition domain of CARs, several VLR-CARs were created. One contained a VLR specific for a murine B-cell leukemia, another contained a VLR specific for the human T cell surface antigen, CD5, and the final VLR CAR was generated against the neuroblastoma cell line SK-N-Be(2). The CAR design consisted of the VLR sequence, myc-epitope tag, CD28 transmembrane domain, and intracellular CD3 $\zeta$  signaling domain. We demonstrate proof of concept, including gene transfer, biosynthesis, cell surface localization, and effector cell activation for multiple VLR-CAR designs. Therefore, VLRs provide an alternative means of CAR-based cancer recognition.

**3.1 Introduction**

CARs provide a method by which immune effector cells can be redirected to recognize specific antigens displayed on tumor cells in a process that is not reliant on the major histocompatibility complex [56, 58, 91, 92]. Since its inception over 25 years ago, CAR technology has had significant advancements, culminating in the breakthrough success of CAR T-cell targeting of the B-cell specific antigen, CD19, in several B-cell lymphomas [63, 64, 66, 93]. With CAR therapy expanding rapidly in its application and design, there is a growing need to increase the number and variety of tumor cell targets available for CAR recognition. There remain difficulties,

however, in the identification and implementation of antibodies against these new tumor cell antigens as studies have revealed significant unintended effects. Many of these side effects arise from either CARs acting off-target, recognizing an antigen or protein similar to the intended target, or on-target but off-tumor, where the target antigen is also found on other, non-tumor cells [55, 60-66]. Thus, improving the impact of CAR technology requires the identification and utilization of a larger repertoire of antigen binding elements, as the majority of successful CAR trials have made use of only a handful of CAR targets. As a means of increasing the potential repertoire of antigens that may be recognized using a CAR complex, we proposed the use of VLRs as the antigen binding domain [67-69, 76, 78]. The advantages of VLRs specifically for CAR technologies are multifaceted including (i) their single chain nature, which enables one-step cloning/screening using any available high throughput surface expression technology, (ii) the evolutionary distance between human and lamprey self-proteins, which presumably facilitates greater diversity in antigen recognition due to a lower degree of self-tolerance based inhibition, and (iii) their unique geometry, which enables distinct binding interaction compared with binding through scFvs. Collectively, these properties provide a platform by which the antigen binding elements of the CAR complex can be expanded to encompass a unique array of clinically-relevant antigens [94].

VLRs, are the primary effector of the adaptive immune system in jawless vertebrates, of which the only two extant species are the lamprey and hagfish. As mentioned, the use of the VLR as the antigen recognition region of the CAR can provide an alternative method that may allow for CAR directed targeting of antigens typically unavailable to immunoglobulin based antibodies. The studies herein used VLRs, directed against three different antigens. The neuroblastoma cell line SK-N-Be(2) was selected to demonstrate the efficacy of the process for generating the VLR library through immunization of the lamprey as well as the method for screening and selecting a VLR capable of binding the SK-N-Be(2) cell line. To provide poof-of-principle data indicating

the VLR was capable of directing CAR activity. A VLR directed against the B-cell receptor of the mouse tumor cell line BCL was used. The target and activity of this VLR had previously been verified and, as such, it provided an appropriate VLR to begin testing the activity of the VLR CAR in effector cells. The final VLR tested was directed against the human CD5 receptor. This VLR provided further evidence of VLR CAR efficacy as well as additional validation the VLR as could function as the antigen recognition region of the CAR through recognition of a third cell surface target.

### **3.2 Materials and methods**

#### **Cell lines**

Jurkat, BCL1-3B3 (BCL), and CCRF-CEM cell lines were obtained from American Type Culture Collection (ATCC, Manassas, VA). The 697 B-ALL cell line was kindly provided by Douglas Graham (Aflac Cancer Center, Atlanta, GA). The primary culture media for the Jurkat, BCL1-3B3 (BCL), CCRF-CEM, and 697 cell lines was Roswell Park Memorial Institute (RPMI) (Corning, Manassas, VA) with 10% fetal bovine serum (FBS) and 1% penicillin/streptomycin. For NK-92 cells, AIMV (Thermo Fisher Scientific, Waltham, MA) was used with 20% FBS, 1% penicillin/streptomycin and 1,000 U/ml recombinant IL-2 (Peprotech, Rocky Hill, NJ) [95].

#### **Cloning the BCL VLR-CAR sequences**

VLR sequences identified as being potential binders to the SK-N-Be(2) cell line via the yeast surface display were sent in for synthesis of corresponding gene fragments (IDT, G-block) . Upon arrival, the gene fragments were cloned into a second generation CAR construct. The construct selected contained the human ubiquitin C promoter, a GFP sequence used for identification of the positively transduced cells, a P2A sequence which allows for co-expression of the CAR construct and the GFP protein, the IL-2 signal sequence, the selected neuroblastoma VLR sequence, a

CD28 region, and the CD3-  $\zeta$  internal signaling domain. Each neuroblastoma VLR CAR was then sequenced to ensure accuracy and used to produce high titer lentivirus.

The BCL-VLR sequence was obtained from the laboratory of Max Cooper (Emory University, Atlanta, GA). The CD5 VLR cDNA sequence was generated from a published protein sequence of a VLR targeting CD526 and then codon optimized for human cell expression. The VLR sequence was then cloned into a vector containing the remaining necessary components for CAR production, which were obtained by gene synthesis from Genewiz (South Plainfield, NJ)[95].

### **Generation of VLR-CAR encoding lentivirus**

Recombinant HIV lentivirus was produced using a four plasmid system. Briefly, the expression plasmid encoding the VLR-CAR constructs as well as packaging plasmids containing the gag, pol, and envelope genes were transiently transfected into HEK-293T cells by calcium phosphate transfection. Cells were cultured in Dulbecco's modified essential medium (DMEM, Thermo Fisher Scientific) supplemented with 10% FBS and 1% penicillin– streptomycin. Twenty-four hours after transfection, the cell culture medium was replaced with fresh medium. At 48, 72, and 96 hours the viral supernatant was collected, filtered through a 0.22  $\mu$ m filter and stored at  $-80^{\circ}\text{C}$ . After the final virus collection, the supernatant was pooled and concentrated overnight via centrifugation at 10,000 x g at  $4^{\circ}\text{C}$ . Pelleted virus was then resuspended in StemPro media (Thermo Fisher Scientific). Titering was performed on HEK-293T cells using quantitative polymerase chain reaction. Titer of the concentrated virus was found to be  $\sim 1 \times 10^8$  TU/ml [95].

### **Lentiviral transduction of cell lines**

Transduction of recombinant HIV lentiviral particles was carried out by incubating cells with virus in appropriate culture medium supplemented with 6  $\mu\text{g/ml}$  polybrene (EMD Millipore, Billerica, MA). Twenty-four hours after transduction, culture medium was replaced with fresh

medium. The transduced cells were then cultured for at least 3 days before being used for downstream applications [95].

#### **Western blotting with CD3 $\zeta$ antibody**

Cells were lysed using radioimmunoprecipitation assay buffer (SigmaAldrich, St. Louis, MO). Cell lysates were clarified by centrifugation and protein was quantified using the Pierce BCA Protein Assay Kit (Thermo Fisher Scientific). Equal quantities of protein were loaded and cell lysates were separated by sodium dodecyl sulfate–polyacrylamide gel electrophoresis (SDS-PAGE) under reducing conditions and transferred to a nitrocellulose membrane (Bio-Rad Laboratories, Hercules, CA). The protein-loaded and blocked membrane was incubated with an anti-CD3- $\zeta$  mAb (1:500) followed by a horse radish peroxidase (HRP)-labeled goat anti-mouse secondary Ab (1:2500) (BioLegend, San Diego, CA) [95].

#### **Flow cytometry analysis and sorting**

Analysis was done using a BD fluorescence-activated cell sorting (FACS) Canto II Flow Cytometer and BD LSRII Flow Cytometer (BD Biosciences, San Jose, CA). Data was analyzed using the BD FACSDiva software. Antibodies used included anti-CD69 APC-Cy7, anti-CD5 PerCP/Cy5.5, antihuman CD45 PE (BD Biosciences) and anti-myc tag fluorescein isothiocyanate (FITC, Abcam, Cambridge, MA). For the cytotoxicity studies, target cells were stained with the membrane dye PKH26 and cell death was assessed using 7-AAD (described below). Flow sorting for GFP was performed using a BD FACS Aria II Cell Sorter (BD Biosciences) [95].

#### **Expansion and lentiviral transduction of primary human T cells**

Commercially available human peripheral blood mononuclear cells were purchased (AllCells, Catalog # PB004F, Alameda, CA). After thawing and washing, a pan T-cell isolation was performed using the manufacturer's recommendations (MACS Catalog #: 130-096-535, Miltenyi

Biotec, San Diego, CA). Cells were then incubated with activation/expansion beads (MACS Catalog #: 130-091-441, Miltenyi Biotec) and cultured for 24 hours after which 100 U/ml IL-2 was added. Cells were stimulated with beads and IL-2 for 3 days prior to transduction. For transduction,  $2 \times 10^6$  T-cells were plated in complete RPMI with IL-2 in each well of a 6-well plate. Virus (300  $\mu$ l) was added at an MOI of  $\sim 20$ . Media was changed after 24 hours and the cells were replated and transduced for the second time. Twenty-four hours after the second transduction, the media was changed to complete RPMI and IL-2 was added at 100 IU/ml. The cells were then allowed to expand for 12 days [95].

#### **Co-culture assay using Jurkat and BCL cells**

The co-culture assay was performed by incubating 50,000 transduced or naive Jurkat cells in a 1:1 ratio with the target BCL cells. This culture was incubated for 4 hours at 37°C and then stained using antibodies for human CD45, the myc epitope tag, and CD69. Cells were then analyzed via flow cytometry to determine levels of activation in the transduced and naive cell groups. Cytotoxicity assay Target cells were labeled with membrane dye PKH26 using the manufacturer's protocol (Sigma-Aldrich). Effector cells were left unstained. Effector (E) and target (T) cells were counted and viability assessed using trypan blue. Labeled target cells were mixed with effector cells in 12 $\times$ 75mm FACS tubes or round bottom 96-well plates at E:T ratios ranging from 0:1 to 20:1 in a total volume of 200  $\mu$ l. Target cells (20,000) were plated per tube/well along with the corresponding number of effector cells. The cell mixture was incubated for 4 hours at 37°C in 5% CO<sub>2</sub>. After incubation, cells were washed and stained with 7-AAD (BD Biosciences). Flow cytometry analysis was then performed to assess 7-AAD positive cells. All experiments were performed in triplicate. To calculate specific cytotoxicity, the number of spontaneously lysed target cells in the absence of effector cells was subtracted from the number of dead target cells, which were identified as PKH26 and 7-AAD double positive in the measured sample [95].

### **Statistical analysis**

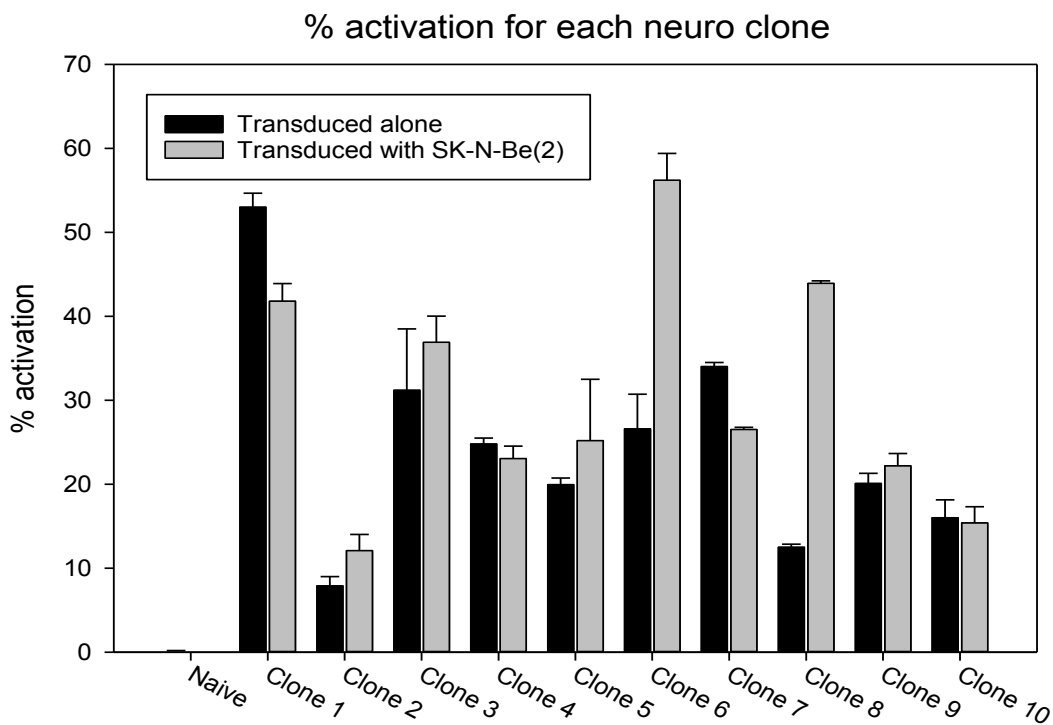
Unpaired two-tailed Student's t-test was used to determine statistical significance. All P-values were calculated with SigmaPlot, version 13.0 (Systat Software, Chicago, IL) [95].

### **3.3 Results**

#### **High-titer lentivirus was created from the VLR CAR constructs and Jurkat cells were transduced then co-cultured with SK-N-Be(2) to show activation**

The high-titer lentivirus created using each neuroblastoma VLR CAR construct was used to transduce Jurkat cells. Jurkat cells were selected as they offer an easily transduced cell type in which CAR activity can be assessed via upregulation of CD69 expression on the cell surface. Following transduction, CAR expression was confirmed by observing GFP expression in the transduced cell types. In each of these transductions, GFP expression was observed to be higher than 50% (data not shown). As a way to determine which VLR clones would most effectively direct the CAR effector cells to the target SK-N-Be(2) cells, a co-culture assay was used. In this assay, effector and target cells are cultured together with the expectation that exposure of the effector cell to the cognate antigen on the target cell surface will result in activation. To apply this assay, transduced Jurkat cells were then either cultured alone or co-cultured with SK-N-Be(2) cells. The transduced Jurkat cells cultured alone provide a background activation level to which the transduced Jurkat cells cultured with the target SK-N-Be(2) cells can be compared. The need for a baseline activation level in the transduced cells is based on the observation that activation occurs in the Jurkat cells following transduction as well as the possibility that the VLR is directing the CAR against an antigen that is common to both the SK-N-Be(2) cells and the Jurkat cell. The results obtained from the co-culture assay demonstrate which VLR sequences can appropriately target the CAR expressing effector cell to recognize the SK-N-Be(2) cell line. From the results in Figure 1, two clones of the 10 assayed showed a significantly increased activation in

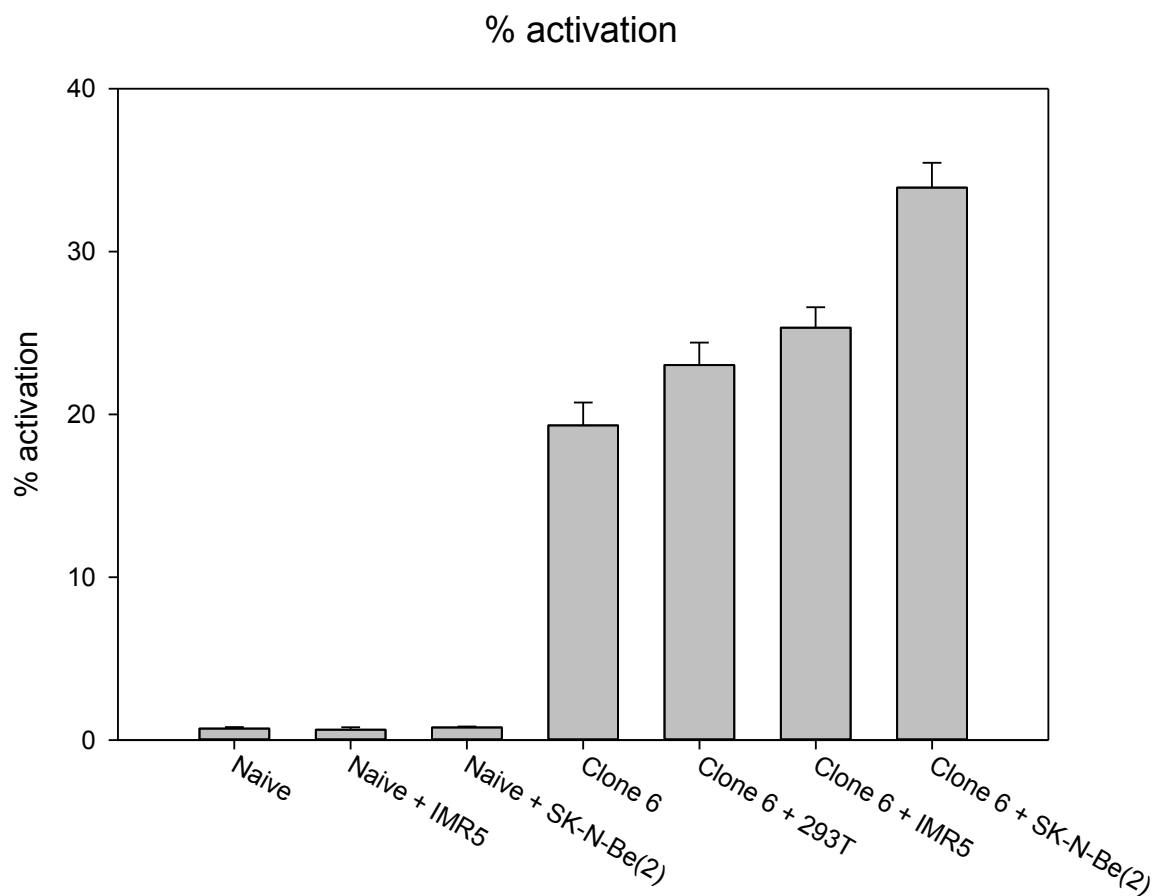
the effector Jurkat cells over the background activation in transduced Jurkat cells cultured alone. Clone 6 showed an increase in activation of approximately 2.5-fold while clone 8 showed an increase in activation of around 3-fold. The remaining clones did not activate significantly above baseline. Based upon these results, clones 6 and 8 were expanded for further investigation.

**Figure 1**

**Figure 1. Screening VLR-CAR constructs** Jurkat cells were transduced with lentivirus containing 10 different anti-SK-N-Be(2) VLRs in a CAR construct. The transduced cells were then screened for activation against SK-N-Be(2) cells in a co-culture assay. The graph shows percent activation as measured by upregulation of CD69 via flow cytometry.

**Clone 6 was selected for further testing and showed moderate improvement in activation level against baseline.**

As the initial co-culture assay indicated Jurkat cells expressing clone 6 were activated preferentially when cultured with the target cells, they were selected for further testing. To better determine the ability of the clone 6 VLR to direct Jurkat cells specifically against the target SK-N-Be(2) cells and not other cell types, Jurkat cells transduced with the clone 6 VLR CAR construct were co-cultured with a larger array of cell types. The purpose of this was to provide evidence that the clone 6 VLR can distinguish between these cell types and SK-N-Be(2) cells. The cell types included were IMR5 cells, HEK 293 cells, and, as a comparison, additional screening against the target SK-N-Be(2) cells. IMR5 cells are another neuroblastoma cell type that may express many of the same cell surface antigens as SK-N-Be(2) cells. HEK 293 cells were selected because they are believed to be derived from a similar origin as the SK-N-Be(2) cells. The results from this assay indicated a modest but still statistically significant improvement in activation over baseline in the Jurkat cells co-cultured with the intended target, SK-N-Be(2) cells (Figure 2). Of the other cell types assayed, co-culture with IMR5 showed the second largest increase in activation above baseline. This was followed by HEK 293 cells. Each was significantly increased above naïve Jurkat cells co-cultured with each target cell type. Based upon the only modest increases observed in activation of the clone 6 VLR CAR expressing Jurkat cells over both baseline and the other assayed cell types, it was determined another clone should be considered to potentially improve upon the specificity of target cell binding.

**Figure 2****Figure 2. Screening of clone 6 anti-SK-N-Be(2) VLR via co-culture assay.** Lentivirus

containing the clone 6 VLR-CAR construct was used to transduce Jurkat cells. The graph shows the results of a co-culture assay in which Naïve cells were cultured alone or with IMR5 or SK-N-Be(2), Clone 6 VLR-CAR expressing cells were cultured alone or with 293T, IMR5, or SK-N-Be(2).

**Clone 8 was selected for further testing and showed significantly increased activation compared to baseline**

Although clone 6 VLR CAR transduced Jurkat cells showed a significant increase in activation above the other cell types assayed, a more significant improvement in activation level is desirable. Because of this, Clone 8 was also investigated as a potential candidate VLR for targeting the SK-N-Be(2) cell line. This was accomplished using a similar assay as was used with clone 6. In this assay, Jurkat cells transduced with the clone 8 VLR CAR construct were co-cultured with a more extensive array of cell types. These cell types include K562, U937, as well as SK-N-Be(2) as a comparison. The results of this assay would indicate any potential cross reactivity of the clone 8 VLR with other cell types. The flow diagram obtained from the co-culture assay is depicted in Figure 3A,B and shows a significant response of the transduced Jurkat cells to co-culture with SK-N-Be(2) cells. The Jurkat cells cultured alone show little activation. When co-cultured with SK-N-Be(2) cells, the population shifts, indicating upregulation of CD69 expression, which correlates with activation. The results of the co-culture are depicted graphically in Supplementary Figure S1, which shows the percentage of total cells in the culture that have been activated following co-culture with SK-N-Be(2) cells. In Figure 3C, the data is adjusted to show only the percentage of gene modified cells that are activated following co-culture. This is a more appropriate method by which to evaluate the results as it discounts the Jurkat cells that are not expressing the CAR and can therefore not activate in the presence of the target cells. The results indicate a significant increase in activation in clone 8 VLR CAR expressing Jurkat cells when co-cultured with SK-N-Be(2) cells. Activation seen in the total cell population increases by approximately 4-fold in Jurkat cells co-cultured with SK-N-Be(2) cells over other cell types. Adjusting to account for only gene modified cells increases the observed effect with an approximate 7-fold increase in activation in the Jurkat cells co-cultured with SK-N-Be(2) cells over all other cell types assayed. The results indicate that the clone 8 VLR may be specific for a cell surface protein expressed primarily on SK-N-Be(2) cells.

**Clone 8 was further screened against SK-N-Be(2) cells, IMR5 cells, and HEK 293T cells**

The clone 8 VLR CAR has shown initial promise as it specifically activates Jurkat cells in the presence of only the target SK-N-Be(2) cells. As a way to further determine the specificity of the clone 8 VLR, Jurkat cells expressing the clone 8 VLR CAR were assayed against cell types of similar origin to the SK-N-Be(2) cell line. These cell types include IMR5 and HEK 293 cells. The results from this co-culture assay are depicted in Figure 3C and indicate the antigen recognized by the clone 8 VLR may be common to these two cell types tested. Although the VLR CAR Jurkat cells do not show specific recognition of the SK-N-Be(2) cells when compared to these other two cell types, it is reasonable to expect these cell types all share common antigens that may not be present on other, more varied cell types. The reason IMR5 cells would have a similar cell surface antigen profile to SK-N-Be(2) cells is that both of these cell type are originally derived from a neuroblastoma tumor. HEK 293 cells are also believed to share a similar origin. In previously reported findings, there are 22 genes that are heavily upregulated in both hematopoietic and neuronal stem cells that have also been found to be highly upregulated in HEK 293 cells. Additionally, there are very similar mRNA expression profiles between HEK 293 cells and stem cells. From this data, the investigators reporting the study concluded that there is clearly, a set of identical or very similar proteins that are strongly expressed in both the HEK 293 cells as well as the various stem cells, also noting that this conclusion is consistent with the view that 293 cells resemble developing neurons and neuronal stem cells. There have also been further studies showing migrating neural crest cells in the kidney which go through apoptosis later in development [96]. From these results, it would be reasonable to assume that HEK 293 cells may share a common expression profile of cell surface antigens and that although the clone 8 VLR CAR targeted both of these cell types, the antigen targeted may not also be on other, more common cell types.

Figure 3A

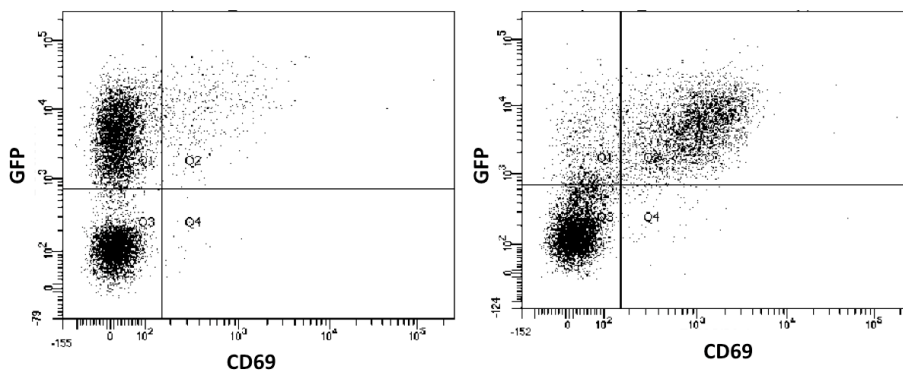


Figure 3B

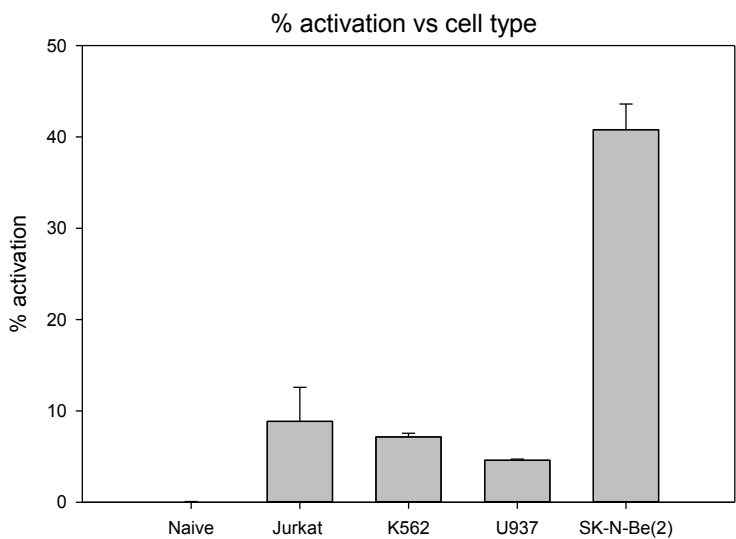
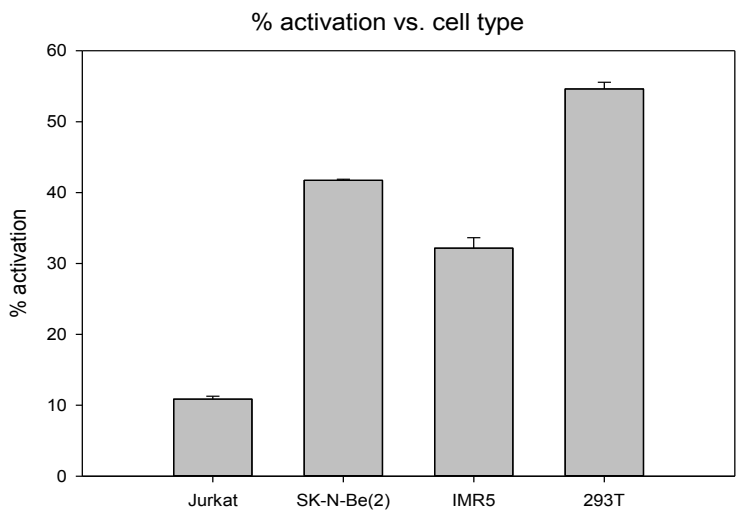


Figure 3C



**Figure 3. Screening clone 8 anti-SK-N-Be(2) VLR in a CAR construct** A. Primary flow cytometry data showing a comparison between clone 8 VLR-CAR expressing Jurkat cells cultured alone and cultured with SK-N-Be(2). The y-axis represents GFP expression and the x-axis represents CD69 upregulation. B. The results of the co-culture assay of clone 6 VLR CAR expressing Jurkat cells cultured alone and co-cultured with the cell types K562, U937, and SK-N-Be(2). C. The results of a co-culture assay of clone 6 VLR-CAR expressing Jurkat cells cultured alone and co-cultured with SK-N-Be(2) cells, IMR5 cells, and 293T cells.

**Construction of the lamprey VLR-based CARs containing VLRs directed against the B-cell receptor of a mouse B-cell leukemia cell line and the human CD5 cell surface protein.**

To generate the next two CAR constructs, sequences were used for a VLR previously shown to be specific for the B-cell receptor of the mouse tumor cell line, BCL (BCL1-3B3), and a VLR shown to be specific for the human T-cell surface protein CD5. The BCL VLR is 600bp and contains one LRR in the LRRV element. The sequence for the CD5 VLR was generated using the previously published protein sequence, and the cDNA sequence designed to express the VLR was codon optimized for human cell expression [77]. The portion of the VLR sequence used in our CAR constructs spanned from the beginning of the LRRNT element and included all sequences through the LRRCT element (Figure 4A). The same portion of the CD5 VLR sequence was used and totaled 573 bps. The two VLR sequences were cloned into the CAR construct as shown (Figure 4B,C). The CAR cassette was a second generation CAR composed of an N-terminal interleukin-2 (IL-2) signal peptide followed by the VLR antigen binding domain, a myc tag for cell surface identification, the transmembrane and intracellular domains of CD28, and the intracellular signaling domain of CD3 $\zeta$  [95].

Figure 4

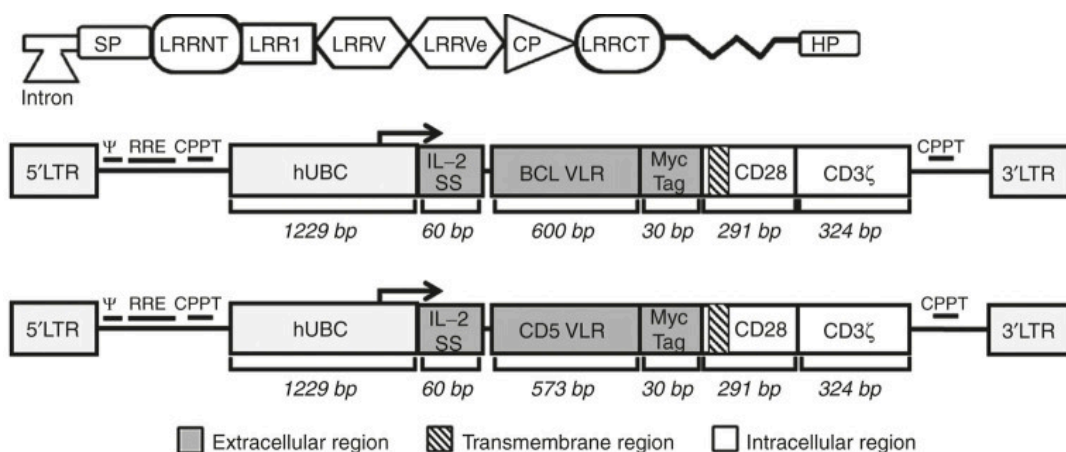


**Figure 4. Schematic of CAR structures containing the BCL or CD5 VLR and the structure of the mature VLR gene.** A. A depiction of the mature *VLR* gene which is assembled from a series of leucine rich repeat (LRR) cassettes spliced from the germ line cell to the mature B-like cell in a combinatorial fashion. SP, signal peptide; LRRNT, N-terminal leucine-rich repeat; LRRV, variable leucine-rich repeats; LRRVe, end leucine-rich repeat; CP, connecting peptide; LRRCT, C-terminal leucine-rich repeat; HP - hydrophobic peptide. B. The structure of the BCL-CAR transgene includes a 5' long terminal repeat (LTR), human ubiquitin C promoter (hUBC), an interleukin-2 signal peptide (IL-2 SP), the BCL VLR, a myc epitope tag, the CD28 region, the CD3- $\zeta$  intracellular domain and a 3' LTR. C. The structure of the CD5-VLR-CAR transgene.

### **VLR-CAR T-cell expression and antigen-specific activation**

High-titer, recombinant, self-inactivating lentiviral vectors encoding the anti-BCL and anti-CD5 VLR-CARs were generated (Figure 4B,C) at titers of  $\sim 1 \times 10^8$  HEK 293 transducing units (HEK-293 TU/ml) and used to transduce the Jurkat T cell line. Quantitative polymerase chain reaction confirmed the successful transduction of these cells. A dose response was observed whereby integrated proviral vector copy number increased directly with multiplicity of infection (MOI) up to a vector copy number of 21 at an MOI of 20 (data not shown). As a means to assess VLR-CAR protein expression in the transduced Jurkat cells, western blot analysis was performed on whole cell lysates. VLR-CAR protein was detected using an anti-CD3- $\zeta$  antibody. Proteins of  $\sim 47$  and  $48$  kDa were observed, which correspond to the predicted sizes of the anti-BCL (Figure 5A) and anti-CD5 (Figure 5D) VLR-CARs, respectively, as well as an  $18$  kDa band, which corresponds to the molecular weight of the endogenously expressed CD3- $\zeta$  protein known to be expressed in the Jurkat cell line. To confirm the cell-surface expression of the anti-BCL VLR-CAR, transduced Jurkat cells were stained with an anti-myc antibody, allowing for CAR detection by flow cytometry (Figure 5B). The BCLVLR-CAR was expressed on the surface of the transduced cells and showed a dose dependent response to vector MOI. The transduced cells also showed persistent surface CAR expression for at least 3 months, with cell viability remaining over 85% (Supplementary Figure S2 and Figure 5F), demonstrating the durability of the VLR-CAR expression [95].

Figure 5

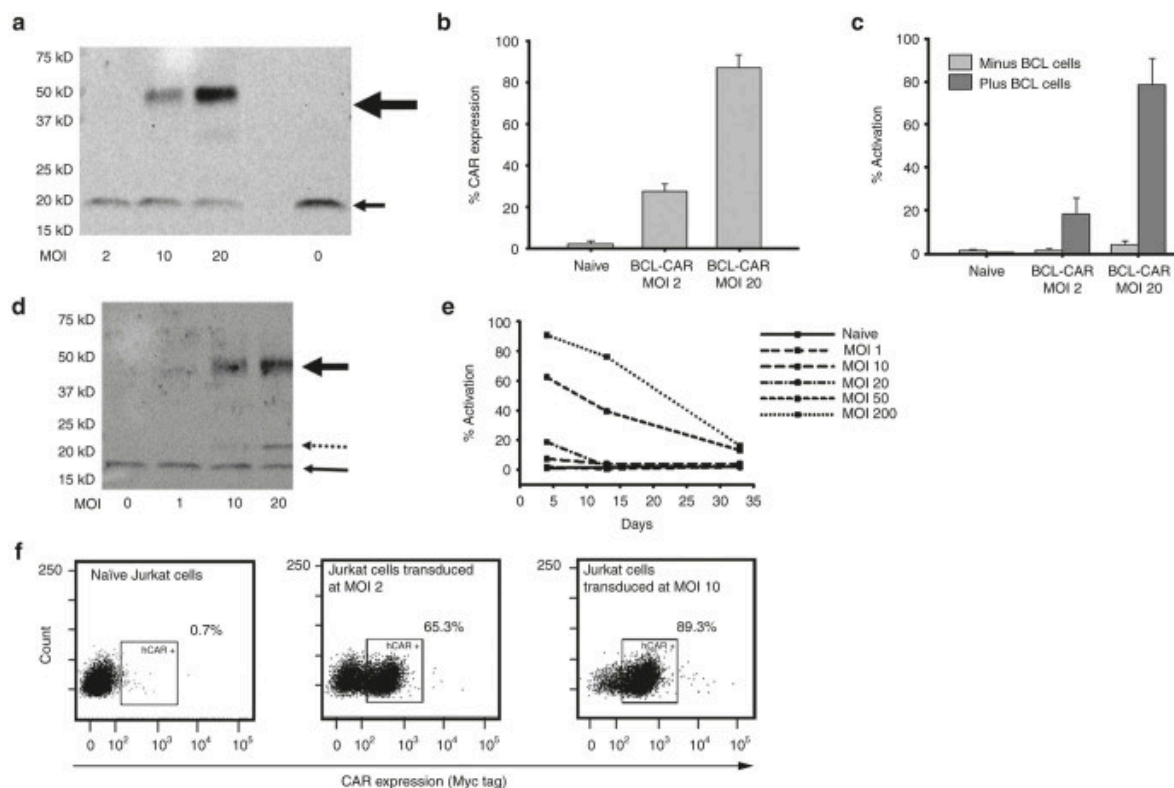


**Figure 5. VLR-CAR expression and activation of Jurkat cells when co-cultured with cells expressing the target antigen A.** Western blot using anti-CD3- $\zeta$  antibody showing BCL-VLR-CAR protein expression in whole cell lysates of Jurkat cells transduced at MOIs from 2 to 20. The bold arrow shows BCL-VLR-CAR and the thin arrow shows endogenously expressed CD3- $\zeta$ . B. Flow analysis of myc expression on the surface of naive and transduced Jurkat cells at MOIs of 2 and 20. C. Flow cytometry analysis of activation (CD69 expression) in naive Jurkat cells and Jurkat cells transduced with BCL-VLR-CAR in the absence or presence of BCL cells. Naive and transduced Jurkat cells not co-cultured with BCL showed minimal activation. D. Western blot using anti-CD3- $\zeta$  antibody showing increased CD5-VLR-CAR expression with increasing MOI. The bold arrow shows CD5-VLR-CAR, the thin arrow shows endogenously expressed CD3- $\zeta$ , and the dashed arrow shows a possible breakdown product of the CD5-VLR-CAR, which is not

observed with the BCL-VLR-CAR. E. Increased activation is observed in Jurkat cells transduced at increased MOIs with the CD5-VLR-CAR, but activation subsequently decreases over time in all transduction conditions. F. VLR-CAR expression 35 days after transduction at MOIs of 0, 2, and 10. Values within the figures show the percentage of VLR-CAR positive cells.

Next, we assessed VLR-CAR functionality by demonstrating effector T cell activation following engagement of the VLR by the target antigen. First, BCL-specific VLR-CAR expressing Jurkat T cells were incubated with target BCL cells. Induction of CD69 expression mediated through the VLR-CAR was demonstrated with activation ranging ~20–80% of the total effector cell population, depending on the initial transduction MOI (Figure 5C and Supplementary Figure S3). Given their inherent surface expression of CD5, we hypothesized that anti-CD5-VLR-CAR expression in Jurkat T cells would result in activation of the transduced cells due to interaction with self or neighboring CD5 on Jurkat T cells. Cells were transduced at varying MOIs ranging from 1 to 200, and green fluorescence protein (GFP) lentivirus was used as a control. Again, western blot analysis using a CD3 $\zeta$  antibody demonstrated increasing CAR expression with increasing MOI (Figure 5D). To determine if CD5-VLR-CAR expression resulted in T cell activation, transduced Jurkat T cells were stained with the T-cell activation marker CD69 and analyzed by flow cytometry (Supplementary Figure S4). Increased activation of Jurkat T cells was observed after CD5-VLR-CAR transduction and the degree of activation was higher with increasing MOI (Figure 5E). No activation was observed in the GFP transduced control group (Supplementary Figure S4). Unlike BCL-VLR-CAR modified cells, the percentage of activated Jurkat T cells decreased over time and returned to baseline after ~5 weeks in culture (Figure 5E). During this time there was also a decrease in copy number, which correlated to the expected decrease in activation, as activated Jurkat cells expanded at a slower rate compared with non-activated cells (data not shown). Therefore, we speculate that this decrease in Jurkat T cell activation and vector copy number resulted from the faster division rate of non-modified versus modified (i.e., VLR-CAR expressing) cells and activation-induced cell death resulting from a continuous activation of the transduced cell population via self and neighboring CD5 interactions, neither of which were observed using the anti-BCL VLR-CAR or GFP-modified cells.

#### **VLR-CAR NK-cell effector cytotoxicity**

Although Jurkat T-cells are capable of CAR-based activation they do not possess cytotoxic effector functionality. Therefore, as a final proof of concept validation test for the VLR-CAR technology platform, next we examined their ability to direct selective effector cell recognition and killing of target cells expressing the cognate VLR antigen. For this study, the well characterized cytotoxic human NK cell line, NK-92, was used. NK-92 is an IL-2 dependent immortalized cell line that has maintained its cytotoxic capabilities [97]. These cells have been studied both preclinically, and now clinically as a stand-alone anticancer therapeutic [98, 99]. In addition, these cells do not display CD5 on their surface, which allows for expression of the CD5-VLR-CAR without self-activation and killing of transduced cells. Given the poor transduction efficiency of NK-92 cells (<10%), a construct incorporating a GFP P2A sequence was created (Figure 6A). This allowed for expression of both GFP protein and the CD5-VLR-CAR protein from a single transgene, which enabled selection of the CAR expressing NK-92 cell population by flow sorting. Initially, this construct was tested using Jurkat cells to confirm VLR-CAR expression and function. Modified Jurkat cells expressing the GFP-p2A-CD5-VLR-CAR construct showed a positive correlation between GFP expression and activation, thus verifying functionality of the new construct (Figure 6B and Supplementary Figure S5). By implementing this construct, we were able to generate a uniform population of anti-CD5 VLR-CAR expressing NK-92 cells by flow sorting for the GFP positive cells. After sorting, the percentage of GFP positive NK-92 cells increased from <5% to >95% (Supplementary Figure S6A). The VLR-CAR positive NK-92 cell population was then expanded in culture for several weeks and, in contrast to the genetically-modified Jurkat T cells, showed sustained GFP expression for a period of >40 days (Figure 6C). QPCR demonstrated an average of 2.3 transduced gene copies/cell in the sorted/expanded cells and western blotting confirmed CAR expression using a CD3- $\zeta$  antibody (Figure 6D). GFP<sup>+</sup>-selected, and thus CD5-VLR-CAR expressing, NK-92 cells were used to assess cytotoxicity against the CD5<sup>+</sup> T-ALL cell line, CCRF-CEM, which is representative of a common T-ALL with robust CD5<sup>+</sup> expression (Supplementary Figure S6B). To assess cytotoxic

potential, CD5-VLR-CAR NK-92 effector (E) cells were cultured with CCRF-CEM target (T) cells in varying E:T ratios. Cytotoxicity was determined via uptake of 7-AAD, a marker for cell death, into target cells that also were pre-labeled with PKH26 allowing for easy distinction from the GFP<sup>+</sup> effector cells (Figure 7A) [100]. This shift indicates a significant increase in cytotoxicity observed with the CD5-VLR-CAR expressing NK-92 cells compared with naive NK-92 cells, even at the lowest E:T ratios ( $P < 0.01$  for all cell groups) (Figure 7B). The observed percent killing increased with incubation time up to 24 hours (Figure 7C). As a negative control, CD5-VLR CAR expressing NK-92 cells were cultured with the CD5 negative B-ALL cell line, 697. No increase in target cell killing was observed with these cells (Figure 7D).

Figure 6

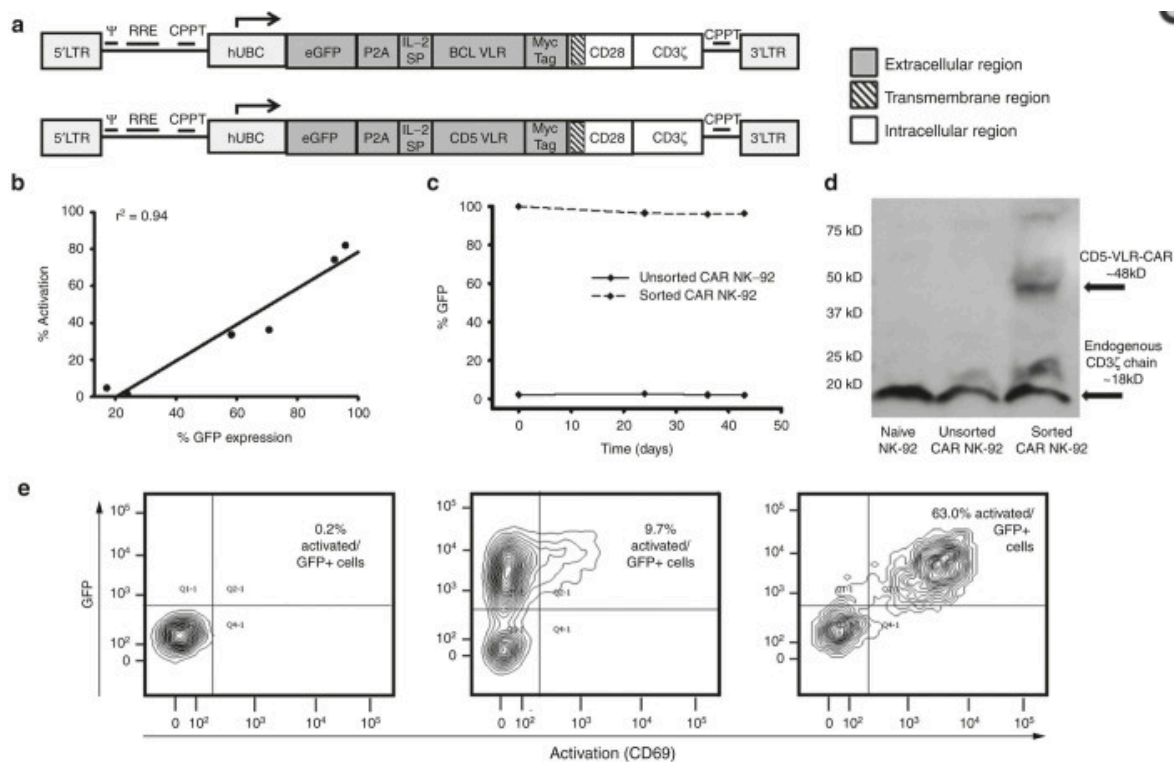


**Figure 6. Cassettes co-expressing GFP and VLR CARs show a correlation between expression and activation.** A. The eGFP P2A CAR construct with either BCL or CD5-VLR. B. Jurkat cells were transduced at various MOIs and a direct correlation between GFP expression and activation is observed in the eGFP P2A CD5-VLR-CAR transduced Jurkat cells, demonstrating dual expression of both proteins and activation of only VLR-expressing cells. C. NK-92 cells were transduced with the GFP-p2a-CD5-VLR-CAR and sorted for GFP expressing cells. The isolated and expanded cells were followed over time for GFP expression. D. Western blot using anti-CD- $\zeta$  antibody on whole cell lysates of NK-92 cells shows the presence of CD5-VLR-CAR protein in the sorted cells. E. Activation of eGFP P2A BCL-VLR-CAR transduced Jurkat cells when co-cultured with target BCL cells. Naive Jurkat cells showed no activation when co-cultured with BCL cells (left panel), cells modified but without co-culture showed

minimal activation (middle panel), and transduced cells co-cultured with BCL cells (right panel) showed robust levels of activation.

Figure 7

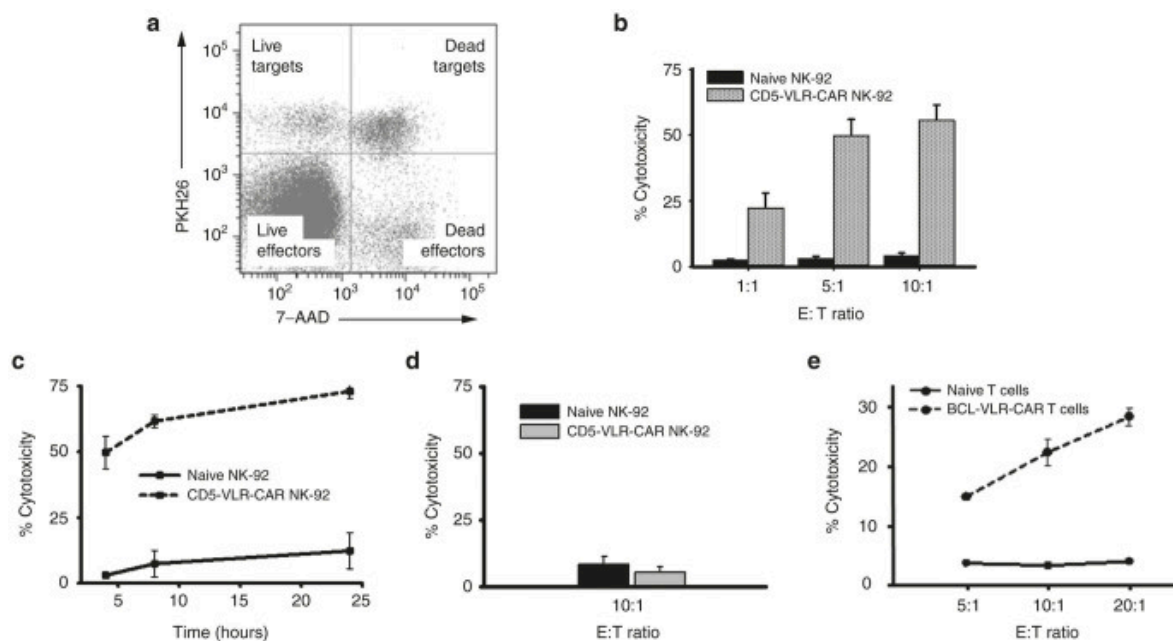


**Figure 7 BCL and CD5 VLR CAR constructs significantly increase the cytotoxic potential of effector cells when cultured with their target cells.** A. Representation of flow cytometry cytotoxicity assay using PKH26 and 7-AAD. Target cells were labeled with PKH26, while effector cells were unlabeled. Cell death was assessed using 7-AAD B. Transduced, sorted, and expanded NK-92 cells were co-cultured with CCRF-CEM cells. Significant increase in cytotoxicity ( $P < 0.01$ ) is observed against CD5-positive CCRF-CEM cells using CD5-VLR-CAR expressing NK-92 cells compared with naive NK-92 cells in a 4-hour assay. C. A cytotoxicity assay was performed over a 24 hours' time course using CD5-VLR-Car expressing NK92 cells and compared with naive cells, which demonstrates continued target cell killing over time at a 5:1 E:T ratio. D. No increase in cytotoxicity against CD5-negative 697 (B-ALL) cells is observed using CAR-expressing NK-92 cells compared with naive NK-92 cells. E. Cytotoxicity assay performed by co-culture of naive or BCL-VLR-CAR transduced primary T cells (E) and

target BCL cells (T) for 4 hours at various E:T ratios, which show increased killing at higher E:T ratios.

To demonstrate the ability of the BCL-VLR-CAR to direct target cell killing, a similar GFP-p2a-VLR CAR construct was generated (Figure 6A). GFP+/BCL-VLR-CAR expressing Jurkat T cells were not activated unless cultured in the presence of BCL cells (Figure 3E and Supplementary Figure S7). To extend these VLR-CAR effector cell line findings to primary human cells, we expanded CD3+ T cells from frozen peripheral blood mononuclear cells for 3 days prior to transduction with VLR-CAR encoding lentiviral vector at MOI of 20, twice on consecutive days. Assessment of cytotoxic potential again was determined by co-culture with BCL cell targets. Flow cytometric analysis showed a significant increase in target cell killing in the transduced T-cell culture compared with naive T cells, and this increase was observed for all E:T ratios tested (Figure 7E). These results show that CARs constructed using two different VLRs, one against a myeloid lineage and another one against a lymphoid lineage, effectively redirect immunocompetent cells to tumor associated antigens.

## Discussion

CAR technology is progressing at an extremely rapid pace and its applications are expanding quickly as new strategies are being applied to achieve tumor specific cell killing. The promising results in human trials involving CARs has fueled increasing interest in the technology and led to improvements in the design of CAR transgenes that have enhanced cell signaling as well as the lifespan of CAR-effector cells. A limitation persists in these approaches, however, as the types of tumor cell target antigens capable of being recognized by the CAR-effector cell still remains limited. Nearly all CAR designs thus far have employed scFvs as the antigen recognition region of the CAR. Our results provide proof of concept for a unique method of replacing the scFv with a VLR, thus increasing the number and diversity of targetable antigens. VLRs, as the functional unit of the lamprey adaptive immune system, allow for antigen engagement in a manner geometrically dissimilar to immunoglobulin, enabling the recognition of antigen epitopes not typically available to immunoglobulin. This results in an expanded selection of tumor cell target antigens/epitopes available for CAR design and application. VLR-CARs can be efficiently expressed on effector cells and are capable of redirecting the effector cells to recognize a specific target cell. Expression of the VLR-CAR on the effector cell improved target cell killing for both BCL directed and CD5 directed CARs. The results provided herein indicate a potentially unique and effective method for activating CAR-effector cells as well as a method by which the array of CAR targeting domains can be expanded.

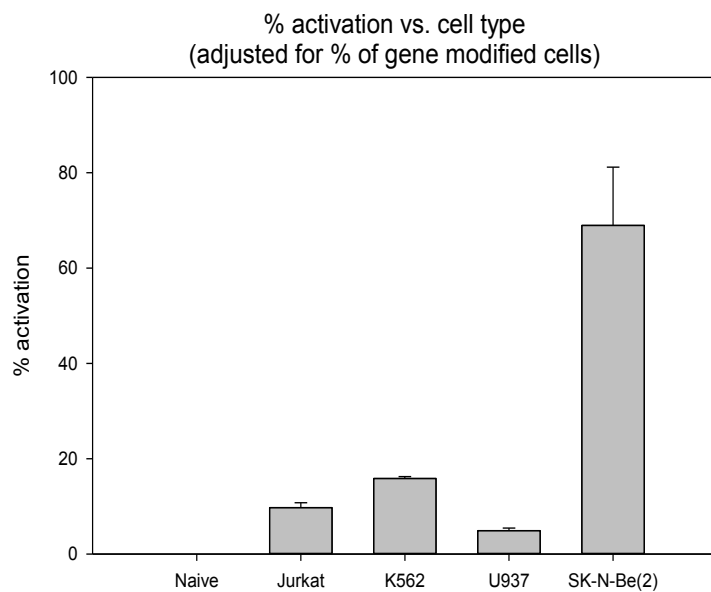
The VLR, as a component of immunity, arose in agnathans, jawless vertebrates, >500 million years ago. The only extant species known to use the VLR-based immune system are lampreys and hagfish. The VLR genes in these two species are produced in a RAG-independent manner that involves assembly of LRR cassettes into the germ line gene of lamprey and hagfish immune effector cells. The VLRs produced by this method represent the functional component of the lamprey and hagfish adaptive immune system. This VLR-based immune system has been shown

in several studies to be equally as competent as the immunoglobulin-based immune system found in other vertebrate species, and is capable of  $>10^{14}$  unique variations in the VLR gene [67-70, 74, 76]. The overall VLR structure is a crescent shape with  $\beta$ -strands lining the convex portion of the molecule, which along with the C-terminal loop provide the binding surface for antigen [73-77]. This structure differs significantly from that of antibodies and their corresponding scFvs used in the conventional CAR design. An example of the unique binding methods of VLRs has been described previously with glycan binding VLRs. In comparison with immunoglobulin-based antibodies where the protein surface is commonly found to contain long grooves that can bind the oligosaccharide chains [101, 102], VLRs bind this same molecule but through recognition of different regions, in a manner wherein the antigen is sandwiched between the loop created by one of the LRRs and the concave surface of the VLR formed from the  $\beta$ -strands [76]. In this example, the VLR structure forces the bound oligosaccharide to bend as a way of adapting to the concave structure of the VLR, while still allowing it to retain contact with the protein. This contrasts with the carbohydrate binding surfaces of antibodies that are generally found to be flat or convex [76]. Therefore, it is becoming clear that the structural differences between VLRs and antibodies impact antigen binding, which can lead to the ability of the VLR to recognize different antigen epitopes as well as impact antigen binding affinity compared with the corresponding antibodies.

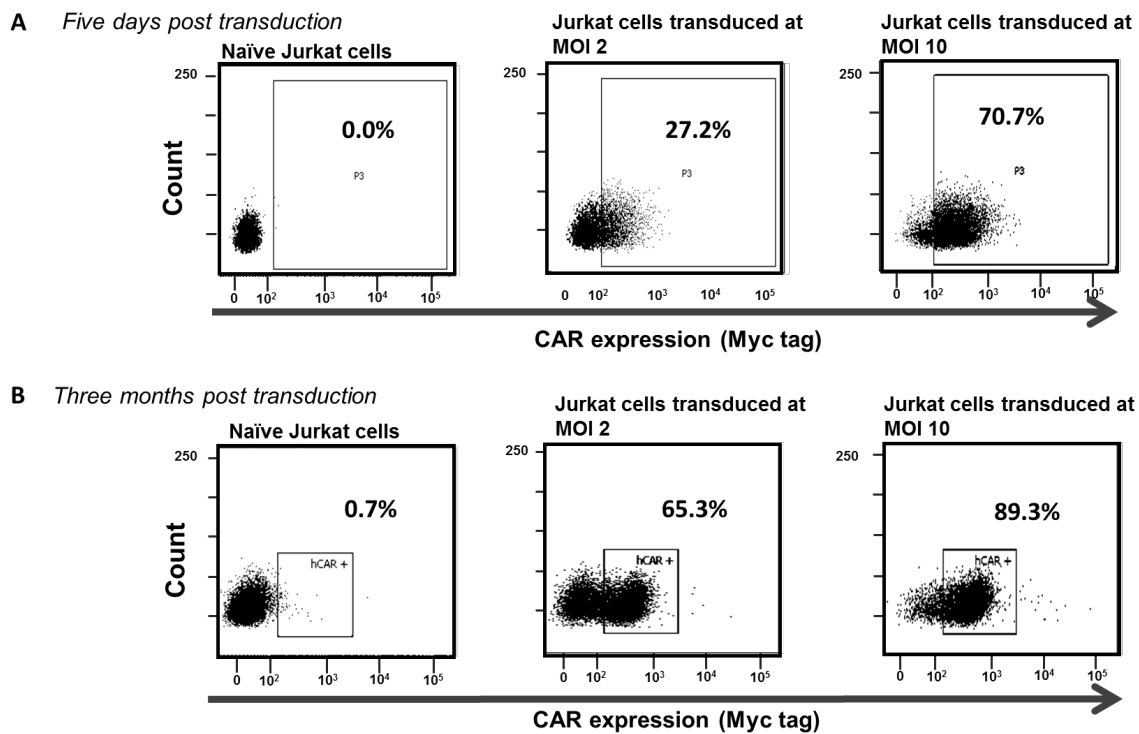
A potential concern needing to be addressed is the immunogenicity of the VLR-CAR construct. LRRs that form the core structure of VLRs are seen in the human innate immune system as part of the extracellular domains of human Toll-like receptors [103, 104]. Therefore, the similar homology of LRRs in human Toll-like receptors may decrease their immunogenicity. However, this remains an obvious and important concern, and several options are being explored to determine the degree of VLR immunogenicity in the setting of CAR technologies and delivery and also to determine issues that may arise from introducing VLRs into mammals.

One of the primary outcomes of this research was the establishment of an effective method for screening and identifying VLR candidates that may work to effectively direct a CAR expressing effector cell to recognize a target cell expressing the cognate cell surface protein. In the results from the development of the VLR against the neuroblastoma cell line SK-N-Be(2), a VLR was identified that binds preferentially to the target cell type when screened against other unrelated cell types. The cross reactivity against similar cell types, indicates the VLR is likely recognizing an antigen common to these cell types. This may be advantageous as it would then allow for a broader recognition of neuroblastoma cells rather than only those closely related to the SK-N-Be(2) cell line.

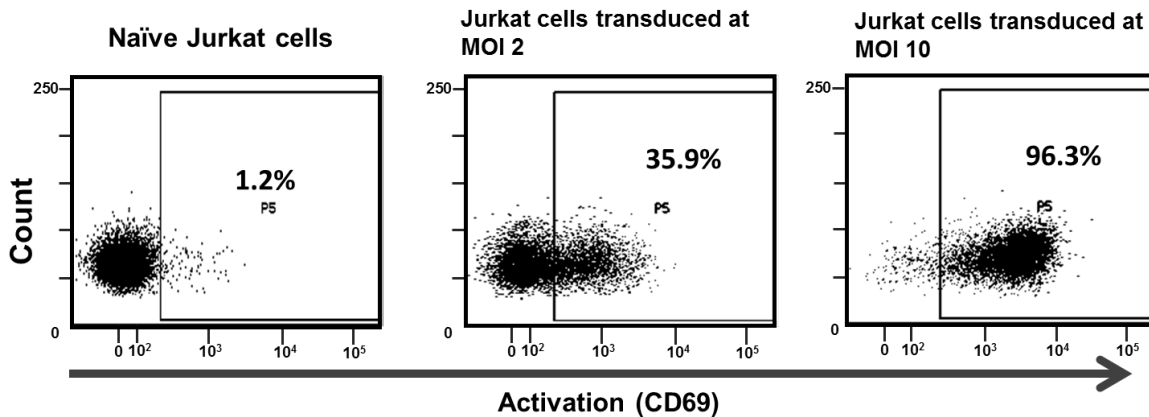
Overall, our results demonstrate VLRs can be used in place of the scFv to serve the function of antigen recognition in a CAR complex. The functionality of the VLR was initially demonstrated in Jurkat cells transduced with two different VLR sequences, a BCL-VLR and a CD5- VLR. CAR protein expression and CAR cell surface expression was confirmed in these cells, indicating a functional CAR design. The BCL VLR-CAR was shown to be capable of effector cell activation when cultured in the presence of target BCL cells. Similar results were shown with a CD5-VLR transduced into multiple lineages of immunocompetent cells. Importantly, it was also demonstrated that the VLR-CARs activated effector cells specifically against their respective antigen expressing target cells. These studies establish the potential of VLRs as the antigen recognition region of the CAR construct and position VLRs as a viable method for redirecting target cells using CAR technologies.

**Supplementary Figure S1**

**Supplementary Figure S1. Activation of clone 8 VLR CAR expressing Jurkat cell.** A co-culture assay was performed that included clone 8 VLR CAR expressing Jurkat cells as well as the cell types K562 and U937. The activation is measured by the percentage of total cells that have CD69 upregulated cell surface expression.

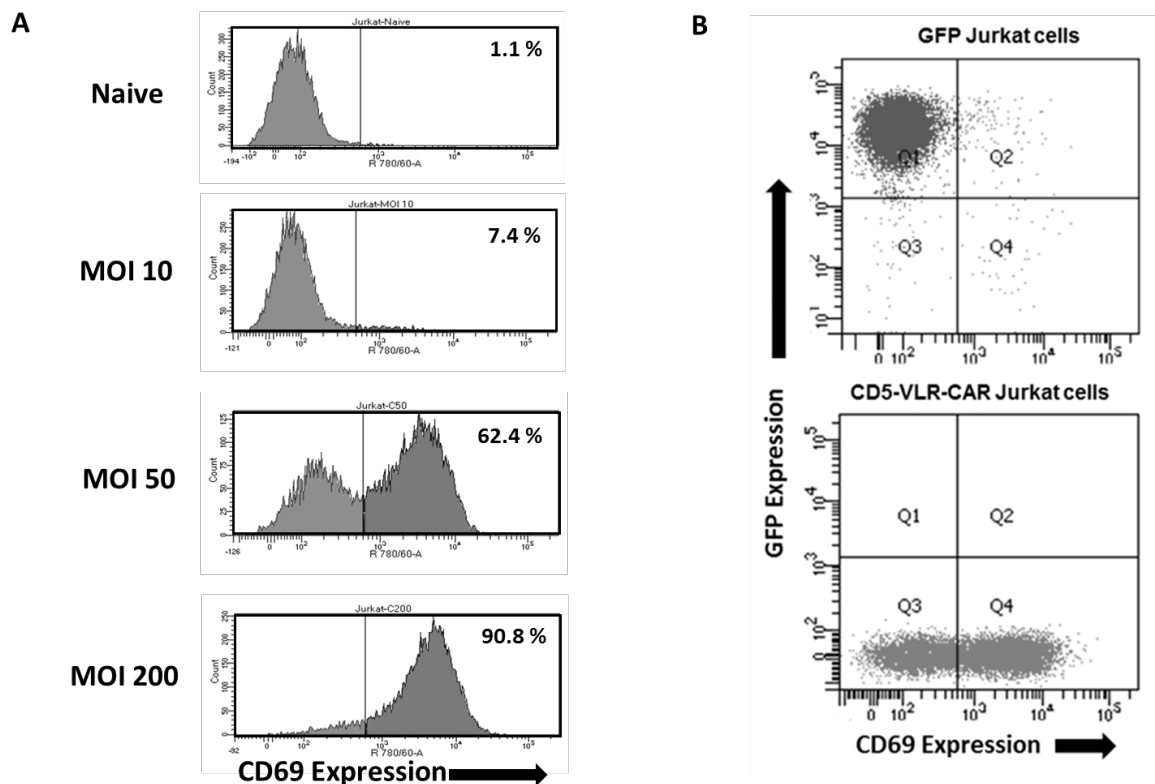
**Supplementary Figure S2**

**Supplementary Figure S2: Stable expression of the BCL VLR CAR in transduced Jurkat cells.** CAR expression as determined by flow cytometry using an anti-myc tag antibody shows a dose response with increased MOI five days after transduction. Values within the figures show the percentage of VLR-CAR positive cells.

**Supplementary Figure S3**

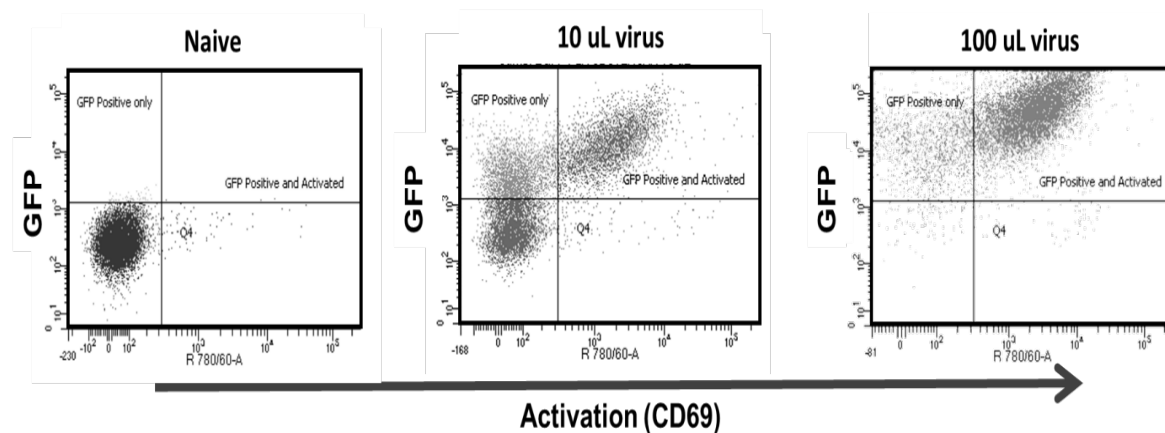
**Supplementary Figure S3: Activation as measured by CD69 upregulation in VLR CAR transduced Jurkat cells.** Flow cytometry results showing activation in BCL-VLR-CAR transduced Jurkat cells with a dose response to transduction MOI when co-cultured with BCL cells.

## Supplementary Figure S4



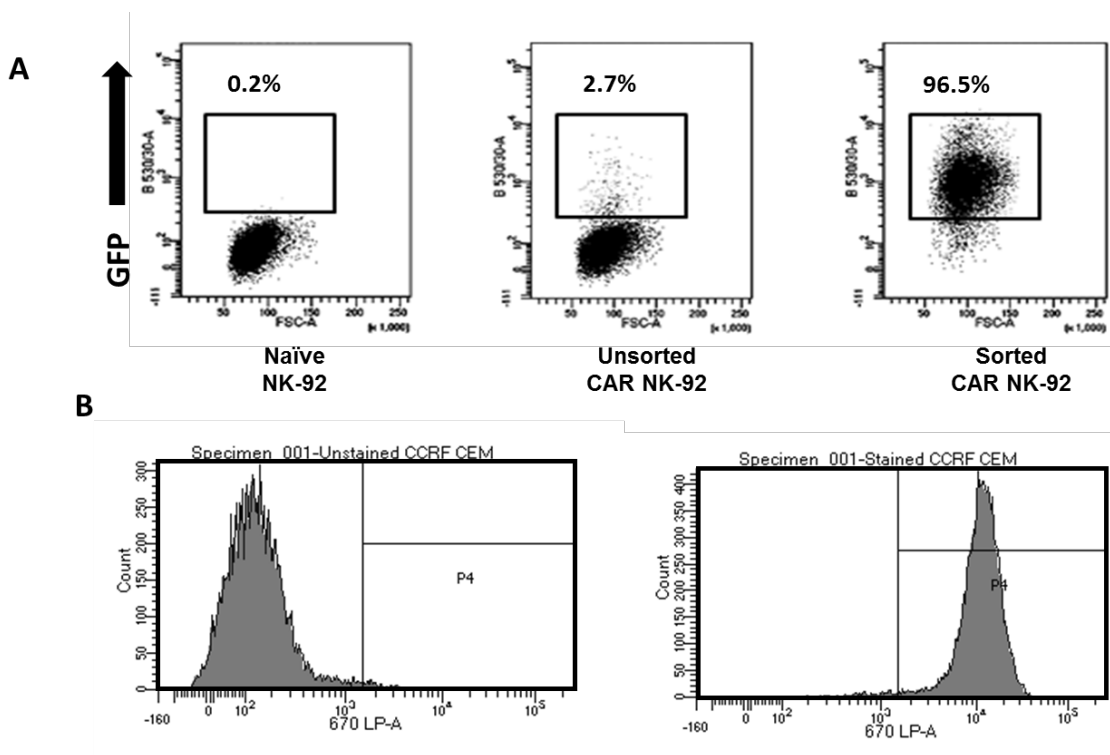
**Supplementary Figure S4: CD5-VLR-CAR expression in Jurkat cells.** (A) Flow cytometry shows increased activation (CD69 expression) in Jurkat cells transduced at increasing MOIs with the CD5-VLR-CAR lentivirus, 4 days after transduction. (B) Flow cytometry showing no activation in Jurkat cells transduced with GFP (top panel) compared to cells transduced with CD5-VLR-CAR lentivirus (lower panel). Both groups were transduced at an MOI of 50.

## Supplementary Figure S5



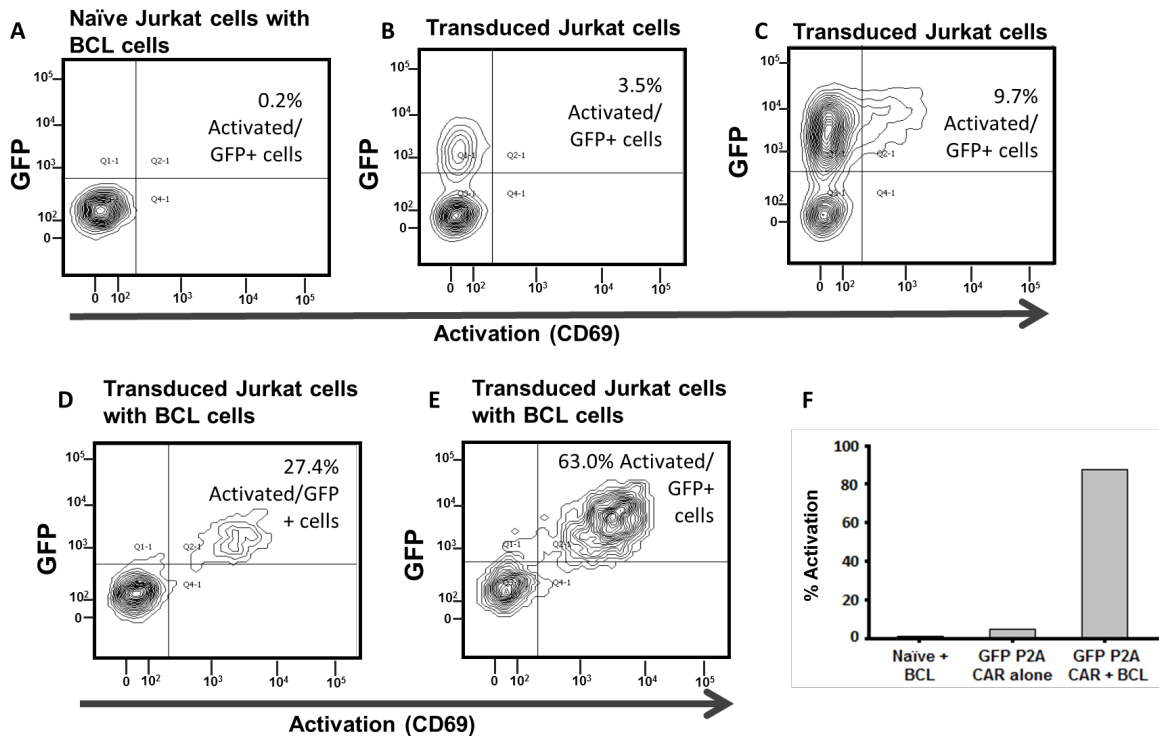
**Supplementary Figure S5: Flow cytometry analysis of Jurkat cells transduced with the eGFP P2A CD5-VLR-CAR construct.** A direct correlation is observed between GFP expression and activation, confirming expression and function of both proteins.

## Supplementary Figure S6



**Supplementary Figure S6: Selection of CD5-VLR-CAR expressing NK-92 cells and CD5 expression on a targeted tumor cell line.** A) Flow cytometry showing GFP expression in NK-92 cells before transduction (left panel), after transduction (middle panel), and after flow sorting (right panel). B) CD5 expression in CCRF-CEM cells. Cells stained with anti-CD5 antibody show robust CD5 expression (right panel) compared to unstained CCRF-CEM cells (left panel).

## Supplementary Figure S7



**Supplementary Figure S7: Flow cytometry analysis from co-culture assay of eGFP P2A BCL-VLR-CAR transduced Jurkat cells with target BCL cells.** A) Naïve Jurkat cells cultured with BCL cells, B) Jurkat cells transduced with an MOI of 2, without BCL cells, C) same as B but cells transduced at an MOI of 20, D) same as B but cultured with BCL cells, E) same as C but cultured with BCL cells. F) Summary of results from a second viral preparation and transduction experiment using cells transduced with an MOI of 20 and cultured with or without BCL cells. These results show a substantial shift in activated GFP positive population in Jurkat cells transduced with BCL-VLR-CAR and cultured with BCL cells. CAR-transduced Jurkat cells without co-culture showed GFP expression with little activation.

## Chapter 4

### **Strategies for genetic engineering of transduction-resistant immunocompetent cells**

This research was published in *Gene Therapy*

Johnston JM<sup>1</sup>, Denning G<sup>2</sup>, Moot R<sup>1</sup>, Whitehead D<sup>3</sup>, Shields J<sup>3</sup>, Le Doux JM<sup>4</sup>, Doering CB<sup>3</sup>,  
Spencer HT<sup>3</sup>.

### **High-throughput screening identifies compounds that enhance lentiviral transduction.**

*Gene Therapy*. 2014 Dec;21(12):1008-20.

- 1: Aflac Cancer and Blood Disorders Center, Department of Pediatrics, Emory University School of Medicine, Atlanta, GA, USA, Graduate Program in Molecular and Systems Pharmacology, Graduate Division of Biological and Biomedical Sciences, Emory University, Atlanta, GA, USA.  
2: Expression Therapeutics, LLC, Tucker, GA, USA.  
3: Aflac Cancer and Blood Disorders Center, Department of Pediatrics, Emory University School of Medicine, Atlanta, GA, USA.  
4: Wallace H Coulter Department of Biomedical Engineering, Georgia Tech and Emory University, Atlanta, GA, USA.

and

### *Biomicrofluidics*

Tran R, Ahn B, Myers DR, Qiu Y, Sakurai Y, Moot R<sup>1</sup>, Mihevc E<sup>2</sup>, Trent Spencer H, Doering C, A Lam W.

### **Simplified prototyping of perfusable polystyrene microfluidics.**

*Biomicrofluidics*. 2014 Jul 30;8(4):046501

- 1: Graduate Program in Molecular and Systems Pharmacology, Laney Graduate School, Emory University, Atlanta, Georgia 30322, USA.  
2: The Wallace H. Coulter Department of Biomedical Engineering, Georgia Institute of Technology and Emory University, Atlanta, Georgia 30332, USA.

**Abstract**

One of the primary challenges to the success of gene therapy is effective and efficient transfer of the transgene of interest to the target cells. Improving upon transduction efficiency would benefit the field by improving the efficacy of the technology and enabling a greater success in the action of the transgene. Herein several methods are explored for improving target cell transduction. The first is the addition of the small molecule PMA to lentiviral transduction. Additionally, PMA is investigated in combination with rapamycin, a molecule already established to improve lentiviral transduction, to determine any potential synergistic effects it may have on transduction with rapamycin. Other methods investigated focused on increasing viral concentration on target cells. These include lentiviral transduction through a magnetic column, transduction in a glass or polymer tube seeded with target cells, and concentration of the virus onto the target cells via a size exclusion filter. The greatest success obtained via this method was in the development of a microfluidics device that showed statistically significant increases in transduction over traditional plate-based transduction methods. Another method to potentially increase transduction was through a separate virus, AAV6. Gene delivery of the CAR has generally been accomplished through transduction with integrating viral vectors, specifically lentivirus. There are, however, limitations in lentiviral transduction such as low level transduction in human innate cells and issues arising from permanent integration of the viral transgene. The experiments presented here indicate AAV6 is a viable alternative for gene delivery to human innate cells as well as a cytotoxic NK-cell line. In studies of PBMC cultures expanded in vitro, gamma delta T-cells, alpha beta T-cells, and NK cells were all transduced at a significantly higher efficiency than a lentiviral vector containing an identical GFP transgene. Additionally, AAV6 was assessed as a potential delivery vector for a CAR transgene. The functionality of a CD5 directed CAR was assessed in NK-92 cells via cytotoxicity assay. The results indicate a fully functional CAR, capable of directing effector cell activity against target, CD5 expressing, Jurkat cells.

#### 4.1 Introduction

One of the primary limitations to successful application of CAR therapy to a variety of effector cell types is a limitation in the transduction efficiency. Without efficient transfer of the CAR transgene, effector function will be limited. There are three options proposed herein as a means to increase transduction efficiency. The first is introducing a small molecule that may act to improve transduction by modulating intercellular pathways. The second is altering the vessel the transduction occurs in to include options such as a microfluidics device and the third is transduction with AAV6. All three of these options are intended to improve the transduction efficiency and ultimately improve the effect of CAR therapy.

One method employed to increase transduction was to identify a small molecule that may act on the cell to increase viral infection efficiency. To accomplish this, a high-throughput screen was performed to identify potential compounds. One compound identified was phorbol 12-myristate 13-acetate (PMA). PMA stimulates protein kinase C (PKC), a family of closely related serine/threonine kinases involved in signal transduction pathways regulating an array of cellular processes. The PKC family consists of 10 isoforms classified into three subfamilies according to which secondary messengers are required for PKC activation. Two of the subfamilies, the conventional (PKC $\alpha$ , PKC $\beta$ I, PKC $\beta$ II and PKC $\gamma$ ) and novel PKCs (PKC $\delta$ , PKC $\theta$ , PKC $\epsilon$  and PKC $\eta$ ) require diacylglycerol (DAG) for activation. PMA, an analog of DAG, activates isoforms within these two subfamilies and associates at the same binding site as DAG in the C1 regulatory domain [105, 106]. In the current study, PMA was confirmed as a positive enhancer of lentiviral transduction, increasing the transduction of hematopoietic cell lines and human CD34+ cells, but importantly not all cells were equally susceptible to the effects of PMA. Additionally, rapamycin has been previously identified as an enhancer of lentiviral transduction [107]. As a way to both compare the effects of PMA and rapamycin on transduction efficiency as well as potentially identify any synergistic effects, a combination of PMA and rapamycin was also tested.

Another of the restrictions that influences the efficiency of lentiviral transduction is that each viral particle needs to interact with a target cell for transduction to occur. Brownian motion in a standard vessel such as a cell culture plate limits the distance a viral particle can travel within its half-life. To improve on transduction efficiency, several methods were tested with the intent to increase the interaction between the viral particles and the target cells. These methods included transduction in a tube that has been seeded with target cells, transduction in a filter that allowed for virus to be concentrated onto the target cells, and transduction of target cells immobilized in a packed column. Although these initial methods proved unsuccessful, one method that did overcome this limitation is the use of an engineered microfluidics device. The concept behind the potential benefit of a microfluidics device is that it improves probability of interaction between the infectious viral particle and the target cell. In previous studies, this concept has already been observed, where transduction efficiency of adherent mammalian cells can be increased using microfluidic systems [108]. Using this same principal, we sought to determine if non-adherent cells, which are pertinent to many clinical gene therapy applications, could be immobilized in a microfluidics device and efficiently transduced via perfusion of viral vector-containing media. The current state of the art for clinical lentiviral vector transduction involves culturing the target cells in viral vector-containing media within Retronectin-coated gas permeable bags [109]. Retronectin is a recombinant human fibronectin fragment that increases the efficiency of lentiviral and retroviral transduction by binding both target cells and recombinant lentiviral or retroviral vector particles and facilitating gene transfer. Despite recent advances in vector production [110], approximately 10–1000 ml of vector are still needed to treat each patient to obtain a high enough transduction efficiency. The scale and yield limitations of vector manufacture and the low efficiency of gene transfer are currently major barriers to the commercialization and widespread implementation of lentiviral vector-based gene therapy, which otherwise has the potential to cure many human diseases. Other widely used gene transfer

techniques, such as nucleofection, electroporation, and lipofection, have been shown to have lower transfection efficiencies and cell viability when compared to lentiviral transduction [111]. For this proof of concept study, K562 cells were used as a surrogate of CD34+ cells to test our hybrid PS-PDMS cell transduction [112]. Using this method of lentiviral transduction, proof of concept was initially established in transduction of K562 cells. These studies showed the microfluidics system was capable of yielding successful transduction. Further studies focused on the transduction of primary human cells improved on these results by showing significant enhancements in transduction efficiency were obtained with the microfluidics system. Overall, these results establish the design and development process of a microfluidics device as well as indicate its potential for improving lentiviral transduction of primary human cells.

The next studies sought to improve target cell transduction using AAV6 as an alternative to lentivirus. AAV is a non-enveloped, single stranded DNA virus around 4.7 kilobases (Kb) long that belongs to the parvovirus family [33]. The general structure of the AAV virus consists of three genes, Rep, Cap, and app [37, 113, 114]. These genes are flanked by two inverted terminal repeats (ITR) that operate as self-priming hairpins and serve as the origins for DNA replication [36, 38]. One of the qualities that make AAV suitable for gene therapy is deletion of Rep protein expression results in formation of a circular concatemer from the viral transgene. This concatemer can then exist in the nucleus of the transduced cell in episomal form rather than integrating into the host genomic DNA [33, 115].

The AAV capsid is composed of proteins VP; VP1/VP2/VP3, which form the capsid shell and encapsulate the viral DNA. The capsid is responsible for determining the AAV serotype and directing the infectivity in different tissue types. A primary consideration in the use of AAV as a gene therapy vector is the type of capsid that will be used. Certain capsid sequence variations can result in differences in sugar binding which have a profound impact on the cell or tissue type that

is most efficiently transduced by the given AAV serotype. Along with the primary interactions mediated through the surface carbohydrates, there are also secondary receptors that can influence cell and tissue specificity between the AAV serotypes [35]. Previous studies have characterized the infectivity profiles of the different AAV serotypes and provided guidance as to which may work best in a particular application [116, 117]. AAV6 has been shown to be the most effective serotype for transduction of hematopoietic stem and progenitor cells (HSPC) while other serotypes have been shown to better transduce tissue such as the liver, heart, or CNS [118, 119]. Because these previous studies have indicated AAV6 transduces cells of hematopoietic origin more efficiently than the other 9 AAV serotypes [39, 120], it was selected as the serotype for use in transduction of the human primary cells and cell lines assessed herein.

Engineering of immune cells for expression of the CAR transgene has typically focused on the use of T-cells [90, 121, 122], of which the majority constituent are  $\alpha\beta$  T-cells [123, 124]. Other T-cell lineages and innate cell types have received less development as CAR T effector cells. The previous studies that have focused on innate cells as potential effectors for CAR mediated therapy have included NK-cells, dendritic cells, and  $\gamma\delta$  T-cells [125]. A common problem noted to hinder progress in development of these cell lines has been the low level transduction obtained with integrating viral vectors. Reports of transduction efficiency in  $\gamma\delta$  T-cells have been relatively low, peaking around 30% CAR positive cells in transduced populations [125]. NK-cell transduction has also been reported as a potential challenge to the development of these cells as a cancer therapeutic. Previous reports indicate transduction levels of 15% in NK-92 cells although other NK cell lines reported transduction efficiencies of 30-40% [126]. Primary NK cells have also proven to be resistant to successful gene transfer with typical transduction efficiencies reported to range from 15-40% gene modified cells. Additionally, there have been reports that lentiviral transduced NK cells are prone to procedural induced apoptosis [127, 128]. Further studies have focused on the resistance to transduction and potential implications for NK based therapy and

implicated an evolved resistance to viral infection that may function to limit gene transfer efficiency [129, 130]. Together, these data suggest that although these other innate cell lineages may offer a promising approach to CAR therapy, inefficient transduction or the need for excessive manipulation of the cells *ex vivo* have delayed progress in the development of these cells as effectors for CAR therapy.

As mentioned previously, AAV expression is diluted out during cell division [131] and, as such, this method for CAR delivery offers an opportunity to effectively control the length of time a particular transgene is expressed in the effector cells. This method of transgene expression offers several benefits over integrating viruses, as there are situations where transient expression of a transgene may be preferable to stable expression. There have previously been studies that have indicated the need for a tighter control over transgene expression [132, 133]. In situations where the side effects of the CAR prove undesirable, limiting the amount of time that the CAR is expressed may prove advantageous [134]. The use of AAV6 as a vector for gene transfer will allow for mitigation of some of the concerns that CAR technology brings by improving control over transgene expression.

Collectively, AAV offers several benefits to CAR delivery that are not realized with lentivirus. The first is the high transduction efficiency in human immune cells including both innate and adaptive immune cells. Another is the transient nature of transgene expression, which may improve the outcome in the case of CAR therapy related side effects. The AAV6 serotype, used herein, was selected due to previously reported studies indicating comparatively high transduction in human cells of hematopoietic origin compared to the other AAV serotypes. Taken together, AAV6 mediated delivery of the CAR transgene provides a beneficial approach that may overcome many of the previously reported limitations.

## **4.2 Materials and Methods**

### **Culture, treatment and transduction of K562 cells and transduction with PMA, rapamycin, or a combination of PMA and rapamycin**

K562 cells were cultured in DMEM/F-12 supplemented with 10% FBS and 1% penicillin/streptomycin. Cells were plated in 24-well tissue culture plates and treated with PMA, rapamycin, or a combination of both (Fisher Scientific). Before treatment, PMA was dissolved in dimethyl sulfoxide to yield an initial concentration of 10 mg ml<sup>-1</sup>. Subsequent dilutions were performed in DMEM/F-12 supplemented with 10% FBS and 1% penicillin/streptomycin. Rapamycin was diluted to the indicated concentrations using the same method as described for PMA. The experimental well were treated for 2 hours with PMA, rapamycin, or a PMA/rapamycin combination. The cells were transduced in minimal volume (300 µl) with a GFP lentiviral vector in the presence of polybrene (8 ng µl<sup>-1</sup>). Transduction efficiency was assessed 72–96 h by flow cytometry. The percentage of GFP positive cells was compared with the percentage of GFP-positive cells from cells transduced in the absence of PMA, rapamycin, or the combination of the two.

### **Transduction using glass or PTFE tubing**

A glass tube 7.5 cm in length with an internal diameter of 0.1mm. PTFE tubing was 0.2mm internal diameter and 15.24cm in length. Each of these tubes were coated with poly-L-lysine (Sigma P7280) as a way to adhere the target cells in the tubing. This was done by adding 50mL of dH<sub>2</sub>O to 5mg of poly-L-lysine then adding the appropriate volume of the poly-L-lysine to completely fill the tube. This was then incubated at room temperature for 5 minutes before washing with dH<sub>2</sub>O. The tubes were then allowed to dry for 2 hours. Following the coating with poly-L-lysine, 1x10<sup>6</sup> cells K562 cells were suspended in complete DMEM and added to the tube. The cells were allowed to adhere for 15 minutes at 37°C. Following the attachment of the cells, silicone tubing was affixed to both ends of the coated tube and attached to a peristaltic pump.

Three hundred  $\mu\text{L}$  of GFP lentivirus was added to 700 $\mu\text{L}$  of complete DMEM that was then loaded into the system. The pump was allowed to flow for 6 hours at 1.5ml/minute before analysis of the cells via flow cytometry.

#### **Transduction with Amicon Filter**

K562 cells were suspended at  $1 \times 10^6$  cells in 3mL of freestyle media (Thermo 12338018) and 300 $\mu\text{L}$  of GFP lentivirus (titer:  $2.3 \times 10^8$ ) was added to the cell suspension. Following addition of the virus, the column was spun at 1500 x g for 20 minutes. The cells were then resuspended in complete DMEM and placed in a 6-well plate. As a control,  $1 \times 10^6$  K562 cells were added to 1mL of complete DMEM in a 6-well plate and transduced with 300 $\mu\text{L}$  of GFP lentivirus (titer:  $2.3 \times 10^8$ ). The transduction was allowed to proceed overnight at 37°C before analysis via flow cytometry.

#### **Transduction with magnetic column**

K562 cells were attached to anti-CD45 dynabeads (Thermo 10608D) following manufacturers instructions. Following attachment to dynabeads,  $1 \times 10^6$  K562 cells were loaded into a MACS manual separation column (Miltenyi 130-041-305) that was placed in a magnetic field. This allowed the cells to remain attached in the column. Next, 300 $\mu\text{L}$  of GFP lentivirus (titer:  $2.3 \times 10^8$ ) was added to 700 $\mu\text{L}$  of complete DMEM and loaded into the column containing the K562 cells. The outflow of the column was then attached to tubing connected through a peristaltic pump to return the virus containing media to the top of the column at 1.5mL/minute. This process was allowed to proceed for 6 hours. As a control,  $1 \times 10^6$  K562 cells were added to 1mL of complete DMEM in a 6-well plate and transduced with 300 $\mu\text{L}$  of GFP lentivirus (titer:  $2.3 \times 10^8$ ). The transduction was allowed to proceed overnight at 37°C before analysis via flow cytometry.

#### **Creation of the microfluidics device for lentiviral transduction**

These experiments were performed through a collaboration with the GA Tech Biomedical Engineering Program and with the assistance of Reginald Tran. PDMS channels were cut from a microfabricated SU-8 master to be used as a PDMS mold, exposed to oxygen plasma for 1 min, and treated with hexamethyldisilazane (HMDS) (Figure 1, step 1). Casting additional PDMS mixed at a 5:1 w/w ratio of elastomer base: curing agent on the HMDS-treated PDMS mold resulted in a PDMS die with raised features as shown in Figure 1, step 2. The PDMS die was then used to emboss channels into a 25 × 75 mm PS microscope slide (Ted Pella, Inc., Redding, CA) using binder clips to apply pressure in a convection oven at 160 °C for 15 min, similar to the embossing method described by Goral *et al.* (Figure 1, step 3). Edge beads formed during the embossing process (Figure 1, step 4) were removed and de-burred to ensure flatness of the PS surface, which is critical for optimal thermal bonding conditions. Holes sized 1/32" were then drilled into the inlet and outlet regions of the channel and de-burred, as shown in Figure 1, step 5. The non-embossed side of the PS was plasma treated for 1 min using either a plasma cleaner (Harrick Plasma, Ithica, NY) or corona gun (Electro-Technic Products, Inc., Chicago, IL) and silanized with 1% v/v aqueous (3-Aminopropyl)triethoxysilane (Sigma-Aldrich, St. Louis, MO) for 20 min at room temperature (Figure 1, step 6) [112]

Figure 1

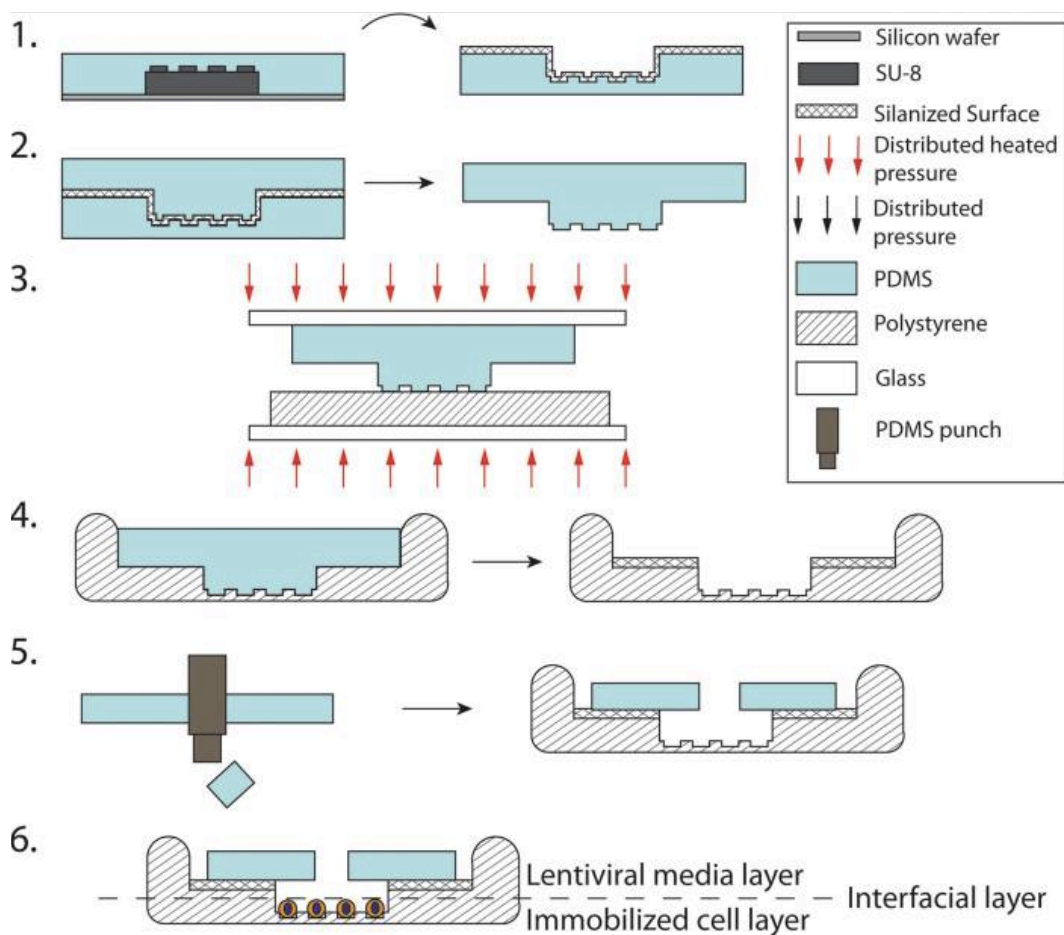


**Figure 1: Schematic of hybrid PS-PDMS device, which can be used for lentiviral transduction.** (1) Cut PDMS from silicon mold and HMDS treat. (2) Pour PDMS (5:1 PDMS:crosslinker) in HMDS-treated PDMS mold to produce a PDMS die. (3) Emboss. (4) Allow to cool and remove die. Additional trimming is not necessary. Silanize the top surface. (5) Punch inlet and outlet ports in a flat slab of PDMS and align with the embossed channels. (6) The completed device will enable non-adherent cells to be immobilized in the embossed divots within the embossed channels, allowing for an immobilized cell layer to come into homogeneous contact with a lentiviral media layer.

### **Seeding cells into the microfluidics device**

Cells were seeded onto a Retronectin-coated PS slide that was embossed with 15  $\mu\text{m}$  divots and bonded to a PDMS channel. Retronectin works best when coated onto PS, cyclo-olefin, polyethylene, or Teflon, which is the reason a hybrid PS-PDMS device was essential for this application [135].

### **Transduction of cells in the microfluidics device**

The PS-PDMS hybrid devices were coated with 50  $\mu\text{g}/\text{ml}$  Retronectin<sup>®</sup> (Takara Bio Inc., Otsu, Shiga, Japan) overnight at 4 °C. K562 myelogenous leukemia cells were then seeded into the channels at a concentration of 23 000 cells/ml; enough to form a monolayer on the Retronectin-coated PS base of the device. The cells were allowed to settle and adhere in an incubator for 4 h. After incubation, the device was connected to growth media (IMDM, L-glutamine, pen/strep, 20% FBS) containing HIV-GFP lentivirus (MOI = 0.75, based on static culture transduction of HEK293 cells) and Polybrene (8  $\mu\text{g}/\text{ml}$ ). The viral vector containing media was perfused through the system for 24 h before switching to growth media to culture the cells for an additional 96 h. After the 96 h incubation period, cells were visualized with epifluorescence microscopy to assess transduction efficiency.

### **Generation of AAV6 and lenti-GFP transgene**

Recombinant HIV lentivirus was produced using methods previously described [136]. Briefly, a four-plasmid system encoding the expression plasmid (GFP or GFP-P2A-CAR transgene), packaging plasmids containing the *gag*, *pol*, and *envelope* genes were transfected transiently into HEK-293T cells using calcium phosphate. The 293T cells were cultured in Dulbecco's modified essential medium (DMEM, Thermo Fisher Scientific) with 10% FBS and 1% penicillin–streptomycin (P/S). Twenty-four hours post-transfection, the culture medium was changed to fresh medium. The viral supernatant was collected at 48, 72, and 96 hours after transfection and

filtered through a 0.22  $\mu\text{m}$  filter. After the 96 hour virus collection, the viral supernatant was pooled then concentrated via centrifugation overnight at 10,000xg at 4°C.

The production of both the AAV6-GFP and the AAV6-CD5 CAR were outsourced to ViGene Biosciences. The AAV6 GFP was obtained by a special preparation of their stock GFP virus. For the AAV6 CD5 CAR, plasmid containing the AAV6 expression vector was shipped to ViGene for virus production.

### **Expansion of $\gamma\delta$ T-cells in serum free media**

Mobilized apheresed PBMC were obtained from consented, deceased, neuroblastoma patients at Children's Healthcare of Atlanta (Atlanta, GA). At the time of stem cell transplant, the patient had undergone two cycles of chemotherapy. Cells were expanded in accordance with previously published protocols [137]. Briefly, cells are cultured with OpTmizer (Life Technologies, Carlsbad, CA) serum free media and supplemented with 2 mM L-glutamine and 1% penicillin/streptomycin. All cultures were stimulated with 500-1000 IU/ml of IL-2 (Peprotech, Rocky Hill, NJ) and 5 $\mu\text{M}$  zoledronic acid (Sigma-Aldrich). Total cell numbers were monitored periodically over a 2 week period via Cellometer (Nexcelom, Lawrence, MA). Dead cells were excluded using trypan blue staining.  $\gamma\delta$  T cell percentage and PBMC cellular composition, were monitored via flow cytometry on days 0, 7, 12, and 14. Flow cytometry methods are reported below.

Cell clumps were broken apart and cell cultures were counted. Based on these counts, 0.25-1x10<sup>6</sup> live cells were stained per sample. Cells were washed with PBS and spun down at 100xg in flow tubes. The cells were decanted and incubated with Invitrogen (San Diego, CA) eBioscience Fixable Viability Dye eFLUOR 780 for 30 minutes with shaking at room temperature. The cells were washed in 10 volumes of PBS. Supernatant was decanted and replaced with the appropriate

antibody cocktail in PBS. The antibodies used from BD Biosciences (Franklin Lakes, NJ), include: BV421 Mouse Anti-Human CD3 (Clone UCHT1), PE Mouse Anti-Human TCR-1 (11F2), and BUV395 Mouse Anti-Human CD56 (Clone NCAM16.2). Antibodies were also used from BioLegend (San Diego, CA): APC anti-human CD314 (NKG2D) (Clone 1D11), Pacific Blue anti-human CD57 (Clone HCD57), Brilliant Violet 711 anti-human CD16 (Clone 3G8), APC anti-human CD62L (Clone DREG-56). Flow cytometric analysis and cells were analyzed using an LSRII (BD Biosciences, Franklin Lakes, NJ).

### **Flow cytometry analysis**

Flow cytometry analysis was performed using an LSRII Flow Cytometer (BD Biosciences, San Jose, CA). Data was analyzed using the BD FACSDiva software. Antibodies used included eFLUOR 780 (eBioscience).

### **AAV6 and lentiviral transduction of NK-92 cells**

Transduction with AAV6 and recombinant HIV lentiviral particles was carried out by incubating cells with each virus in the appropriate culture medium. Lentiviral transductions were supplemented with 6 µg/ml polybrene (EMD Millipore, Billerica, MA). Twenty-four hours after transduction, culture medium was replaced with fresh medium. The transduced cells were then cultured for at least 4 days before being used for downstream applications.

### **Functional titer calculation**

As a way to standardize titer calculation between AAV6 and lentivirus, a functional titer was used. To perform this assay, Jurkat cells were plated at  $1 \times 10^5$  cells per 100µL of DMEM containing 10% FBS and 1% P/S in a 96-well plate. AAV6 was added to the culture at 1µL at a 1:5 dilution. Lenti-GFP virus was added under the same conditions with 1µL at a 1:5 dilution but also included Polybrene. Four days post-transduction, the transduced Jurkat cells were analyzed

via flow cytometry to determine the percentage of GFP positive cells. Functional titer was calculated as (cell number) x (% of transduced cells) x (1000) x (virus dilution)/(volume of virus).

#### **Transfection of NK-92 cells with CD5-CAR in an AAV vector**

NK-92 cells were transfected with the CD5 CAR construct in the AAV expression vector. This was accomplished by removing  $2 \times 10^5$  NK-92 cells from culture and washing once with PBS then plating in a 24-well plate in 50 $\mu$ L of Opti-MEM (Gibco 51985091). The DNA/Lipofectamine 2000 (Thermo 11668) mixture was created by mixing 5 $\mu$ g of CD5-CAR plasmid DNA with 250 $\mu$ L of Opti-MEM. Fifty  $\mu$ L of this mixture was then removed and added in a separate tube to 50 $\mu$ L of Lipofectamine 2000. This was incubated at room temperature for 5 minutes then added to the 50 $\mu$ L of NK-92 cells in the 24-well plate. The cells were incubated at 37°C for 24 hours. Following the incubation, the cells were washed once in complete RPMI (Sigma RO883) and replated in complete RPMI.

#### **Binding of CD5 transduced effector cells to purified CD5 fusion protein to Fc region**

The binding assay for CD5 transduced effector cells was performed by removing  $5 \times 10^5$  NK-92 cells from culture and washing twice in PBS. The cells were then resuspended in 200 $\mu$ L of PBS. 0.2 $\mu$ g of the CD5-Fc-fusion protein was obtained through a 1:5 dilution of the stock solution and 2 $\mu$ L of this solution were then added to the tube containing the NK-92 cells. The cell mixture was allowed to incubate at room temperature for 30 minutes then washed once with PBS. Two  $\mu$ L of a 1:100 dilution of IgG-Fc-PE antibody (Biolegend HP6017) was then added to the tube, which was covered and incubated at room temperature on a rotating shaker for 15 minutes. Following the incubation, the cells were washed and resuspended in PBS with 1% BSA. Flow cytometry was then used to determine binding of the CD5 expressing NK-92 cells to the CD5-Fc-fusion protein

### **Cytotoxicity assay**

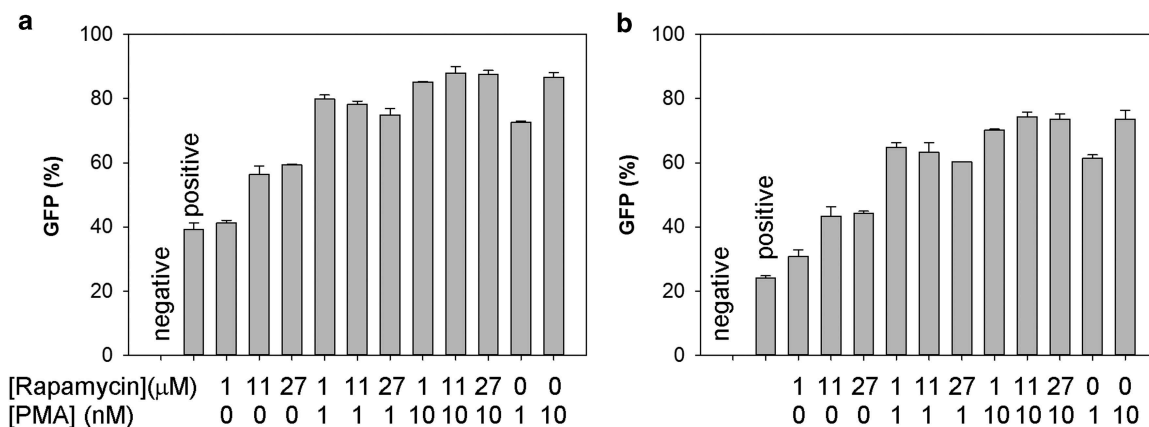
The cytotoxicity assay was run as previously described [95]. Briefly, it was performed as follows: target Jurkat cells were collected from culture and washed once then counted. From the total population,  $2 \times 10^7$  cells were then labeled with PKH26 red membrane dye (Sigma PKH26GL) according to manufacturer provided instructions. After labeling, the cells were washed again in complete medium and re-suspended in RPMI containing 10% FBS and 1% Pen/Strep. The transduced NK-92 cells were added to a round bottom 96-well plate at the appropriate cell number. The membrane stained Jurkat cells were then added at the appropriate effector to target ratio. The cell mixture was then incubated at 37°C for 4 hours. Following incubation, the cells were washed with PBS. The culture was then re-suspended in 200 $\mu$ L PBS containing 1% BSA to which 2 $\mu$ L of 1:1000 dilution of Fixable Viability Dye eFLUOR 780 (eBioscience) was added. The cells were incubated at room temperature on a rotating shaker for 15 minutes before being washed again and re-suspended in 200 $\mu$ L PBS with 1% BSA.

## **4.3 Results**

### **Increasing transduction with PMA or rapamycin**

The effect of pretreatment with PMA, rapamycin, or a combination of both was evaluated in the K562 cell line. PMA was identified in a high-throughput screen of a library of small molecules and rapamycin had previously been shown to enhance CD34 cell transduction [107]. K562 cells were plated in 300  $\mu$ l of complete Dulbecco's modified Eagle's medium (DMEM). The cells were treated with PMA and/or rapamycin for 2 h at the dose indicated in Figure 2, after which the cells were washed and re-plated. The cells were then transduced at an MOI of 2 (based on viral titer after transduction of 293T cells) immediately after re-plating. Twenty-four hours after transduction, the cells were washed and re-plated in a 24-well plate. To determine the effect of treatment, flow cytometry was performed 3 (Figure 2A) and 10 (Figure 2B) days after transduction and the percentage of GFP-positive cells was compared with control cells that

received no treatment but identical culturing conditions. Compared with the no treatment control, there was an increase in the transduction percentage of all treatment conditions with higher transduction efficiencies observed at higher drug doses. Of the conditions tested, the largest increase in transduction was obtained with rapamycin concentration at 10.9  $\mu\text{M}$  and PMA concentration at 10 nM, however, this was not dramatically higher than PMA alone. Therefore, under these conditions, PMA and rapamycin increased transduction efficiencies but there appears to be only a very modest benefit to combining these two compounds. The mean fluorescent intensity was also increased to similar levels over the control in these conditions (data not shown).

**Figure 2**

**Figure 2 Determination of the effect on the transduction of K562 cells by varying concentrations of rapamycin and PMA, both independently and in combination.** K562 cells were transduced with an GFP containing lentiviral vector at an MOI of 2. The concentrations tested were 1.1, 10.9 and 27.3 $\mu\text{M}$  of rapamycin. The individually tested concentration of PMA was 1 and 10nM. The combined concentrations tested were 1.1, 10.9 and 27.3 $\mu\text{M}$  rapamycin with 1 and 10nM PMA. Transduction efficiency was assessed by flow cytometry 3 (a) and 10 (b) days after transduction.

**Transduction in a tube as a means of increasing transduction efficiency**

Lowering overall transduction volume while maintaining the viral volume would provide a way to increase virus concentration on the target cells and may improve the chance for contact between a viral particle and the target cells. K562 cells were selected as the target cell type as they represent an easy to propagate and transduce cell line that were originally derived from human WBCs and therefore bear many similar characteristics to the primary cells this method will eventually be applied to. The first method attempted involved the use of glass or PTFE tubing that was coated with poly-L-lysine as a way to bind cells in the system. Virus containing media was then flowed through the tubing and into a plate using a peristaltic pump. The virus containing media was then recirculated back through the pump and flowed through the column in a continuous fashion. The standard plate based method was used as a control, wherein an equivalent number of cell and virus was added to the plate along with polybrene. The transduction efficiency was determined via flow cytometry (Figure 1A-C). The results from this method are detailed in Table 1 and show that although the process did decrease the overall transduction volume, it was unsuccessful in improving transduction over the standard plate based transduction. One of the primary issues that arose in this method was the inability to effectively bind the target cells in the tubing. Following every test, a significant number of the target cells were found to have dislodged from the tube and flowed into the plate. This issue persisted despite the type of tubing used as well as the concentrations and incubation time with the poly-L-lysine.

Figure 3

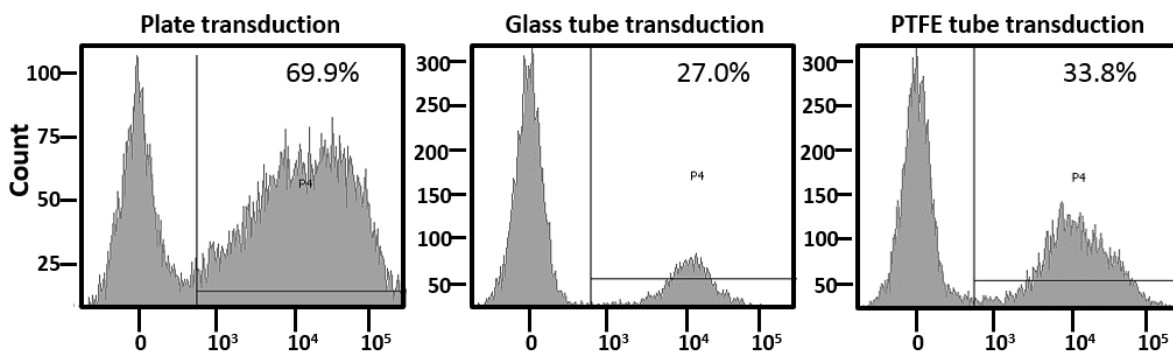


Table 1

Transduction method	Total volume	Amount of virus	% GFP positive cells
<b>Tube transduction</b>			
Glass	500 $\mu$ L	300 $\mu$ L	27.7
PTFE	500 $\mu$ L	300 $\mu$ L	33.8
<b>Plate</b>	1mL	300 $\mu$ L	69.9

**Figure 3/Table 1 Comparison of tube-based method of transduction with standard plate based method of transduction.** Figure 3 shows the flow cytometry data from the K562 cells transduced with either the glass or PTFE tube compared to the standard plate based method. Table 1 indicates the transduction efficiencies for each of the methods used along with that obtained via the standard plate based transduction system. None of the techniques attempted increased transduction over the 6-well plate (Table 1).

**Transduction in a concentrating filter as a way of increasing transduction efficiency**

The second method designed to improve lentiviral transduction used an Amicon Ultra centrifugal filter unit as a means to concentrate the virus onto K562 cells. This method of transduction was performed by seeding the Amicon filter with the target K562 cells, then adding virus containing media to the filter. The column was then centrifuged to allow the virus to flow through this system with the intention of increasing virus interaction with the stationary target cells. The results of this study were analyzed via flow cytometry (Figure 4) and indicate a decrease in transduction efficiency when using the column transduction compared to the standard plate based transduction method (Table 2). The main reason for a decrease in the transduction efficiency with the Amicon filter was a likely due to the observed decrease in target cell viability after using the filter-based method. Although the spin speed was decreased as a means to potentially improve the viability of the target cells, flow of the virus containing media through the column was not achieved at the spin speeds low enough to maintain cell viability.

Figure 4

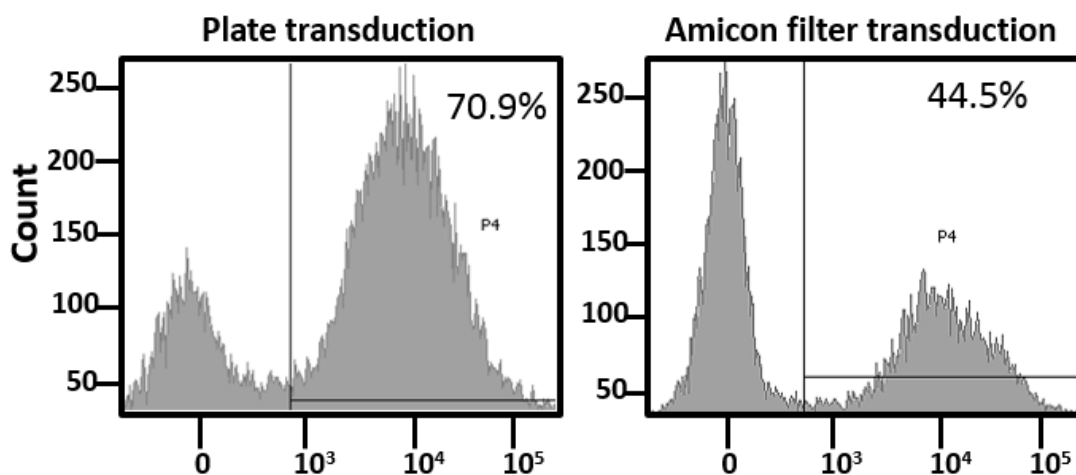


Table 2

Transduction method	Total volume	Amount of virus	% GFP positive cells
Plate	1mL	300 $\mu$ L	70.9
Amicon filter	3mL	300 $\mu$ L	44.5

**Figure 4/Table 2 Comparison between transduction using an Amicon filter and the standard plate based method.** Target K562 cells were analyzed via flow cytometry for the presence of GFP. The flow cytometry data from the transduction of K562 cells with GFP lentivirus using the Amicon-based filter method was compared to the standard plate based method to assess for increases in transduction efficiency obtained with the filter based method. Table 2 shows a direct comparison between transduction carried out via the Amicon filter-based method and the standard plate based method. The results indicate a decrease in transduction efficiency when using the Amicon filter based method (Table 2).

**Transduction of target cells labeled with magnetic beads and immobilized in a packed column as a method to increase transduction.**

The third method tested to increase the concentration of virus on the target cells involved the use of CD45 conjugated dynabeads. In this experiment, the target K562 cells were labeled with magnetic dynabeads and immobilized in a packed magnetic column. This method was designed to allow for increased virus interaction with the target cells by decreasing the overall volume in which the cells are transduced. By flowing the virus over the immobilized cells, in a perpetual manner, the chance of interaction between the virus and target cells should be increased. The transduction efficiency was assessed via flow cytometry for GFP expressed in the target cells (Figure 5). Although the total volume of the transduction was decreased, the results from this experiment indicate a lower transduction percentage than that obtained via the standard plate based transduction method (Table 3). Upon further examination into the reason for the decrease in transduction efficiency, it was revealed that transduction was decreased in the several days immediately following the labeling of the target cells with dynabeads (data not shown).

Figure 5

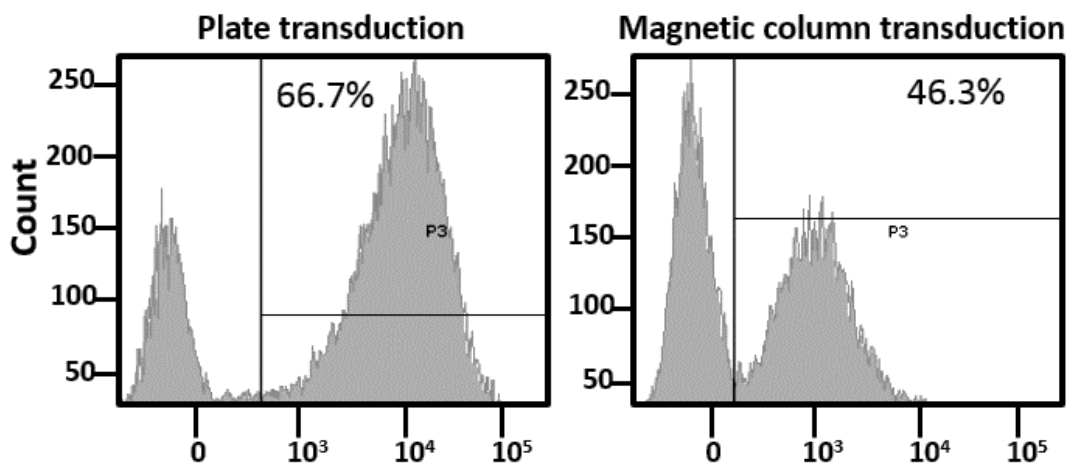


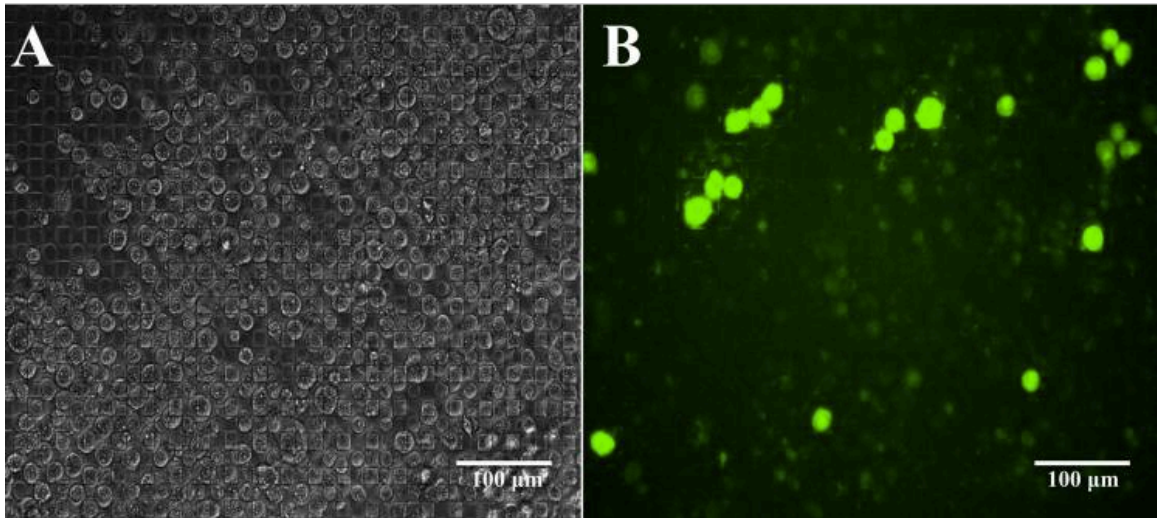
Table 3

Transduction method	Total volume	Amount of virus	% GFP positive cells
Plate	1mL	300 $\mu$ L	66.7
Magnetic column	750 $\mu$ L	300 $\mu$ L	46.3

**Figure 5/Table 3 Transduction of cells immobilized in a packed column and the standard plate based method of transduction.** Target K562 cells were labeled with anti-CD45 dynabeads and loaded into a column. Analysis of the transduced cells was carried out via flow cytometry (Figure 5). The percentage of GFP positive cells present in the transduced cell population was used as the measure of transduction efficiency. The plate-based method yielded a higher transduction percentage than the column-based method (Table 3).

**Engineering of a microfluidics device for use in lentiviral transduction**

The novel microfluidics device design (Figure 1) enables an immobilized non-adherent cell layer to be homogeneously exposed to lentiviral media. All fluorescent cells were counted in a binary manner and compared to the total amount of cells counted in the phase contrast image. Via image analyses with ImageJ (National Institutes of Health, Bethesda, MD), cells with a gray value between 1350 and 4095 (at 12 bpp) fluorescence units were considered to be positive for GFP, which served as our marker for successful lentiviral vector gene transfer. The variability in transgene expression, demonstrated by the heterogeneity of fluorescence intensity among the cells, is due to position-effect variegation, which is caused by integration of the transgene at semi-random genomic sites that display differential permissivity to the transcriptional machinery and subsequently lead to varying levels of mRNA production [110]. It was expected from our previous lentiviral transduction studies using this cell line under static tissue culture conditions that, at the MOI utilized, approximately 5%–10% of the K562 cells would be genetically modified [136, 138]. Previous results have shown that transduction efficiency can be improved by automating a syringe pump to perfuse, come to rest, and reperfuse in cycles to allow viral particles to come into contact with cells through Brownian motion before exchanging viral media through perfusion [139]. A similar protocol should be amenable to the hybrid PS-PDMS device and should allow for even more efficient transduction and reduced viral vector requirements, which currently is a major barrier to clinical use as vector manufacturing is inefficient and costly. The results indicate a successful transduction of the K562 cells using lentivirus containing the GFP transgene perfused through the microfluidics device (Figure 6).

**Figure 6**

**Figure 6 K562 cells transduced in the hybrid PS-PDMS device.** (a) Phase contrast image of K562 cells immobilized in the divots. (b) Fluorescence image of cells expressing GFP after 24 h of perfusion of lentiviral media followed by a 96 h incubation period. Cells can be seen expressing GFP at various levels. Scale bar = 100  $\mu\text{m}$  [112].

**Factors That Increase Transduction in Standard Systems Are Amplified in Microfluidics.**

Having established the method for producing a microfluidics device capable of transducing the human cell line K562, the next steps were to compare transduction in this device to similar conditions in a 6-well plate. These experiments used a microfluidic system that could accommodate  $1 \times 10^6$  cells for direct comparison to transduction in a 6-well plate. In this setup, the number of infectious viral particles, cell numbers, and time of transduction were kept constant between the two systems. Increasing the number of infectious units (and thus the MOI) improved transduction in both systems, which further highlights the concentration dependence of LV transduction. However, the microfluidics system outperformed the six-well plate in all head-to-head comparisons. Higher transduction in the six-well plate was only achieved by using 6-fold more virus than the microfluidic and for transduction times greater than 12 hr. The viral supernatant collected at each time point and used for secondary transductions on naive Jurkat cells also confirmed that less lentivirus was wasted in the microfluidics device [140]. Overall, these data indicate the successful development and use of an alternative to plate transductions that can produce increases transduction efficiency.

### **Transduction of $\gamma\delta$ T-cells with AAV6 GFP**

The AAV6 vector used in these experiments is depicted in figure 7A. It contains AAV2 ITRs, along with a CMV promoter controlling expression of a  $\beta$ -globin intron as well as the GFP gene. The SV40 polyadenylation (poly-A) sequence is included to increase transgene expression. The lentiviral vector used to produce virus contains an eFl $\alpha$  promoter driving expression of the GFP gene (figure 7B). To titer the virus created from these two constructs, a functional titer was calculated. In this assay, Jurkat cells are transduced with each GFP containing virus. The titer is based upon the percentage of transduced cells per viral volume. In the AAV6-GFP virus, the functional titer was calculated to be  $5.53 \times 10^7$  (figure 7C). For the lenti-GFP virus, the titer was calculated to be  $9 \times 10^7$  (figure 7D). Each of these constructs was used to transduce  $\gamma\delta$  T-cells obtained from culture of human peripheral blood mononuclear cells (PBMCs). The  $\gamma\delta$  T-cells were distinguished in culture using antibodies to CD3 and  $\gamma\delta$  TCR (figure 7E). The AAV6 transduction was performed at MOI 0.5, 1.5, 15 while the lentiviral transduction was performed at MOI 30. The transduction efficiency was assessed via flow cytometry and showed a dose response to increasing MOI as it rose from MOI 0.5 to MOI 15. At the highest MOI,  $\gamma\delta$  T-cells were nearly 100% transduced (figure 7F). In comparison, the highest percentage of GFP positive cells obtained through lentiviral transduction was below 20% (figure 7G). The limit to lentiviral transduction MOI is determined as the maximum volume of virus that still maintains a high population of viable cells. In previous studies, the volume virus that could be added before adversely affecting the transduced cell viability was determined to be approximately 30% of the culture volume (data not shown). In the AAV6 transduced samples, although the level of transduction decreased as the MOI was lowered, there remained relatively high levels of transduced cells as compared to lentiviral transduction (figure 7H).

Figure 7

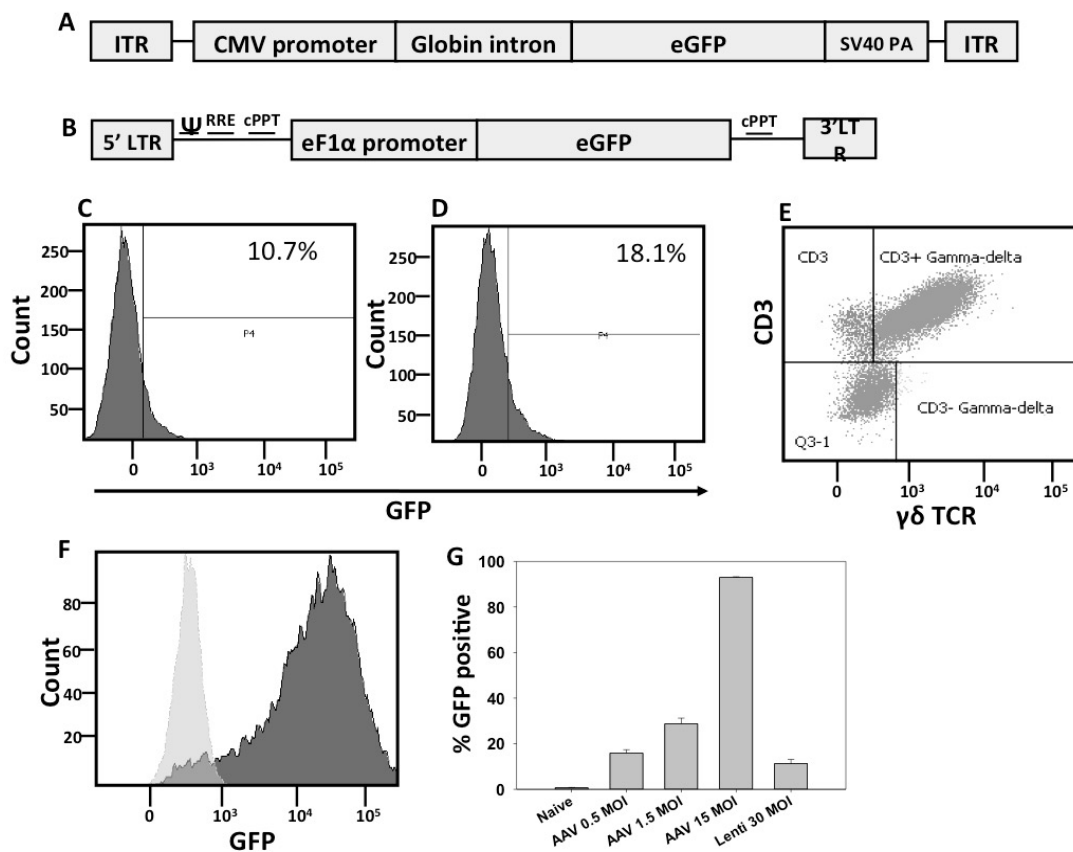


**Figure 7. Schematic of AAV6 and Lenti GFP transgene, gamma delta T-cell enrichment, and transduction with AAV6 GFP.** A. Schematic of AAV6 GFP transgene. ITR: inverted terminal repeat, CMV: cytomegalovirus, eGFP: enhanced green fluorescent protein, SV40 PA: simian virus 40 polyadenylation signal. B. Lenti-GFP transgene; Percentages of gamma-delta T-cells in transduced culture as measured by flow cytometry. C. Functional titer of AAV6-GFP on Jurkat cells with virus diluted 1:5. D. Functional titer of lenti-GFP on Jurkat cells with virus diluted 1:5. E. Separation of PBMC culture using antibodies CD3 and  $\gamma\delta$  TCR. F. GFP positive gamma-delta cells 4 days post transduction at MOI 15. G. Graph showing the transduction of gamma-delta T-cell enriched culture with Lenti-GFP at MOI 30 and AAV6 GFP at MOI 0.5, 1.5, and 15.

**Transgene expression in primary cells after AAV6 GFP transduction**

In the population of primary human PBMCs that were transduced with AAV6-GFP,  $\alpha\beta$  T-cells and NK cells cell types were analyzed for expression of GFP via flow cytometry.  $\alpha\beta$  T-cells were analyzed in the population using CD3 and  $\gamma\delta$  TCR antibodies and selecting for the CD3+,  $\gamma\delta$  TCR- population. Of the analyzed populations, the  $\alpha\beta$  T-cells exhibited the most comparable transduction levels between lentivirus and AAV6, however even at the lowest MOI, AAV6 transgene expression was significantly higher than that obtained via lentiviral transduction (figure 8A). The NK-cell population was selected for as the CD3-,  $\gamma\delta$  TCR- population. The results indicate low-level transduction in all populations analyzed, excluding the highest MOI of AAV-GFP (figure 8B). In both NK and  $\alpha\beta$  T-cells, transduction at the highest MOI showed greater than 60% transduction. In the lentiviral transduction, percentage of GFP positive cells remained below 30%. Viability was also assessed in the transduced populations as a percentage of the total viable cells in the PBMC transduced compared to naïve culture. In each transduced population, viability remained above 70% (figure 8C), indicating a low level of transduction associated cell toxicity.

Figure 8

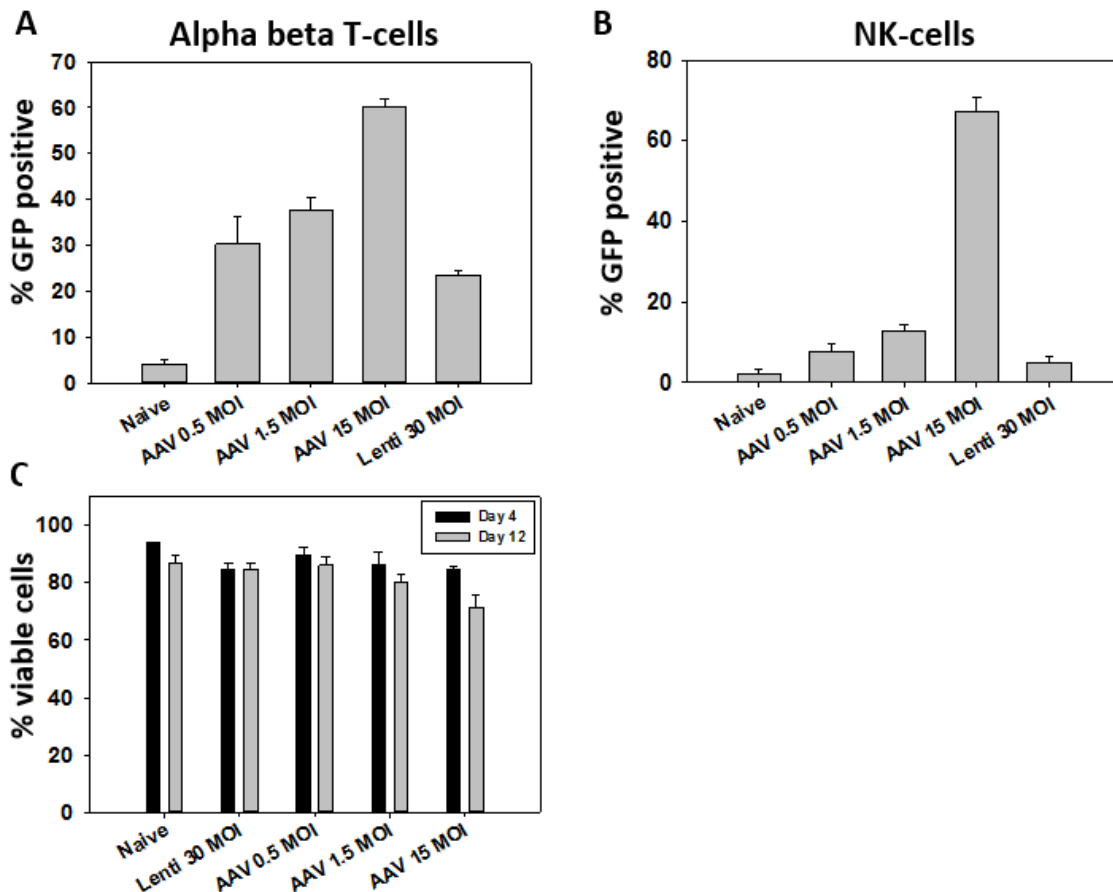
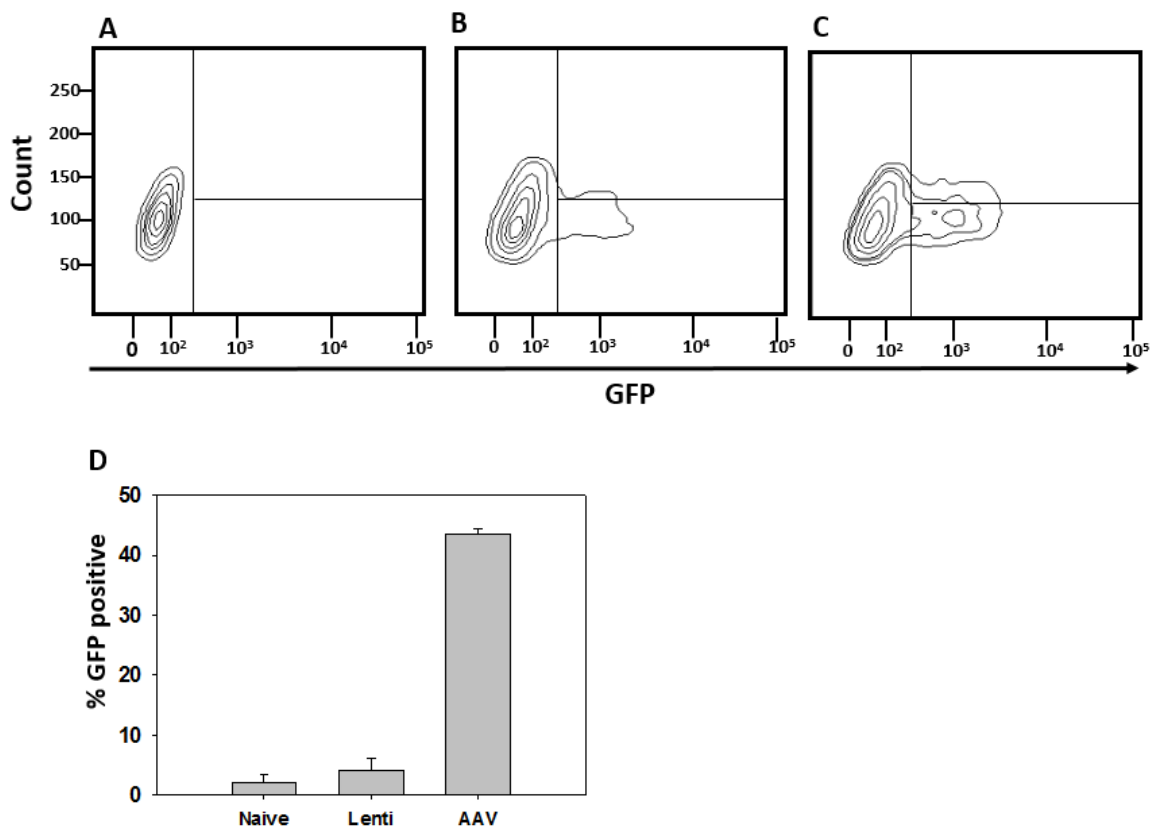


**Figure 8. GFP expression and viability in AAV6 GFP and Lenti-GFP transduced cell lineages.** A. GFP positive percentage of alpha beta T-cells in a culture transduced with Lenti-GFP at MOI 30 and AAV6-GFP at MOI 0.5, 1.5, and 15. B. GFP positive percentage of NK-cells in a culture transduced with Lenti-GFP at MOI 30 and AAV6 GFP at MOI 0.5, 1.5, and 15. C. Graph showing cell viability over time in cultures transduced with Lenti-GFP at MOI 30 and AAV6 GFP at MOI 0.5, 1.5, and 15.

**AAV6 and lentiviral transduction of cells with AAV6 GFP**

NK-92 cells are an immortalized cytotoxic cell line derived from human NK cells [97, 98]. They can be propagated in culture in the presence of IL-2 and provide an effective cell type through which the CAR construct may act to direct target cell killing [141]. In previous transductions [95] and also reported in Figure 9B, lentiviral vectors show low levels of transduction (~5%) in NK-92 cells. Transduction with AAV6 significantly increases the percentage of GFP expression in transduced cells compared to that observed with lentivirus and has shown transduction levels around 45% with MOI 15 (Figure 9C). A comparison of the transduction efficiency between lentivirus at MOI 30 and AAV6 at MOI 15 shows the improved transduction obtainable through the AAV6 vector (Figure 9D). The results from these transductions show the same trend that was observed with transduction of human primary cells, where AAV6 provides an improved method for gene transfer over lentivirus.

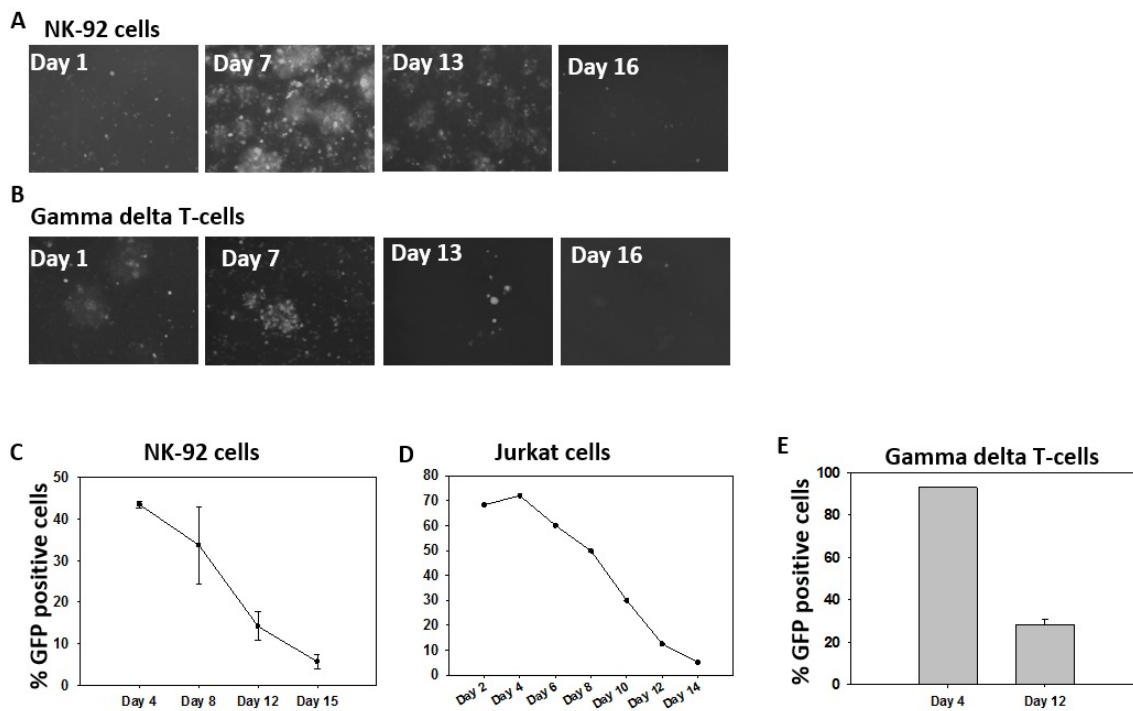
Figure 9



**Figure 9 AAV6 GFP transduction of NK-92 cells.** A. Naïve NK-92 cells show no GFP expression. B. Lenti-GFP transduction of NK-92 cells show a slight shift in GFP positive cells to 9.8% when analyzed via flow cytometry. C. AAV6 GFP transduced NK-92 cells show a significant shift in GFP positive cells to 45.6% as analyzed via flow cytometry. D. Graph depicting the GFP positive percentages in transduced NK-92 populations compared to naïve cells.

**AAV6 transgene expression over time**

To determine the length of transgene expression in the selected effector cell types NK-92, Jurkat cells, and  $\gamma\delta$  T-cells were monitored for GFP expression over time. GFP expression can be seen to visually decrease in transduced cells: NK-92 (Figure 10A) and  $\gamma\delta$  T (Figure 10B) when examined via fluorescence microscopy. The same cells were also assessed for GFP expression via flow cytometry. The results indicate transgene expression in NK-92 cells transduced at MOI 10 peaks around 45% and decreases steadily to below 10% by day 12 post-transduction (Figure 10C). In Jurkat cells, a similar trend is observed where transgene expression decreases steadily to drop below 10% GFP positive cells by day 14 (Figure 10D). Transduced populations of  $\gamma\delta$  T-cells were assessed for GFP expression via flow cytometry on day 4 post-transduction and day 12 post-transduction (Figure 10E) and show a similar rate of loss in GFP expression. Overall, GFP expression is maintained above detectable levels for approximated 14-15 days in the assessed cell types.

**Figure 10**

**Figure 10 AAV6 transgene expression decreases over time.** Fluorescent microscopy images showing the initial GFP expression following transduction with AAV6 GFP and the decline in GFP expression over the course of 16 days in A. NK-92 cells and B. Gamma Delta T-cells. C. NK-92 cells were transduced with AAV6 GFP and GFP expression was followed over a 15 day time course via flow cytometry. D. Jurkat cells transduced with AAV6 at MOI 0.5 and monitored over a 2-week time course. Gamma delta T-cells were transduced with AAV6 GFP and GFP expression was measured via flow cytometry on day 4 and day 12 following transduction.

**Expression and functional assessment of CD5 CAR transgene in transduced NK-92 cells**

Due to the promising results obtained from AAV6 transduction of primary human cells and human cell lines, we next sought to determine the functionality of the CAR construct in transduced cells. To accomplish this, a CD5 directed CAR was cloned into the AAV6-GFP vector used previously. The resulting transgene contains a CD5 directed CAR separated from a GFP gene by a P2A sequence (Figure 11A). This arrangement would allow for co-expression of GFP and the CD5 CAR construct and subsequent identification of positively transduced cells. A functional titer was also performed using virus created from this transgene. The results give a titer of  $2.2 \times 10^6$  (Figure 11B). NK-92 cells were selected as the effector cell type based upon their ability to kill target cells as well as the absence of the CD5 receptor on their cell surface. Naïve (Figure 11C) and transduced (Figure 11D) NK-92 cells were assessed via flow cytometry. Transduction of these cells with AAV6 at MOI 2.5 resulted in GFP expression in ~50% of cells (Figure 11D). Jurkat cells transfected with the AAV6 CD5 CAR were also shown to bind to the CD5 protein in an assay involving co-culture of purified CD5 protein fused to an antibody Fc region (Supplementary Figure S1). The results of this assay demonstrate that the CD5 CAR construct on transduced effector cells is both present and functional (Figure 11E).

Figure 11

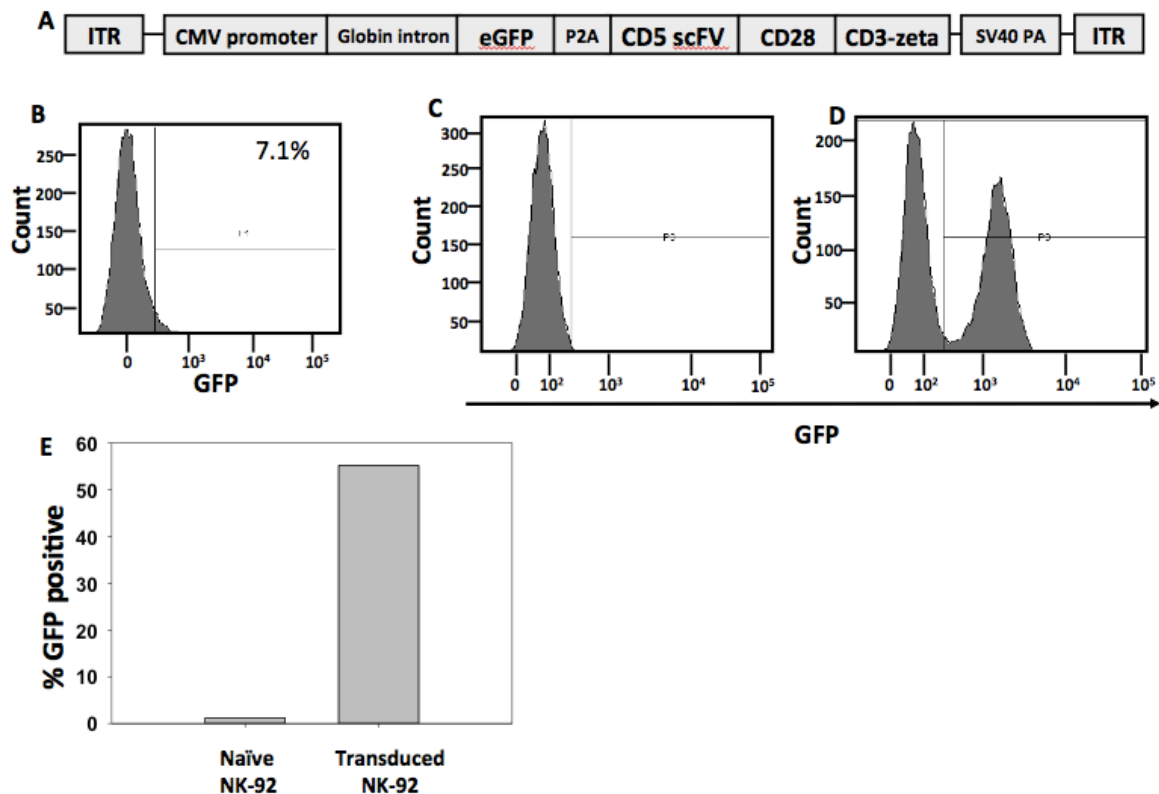


**Figure 11: Schematic of CD5 AAV6 transgene and GFP expression in naïve and transduced NK-92 cells.** A. Schematic showing the AAV6 CD5 transgene; ITR: inverted terminal repeat, CMV: cytomegalovirus, eGFP: enhanced green fluorescent protein, P2A: porcine teschovirus-1 2A, SV40 PA: simian virus 40 polyadenylation signal. B. Functional titer of AAV6-CD5 CAR virus. C. Naïve NK-92 cells show no GFP expression. D. NK-92 cells transduced with the GFP CD5 AAV6 vector show ~55% GFP positive cells. E. Graph showing GFP percentage in transduced vs. naïve NK-92 cells.

### **Targeted cell killing via AAV6 delivered CAR transgene**

To demonstrate the functionality of the AAV6 delivered CAR transgene in vitro, a cytotoxicity assay was performed. In this assay, AAV6 CD5 CAR virus (Figure 11A) was used to transduce NK-92 cells at MOI 2.5. The assay was then performed by co-culturing the transduced NK-92 cells with Jurkat cells expressing CD5, the CAR target antigen. After incubation, the relative target cell death was determined via flow cytometry. In the co-culture assay on naïve NK-92 cells performed at effector: target (E:T) ratio of 1:1 (Figure 12A) or 5:1 (Figure 12B) there was no observable target cell death. When CD5 CAR transduced NK-92 cells were co-cultured with the target Jurkat cells at E:T ratio of 1:1 there was a statistically significant increase in target cell death to ~30% (Figure 12B). The ratio of effector to target cells was then increased to 5:1, and there was again observed a significant rise in target cell death as it increased to ~60% (Figure 12D). The overall dose response to an increase in the AAV6 transduced effector cell to target cell ratio compared to naïve can be seen in Figure 12E. The results from this assay indicate that the AAV6 CAR transduced NK-92 cells were able to effectively identify and kill the target cells at a higher rate than naïve NK-92 cells, implying the transduced cells are appropriately producing and expressing the CAR protein.

Figure 12

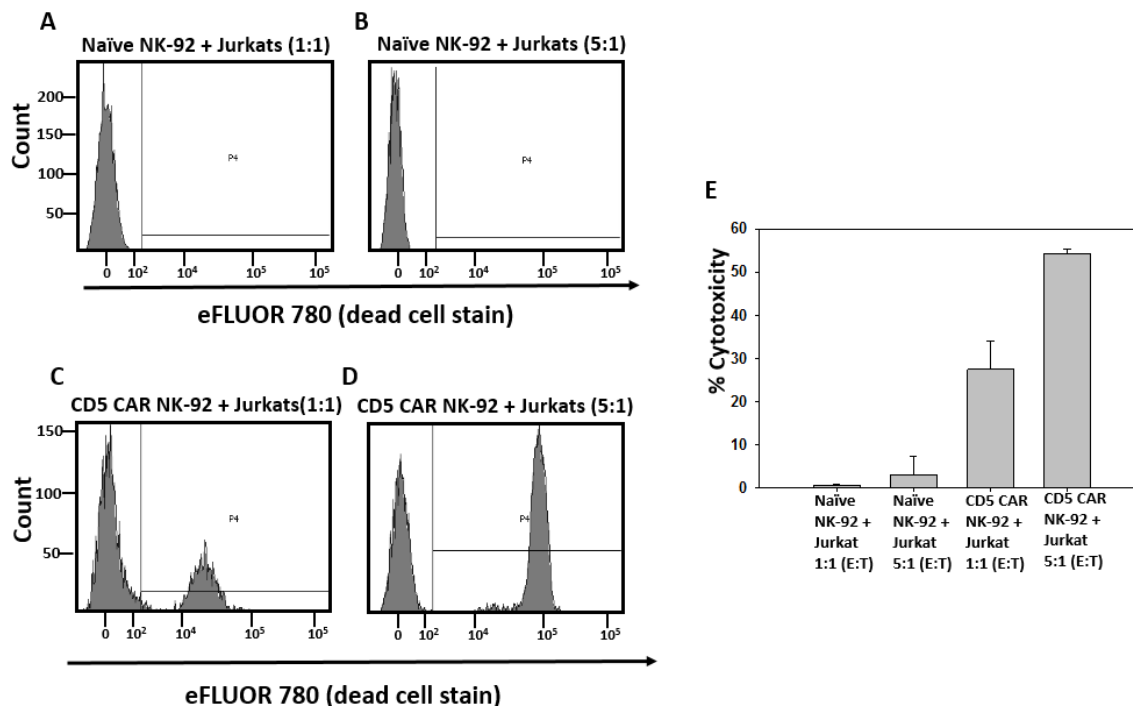


**Figure 12: NK-92 cytotoxicity assay with Jurkat cells** NK-92 cells were labeled with a membrane dye then co-cultured with Jurkat cells for 4 hours. Results from flow cytometry show percentage of dead cells in culture as measured as percentage of cells positive for eFLUOR 780 dead cell stain. A. Naïve NK-92 cells were co-cultured with Jurkat cells at E:T ratios of A. 1:1 and B. 1:5. NK-92 cells were transduced with CD5 CAR AAV6 virus and co-cultured at E:T ratios of C. 1:1 and D. 1:5 with Jurkat cells. E. Graph depicting the results of the cytotoxicity assay.

#### 4.4 Discussion

In these experiments, several alternate methods to improve transduction were investigated. The first method focused on the use of a small molecule as a means to increase target cell transduction. The subsequent 4 methods focused on increasing the concentration of virus on the target cells. Although several of these techniques were unsuccessful, the microfluidics device was able to overcome many of the limitations imposed on transduction by Brownian motion and successfully increase the transduction efficiency in target cells. Another alternate method for improving gene transfer used AAV6 as the viral vector as opposed to the lentivirus used in the previous transductions. In transduction experiments with AAV6, there were significant benefits observed across several cell types of both innate and adaptive immune cells. Together, these methods provide a promising approach to increase transgene expression in the effector cells.

The first method investigated to improve transduction aimed at identifying a small molecule that would allow for increases in target cell transduction. Through a high-throughput screening process, a library of 1280 pharmacologically active compounds was screened for the purpose of identifying enhancers of lentiviral transduction. Through this screen, PMA was identified as a positive hit. Assessment of the impact of pretreatment with PMA was performed with K562 cells. In these experiments, a fourfold increase in modified cells was apparent when culturing with PMA before transduction. This increase was achieved at a concentration as low as 2.5nM PMA. Observation of the cell treated with PMA indicated that cellular proliferation was inhibited, suggesting that this inhibition of the cell cycle might be a method whereby PMA exhibits its effects, however, the exact method whereby arresting cellular proliferation results in a favorable cellular condition for lentiviral gene transfer is unknown. As a phorbol ester, PMA binds to the C1 domain of PKC resulting in PKC translocation and activation. Eight PKC isoforms are activated by PMA and have been implicated in an array of cellular processes. Further analysis is needed to assess the mechanism by which PMA is enhancing lentiviral transduction [136]. In

addition to PMA, the combination of PMA with rapamycin was also assessed. Rapamycin has previously been identified as an enhancer of lentiviral transduction [107] and combination of rapamycin with PMA may have potentially synergistic effects that would allow for even greater increases in transduction. The results of these studies indicate a modest increase in transduction efficiency obtained with a combination of PMA and Rapamycin, however, there was also a corresponding increase in toxicity associated with the use of both compounds. Overall, these results indicate PMA may provide benefit to lentiviral transduction and that combination with rapamycin may improve upon this increase if cell viability can be maintained.

Initial studies aimed at improving transduction efficiency focused on decreasing the reliance on Brownian motion as the determining factor of whether a particular viral particle would make contact with a target cell. In these studies, several methods were tested with the intention of increasing the concentration of virus on the target cells. The first method attempted involved the use of poly-L-lysine coated glass or PTFE tubing with diameters of between 0.005 and 0.01 inches. A major difficulty limiting the success of this method was the inability to effectively bind the target cells in the tubing. The result was a loss of cells from the device and a corresponding drop in transduction efficiency. Another method sought to concentrate the virus onto the target cells using Amicon Ultra centrifugal filter units. These units were selected for this study with the idea that they would concentrate lentivirus onto cells that had been seeded into the column. Despite several attempts, cell viability following transduction remained a significant obstacle. A third technique, also designed to increase viral concentration on target cells, used a packed column in a magnetic field in which labeled target cells would be immobilized. This method was also unsuccessful likely due to the observation that transduction of target cells was reduced in the several days following labeling with the magnetic dynabeads. Although none of these methods succeeded in increasing transduction in the target cells, the concept of increasing viral

concentration on target cells and therefore increasing the probability of viral infection was eventually validated through the use of a microfluidics device.

To overcome the limitations of the previous studies, a collaboration was established with GA Tech to develop and test a microfluidics system that could be tailored to the needs of lentiviral transduction. The device eventually developed was PS-based and engineered specifically for use in biological experiments. It was intended to demonstrate that the inclusion of controlled perfusion rather than passive pumping or other methods of fluid exchange could improve this class of devices to create more physiological cell culture environment, as well as improve the transduction efficiency in target cells. Along with establishing the method of producing the microfluidics device, these initial studies were followed by results in which the microfluidics device showed successful increases in transduction initially in K562 cells and then as follow up studies in primary human cells when compared to the standard plate based method of transduction. These results confirm the effectiveness of the device as a method of lentiviral transduction and provide a platform upon which future studies may increase transduction efficiency.

The objective of the next set of experiments was to establish AAV as an effective vector for transfer and expression of a CAR transgene in immune effector cells as well as demonstrate the functionality of the CAR construct when expressed in these effector cells. The selection of AAV6 as the serotype for use in these studies was based upon previously published results in which AAV6 was shown to transduce cells of the hematopoietic lineage at significantly higher levels than any of the other 9 serotypes evaluated [39, 142, 143]. Based upon these studies, we hypothesized that the AAV6 serotype would provide an alternative method for efficient delivery of a CAR transgene into several immune cell types that have previously proven difficult to transduce.

Although a majority of previous studies have focused on the use of alpha beta T-cells as the primary driver of CAR activity, there are several innate cell types that may each provide some benefit to CAR mediated tumor cell killing that is not realized with alpha beta T-cells [144]. Herein, we sought to establish AAV6 as an effective vector for gene transfer into several of the innate cell types relevant to CAR immunotherapy. These included human primary NK cells, NK-92 cells, and  $\gamma\delta$  T-cells.  $\gamma\delta$  T-cells, in particular, have several unique characteristics that can act to enhance the impact of CAR therapy. Included among these are the ability for alpha beta T-cell priming, an apparent lack of alloreactivity, MHC-unrestricted antigen recognition, and broad recognition of cancerous ligands [144]. NK cells as well as NK-92 cells have also been shown to be a potent alternative to alpha beta T-cells in CAR therapy, with reports indicating many of the same benefits of  $\gamma\delta$  T-cells, such as MHC-unrestricted antigen recognition [144]. Additionally, both primary NK cells and the NK cell line NK-92 have been shown to be capable of tumor cell targeting in vivo [98, 145, 146]. One restriction in the development of these innate cells as a CAR effectors has been in the limited gene transfer efficiency obtained with lentiviral transduction [127]. Transgene expression in  $\gamma\delta$  T-cells transduced with lentiviral vectors has been previously reported to be approximately 20-30% [125, 137]. A similar trend has been observed in primary NK and NK-92 cells, where average transduction efficiency of primary NK cells has been reported across a majority of studies to be in the range of 15-40% [127, 147]. Limited transduction efficiency in NK-92 cells has been reported with some studies indicating a maximum of 25% gene modified cells [128]. Due to these limitations and the potential of these innate cells to deliver several unique benefits not realized with alpha beta T-cells, a method for efficient viral transduction is needed. The results provided herein, with gene transfer efficiency of approximately 50% in transduced NK-92 cells and nearly 100% in  $\gamma\delta$  T-cells, indicate AAV6 may overcome many of the limitations in innate cell transduction experienced with lentivirus. These high levels of transduction relative to that obtained with lentivirus and the potential for

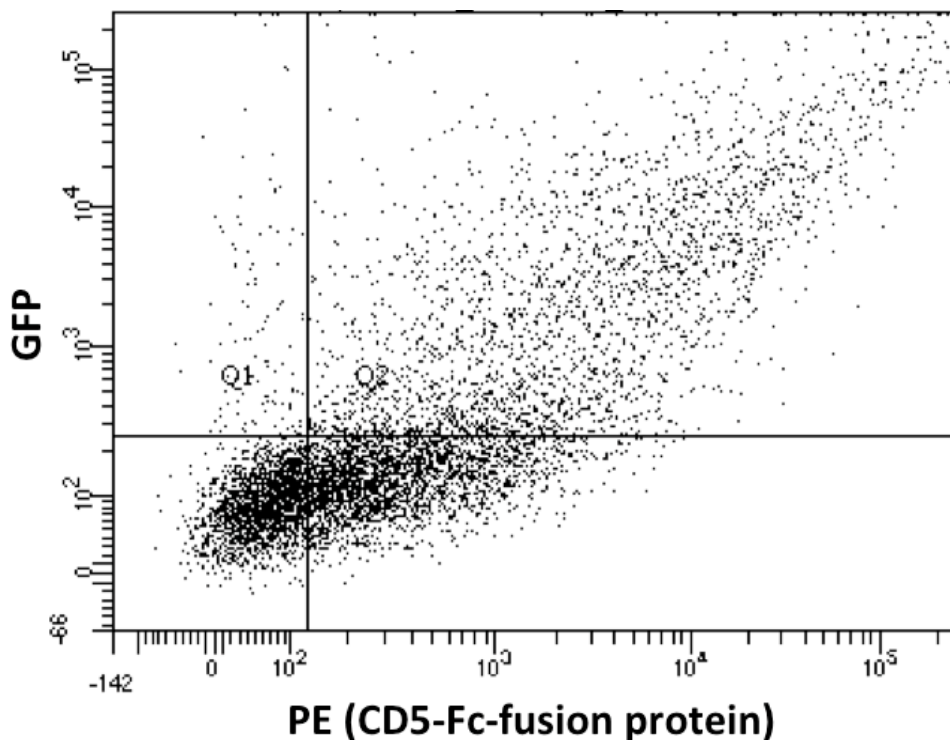
increasing MOI while maintaining cell viability position AAV6 as a promising viral vector for CAR therapy.

Another consideration in the use of CARs as a cancer therapeutic is the longevity of the transduced cells and subsequent length of expression of the CAR transgene in the patient. Because AAV6, used in these studies, is a non-integrating virus, its expression is diluted out during cell division [35]. This characteristic of AAV consequently provides a much greater control over the length of expression of the viral transgene. In previous studies it has been noted that there would be a benefit to a more controlled expression of the therapeutic transgene in cases where continued expression of the CAR after serving its therapeutic purpose is undesirable [122, 148]. An example of this would be in trials where the CAR directs T-cell killing toward a common cell type with the intent to eliminate the entire population of cells, included in them the tumor cells. After the patient enters remission, continued targeting and killing of these cells may be deleterious to the patient as it prevents regeneration of the original, healthy cells [149]. In the results above, a tentative timeline for transgene expression was established in  $\gamma\delta$  T-cells and NK-92 cells. The approximately 2-week timeframe for expression would allow for more precision in transgene delivery as well as finer control over side effects.

To finalize the studies and demonstrate the functionality of the CAR delivered via AAV6, a CAR containing an scFv directed against CD5 was cloned into the AAV6 vector to be co-expressed with GFP. Transduction of NK-92 cells with this vector was used to demonstrate the functionality of the CAR construct after AAV6 delivery of the transgene. NK-92 cells are an innate cell type that have been used previously as effector cells in CAR trials [141, 150]. The results from the cytotoxicity assay performed with CD5 expressing Jurkat cells indicates the CAR construct expressed in the effector cells is functional and capable of directing the transduced NK-92 cells to specifically target and kill the CD5 expressing Jurkat cells. These results establish AAV6 as an

effective alternative for delivery of a CAR transgene and provide confirmation of the functionality of the CAR in transduced cells.

In conclusion, and based upon the results presented herein, two potential methods for increasing target cell transduction have been established. The microfluidics technique established a method for seeding and transducing cells in an engraved polystyrene device as well as allowed for increases in lentiviral transduction efficiency over the standard plate-based method. In transduction with AAV6, it was shown to be a more effective transgene delivery vector than the more commonly used lentivirus as it demonstrated an improved efficiency in transduction of several innate effector cell types as well as other cytotoxic cells. Together, these results position both the microfluidics approach as well as AAV6 as two viable options for improving transduction moving forward.

**Supplementary Figure S1**

**Supplementary Figure S1: Flow cytometry showing binding of CD5 CAR transfected HEK 293 cells to CD5-Fc fusion protein 293T cells transfected with the CD5 CAR transgene in the AAV expression vector co-culture with CD5-Fc-fusion protein** Flow diagram showing the binding of CD5 CAR expressing 293T cells that are capable of binding the CD5 protein after transfection. The cells in quadrant Q2 are expressing the CAR transgene as measured by GFP expression and have successfully bound the CD5 protein as measured by staining with PE anti-CD5 antibody.

## **Discussion and future directions**

## Chapter 5

### 5.1 Discussion

Together, the results provided herein improve on the technology available for antigen recognition by cellular immune receptors as well as introduce a method to increase viral gene transfer efficiency. Broadening immune receptor antigen recognition is accomplished through the generation of an antigen-specific VLRs. As the structure and binding geometry of VLRs differs greatly from that of immunoglobulin based antibodies, these receptors may afford the potential for binding a greater diversity of antigens than that obtainable through immunoglobulin-based antibodies alone. To further develop this technology, VLR-CARs have been constructed from the antigen specific VLRs and cloned into an expression vector. Introducing this CAR construct into an immune effector cell has shown evidence of CAR functionality in the form of effector cell activation and directed target cell killing. The impact of this research is that it offers a procedure to produce VLRs thereby expanding the repertoire of potential target antigens by allowing for binding to either novel antigens or novel antigen epitopes [76]. Two methods to improve the efficiency of gene transfer into a selected immune effector cell are also provided along with this evidence of VLR generation and function in a CAR. These two methods include transduction using a microfluidics system and transduction with AAV6. The improvements in transduction achieved via the methods detailed above present a means of overcoming the low gene transfer efficiency of lentivirus as well as a method for effective gene transfer to innate effector cells.

The methods described for antigen-specific VLR generation hold relevance in numerous applications. Monoclonal antibodies have revolutionized research approaches as well as disease treatment, but refining of these methods has traditionally focused on improving the antibody delivery or specificity with little research dedicated to uncovering any alternatives to these antibodies. As the primary lamprey immune receptor and counterpart to immunoglobulin based

antibodies, the VLR provides a unique approach to targeted antigen recognition. The lamprey immune system is comprised of clonally diverse lymphocytes, each displaying a unique VLR, which, through alternate splicing, can generate a diversity of unique immune receptors in the range of  $10^{14}$  [74]. Generating receptor diversity in the lamprey VLR is accomplished in the maturing lamprey immune cells. Germ line cells responsible for production of the VLR bearing mature immune cells have an incomplete VLR gene. Combinatorial splicing of LRRs flanking the VLR gene into predetermined regions within the gene generates a unique receptor in the mature immune cell. This method of VLR generation is used in the lamprey to produce three distinct types of immune cells: VLR-A, VLR-B, and VLR-C, with VLR-B responding to immunization with an exogenous antigen by clonal expansion and secretion of a soluble VLR-B protein [151]. The VLR-B protein produced in this process contains a large concave surface containing  $\beta$ -sheets of high sequence variability, which are believed to be the region responsible for antigen binding [74]. As a result of the structural disparities between the lamprey VLR and immunoglobulin-based antibodies, VLR binding can result in interactions with antigen epitopes unique to the VLR and not recognized by antibodies [76]. Additionally, in generating VLRs, lampreys are not subject to the same constraints of self-tolerance that make certain antigens invisible to the immune system of traditional animal models used in antibody generation [152]. Because of this, immunization of the lamprey, may uncover antigens previously unavailable for targeting by immunoglobulin-based antibodies. Taken together, these qualities of the VLR position it as a promising candidate for development as alternative to traditional antibodies.

## **5.2 Results and implications**

The process to generate VLRs against a pre-specified antigen, as outlined herein, was used to produce VLRs against both a B-domain deleted human-porcine chimeric FVIII protein as well as the neuroblastoma cell line SK-N-Be(2). Through these experiments, a process was defined for VLR generation against both a soluble protein as well as a tumor cell line. Although each

experiment was developed to a different stage, collectively the results demonstrate an effective method for antigen specific VLR production. The production of anti-FVIII VLRs was successful in demonstrating a positive immune response in immunized lampreys as well as the presence of anti-FVIII VLRs in the plasma of the immunized lampreys. Although the ELISA data indicating the presence of anti-FVIII VLRs did not show a dose response, this result is to be expected as each lamprey is expected to respond differently to immunization.

To begin the task of identifying an anti-FVIII VLR, the entire assembly of unique VLR genes present in the immunized lamprey was amplified from the cDNA obtained from the RNA of the lamprey lymphocytes. Successful amplification of the VLR genes from the FVIII immunized lampreys was demonstrated through gel electrophoresis and imaging that showed the collection of VLR genes ranging in size from ~500 base pairs to over 800 base pairs. To refine the pool of VLRs to include only those containing the anti-FVIII VLRs, a plasmid was designed that the polyclonal VLR assortment could be cloned into. When transformed into yeast, a fusion protein between the VLR and a yeast cell surface flocculation protein would be produced allowing for high-throughput screening of the VLR library. Currently the polyclonal library of anti-FVIII VLRs has been amplified with primers that created a unique restriction enzyme cut site that would allow these sequences to be cloned into the yeast expression plasmid.

To develop the anti-neuroblastoma VLRs described above, lampreys were immunized with SK-N-Be(2) cells in three injections spread across 6 weeks. Presence of anti-SK-N-Be(2) VLRs in the lamprey plasma was verified using a flow cytometry based method wherein the target cell line was incubated with the lamprey plasma. SK-N-Be(2) binding VLRs were then identified by labeling with an anti-VLR antibody and screening the cells via flow cytometry. Once confirmed, the total collection of VLR genes were amplified from the lamprey RNA using the same method described for FVIII. The resulting VLR library was cloned into a plasmid expression vector that,

when transformed into yeast, displayed the VLR on the yeast cell surface. This yeast surface display was then used to narrow the VLR library to include only binders to SK-N-Be(2) cells by sorting for yeast cells displaying a VLR capable of binding molecules present in biotinylated SK-N-Be(2) cell lysate. To further refine the VLR library after sorting, individual VLR-yeast clones were selected and grown. Screening to show binding to biotinylated SK-N-Be(2) lysate allowed for selection of 10 clones displaying SK-N-Be(2) binding VLRs. The VLR genes in these yeast clones were then sequenced and used to create synthetic DNA fragments that could be cloned into a CAR transgene. Expression of these VLR-CAR constructs in Jurkat cells via lentiviral transduction was then used to further identify VLRs that would function to effectively direct the Jurkat cell to recognize the target SK-N-Be(2) cell line. The results of this assay reduced the potential VLR pool to 2 candidate VLRs. Further testing of these two VLR clones was performed on a range of cell lines. The results of these tests identified a single VLR that bound preferentially to the SK-N-Be(2) cell line. Overall, the lamprey immunization and successive enrichment of the VLR library described herein, provides a validated technique to produce and identify antigen-specific VLRs.

As a way to substantiate the function of the VLR as the antigen recognition region of a CAR, a previously well-characterized VLR directed against the B-cell receptor of a mouse B-cell leukemia was used. This particular VLR was selected because the binding partner of this VLR had previously been identified. This obviated the need to determine the cell type and antigen to which the VLR was directed and move directly to testing the VLR in a CAR. To accomplish this, the BCL VLR was cloned into a second generation CAR construct under control of the human ubiquitin C promoter. The CAR construct was composed of an IL-2 signal sequence followed by a myc epitope tag, which joined to the BCL VLR. The BCL VLR was adjacent a CD28 co-stimulatory region which spanned the cell membrane and linked to the CD3-  $\zeta$  internal signaling domain. The purpose of this next phase in development of the VLR was to provide evidence the

BCL VLR CAR could be successfully produced in a human immune cell and direct that cell to recognize the intended target. Initial validation of the BCL VLR CAR was accomplished through lentiviral mediated transduction of Jurkat cells with the CAR construct. Integration into the cellular genomic DNA was confirmed using qPCR while production of the BCL VLR CAR transgene protein was confirmed using Western Blot. Cell surface expression of the BCL VLR CAR was confirmed using flow cytometry to detect transduced cells labeled with anti-myc antibody. Once expression of the VLR was confirmed, the BCL VLR CAR expressing Jurkat cells were assayed to determine CAR function. This was accomplished using a co-culture assay, the results of which demonstrated upregulation of the activation marker CD69 at a significantly higher level in Jurkat cells expressing the BCL VLR CAR co-cultured with the target BCL cells. To further assess the function of this construct, high-titer lentivirus was used to express the VLR CAR in human primary T-cells. Co-culture of these cells and subsequent staining with a dead cell marker indicated a targeted cell killing of BCL cells as assessed by flow cytometry analysis. The function of the VLR-CAR was further validated using a separate VLR, directed against the CD5 receptor. Lentiviral transduction of NK-92 cells and subsequent cell sorting for gene-modified cells yielded a population of CD5 VLR CAR expressing cytotoxic NK-92 cells. A co-culture assay performed on these cells with target cells demonstrated their ability to target and kill CD5 expressing cells. Collectively, these results suggest the VLR can effectively function as the antigen recognition region of a CAR receptor and direct the effector cell to specific recognition and killing of the predetermined target cell.

One of the primary limitations noted to impede the progress of CAR therapy is the limited gene transfer efficiency observed in effector cell transduction. Although this has been a topic of continued research, there is still significant room for improvement. The results herein indicate several potential methods that may provide a more efficient approach to gene transfer. These methods include addition of a transduction enhancing small molecule, transduction in a

microfluidics device, and transduction with AAV6. These approaches have been successful in improving gene transfer and may provide a method for overcoming obstacles posed by limited transduction efficiency in effector cells.

The first method for improving transduction involved pretreatment of the target cells with a small molecule. Compounds that may improve transduction were identified using a high-throughput screen of a library of small molecules. Using this screening method, several compounds were identified as potentially improving transduction. Of these compounds, PMA was identified as the most promising candidate based upon its limited cytotoxicity and success in improving transduction. In follow up studies that used K562 cells as the target cell line, pretreatment with PMA or PMA/rapamycin increased transduction in the cell compared to cells that did not receive pretreatment. These results indicate that addition of PMA may provide a promising method for improving transduction efficiency.

The second series of experiments sought to increase transduction by minimizing the limitations imposed by Brownian motion on the diffusion of virions in a plate transduction. Initial studies, intended to lower the transduction volume, focused on the use of either coated tubes or filters. Despite the limited success of these methods, the concept was developed further through the use of an engineered microfluidics device intended specifically for use in transduction. This device involves the use of a perfusable polystyrene microfluidics device for cell culture that can be fabricated using standard lithography and wet laboratory equipment to enable stable perfusion at shear stresses up to  $300 \text{ dyn/cm}^2$  and pumping pressures up to 26 kPa for at least 100 h. The benefit of this system is that it allows for increased efficiency of viral transduction in non-adherent suspension cells by leveraging the high surface area to volume ratio of microfluidics and adhesion molecules [112]. The rationale behind this method is that it provides a method to increase the interaction between a viral particle and the target cell. The results of this study have

identified a reproducible method to improve viral transduction. In follow up studies, this method of lentiviral transduction was shown to significantly improve transduction efficiency in human CD34 cells and mouse Sca-1+ cells. These results showed a 5-fold faster transduction time that required one-twentieth the amount of virus to achieve the same transduction levels [140].

The third method for improving transduction focused primarily on improving delivery of a CAR transgene to cytotoxic effector cells, particularly human innate immune cells. This was accomplished using AAV6. The transgene cloned into the AAV expression vector contains AAV2 ITRs, a CMV promoter controlling expression of either a single GFP gene or a GFP gene co-expressed via a P2A sequence with the CD5 CAR gene. A  $\beta$ -globin intron was included in the construct to improve AAV transgene expression in transduced cells as indicated previously [153]. The SV40 poly-A signal was added to the transgene as it has previously been shown to enhance the efficiency of the transgene expression [154]. There are currently 10 AAV serotypes in use as a viral vector for gene therapy, with each serotype having a unique integration profile. AAV6 was selected as the serotype for use in these studies based on previous results implicating it as the most effective for transduction of hematopoietic stem and progenitor cells. It was found in these studies that AAV6 transduced cells of the hematopoietic lineage at considerably higher efficiency than any of the other 9 serotypes evaluated [39, 142, 143]. The implication of these results is that AAV6 provides an effective method for gene transfer to the effector cell lines selected in this study. These cell lines include the innate cells: gamma-delta T-cells, primary NK cells, and NK-92 cells, as well as the T-cell line, Jurkat cells.

As a means to standardize the titer calculations between lentivirus and the two AAV6 vectors, we also developed a method for calculation of a functional titer. This method allows different types of virus to be titered using an identical method with calculations based upon the functional output of transduction in a selected cell type. In the previous methods, the number of genome copies of

AAV is determined using qPCR on a concentrated AAV sample while lentiviral titering is performed after transduction of a target cells and based on transgene presence in the genomic DNA of the target cell as determined by qPCR analysis. Comparing between viruses that are each titered using an alternate method is less informative than that performed using a standardized assay that can be applied equivalently to each virus. The functional assay is performed using Jurkat cells as a target cell type to which a pre-established volume of virus is added. When calculating titer using the described functional assay, a comparative titer between the two viral types can be established.

Having established AAV6 as the serotype that would yield the most effective gene transfer, initial studies were performed to determine the viability of AAV6 as a method for transduction of several cell types relevant to CAR therapy. To show transduction capacity, the AAV6 used in the initial studies contained a GFP transgene. This is compared directly to lentivirus also containing an identical GFP transgene. These AAV and lentiviral constructs were selected as they provided the opportunity for a direct comparison with an output that is easily quantifiable. The results of transduction of gamma delta T-cells with AAV6-GFP shows a high level of GFP expression as well as a dose response to increasing viral MOI. Comparison to lentivirus shows a significant increase in transduction efficiency as measured by GFP expression. This trend is also observed in the primary NK as well as  $\alpha\beta$  T-cells with transduction efficiencies increased several fold above that obtained with lentivirus. When tested on two cell lines, Jurkat and NK-92, AAV6 again provided more efficient transduction. This improvement was most significant in the NK-92 cells in which transduction with AAV6 increased more than 20 fold over that of lentivirus. Because the transduction improvements are consistent throughout the cell types tested the results suggest that AAV may provide a means of overcoming the low levels of transgene expression typically obtained in lentiviral transduction of several effector cell types. The results of these transductions indicated that AAV6 provides an effective method for gene transfer to several innate cell types.

The benefit of this is it provides a method to overcome the limited transduction efficiency seen in many studies that have investigated innate cell types as a CAR effector cell [125, 127, 137].

### **5.3 Future directions**

Follow up studies are necessary to finalize the data in several of the studies outlined above. In the studies involving the anti-FVIII VLR, the VLR library needs to be cloned into the yeast expression vector and transformed into yeast. This will allow the polyclonal library to be refined sequentially through further screening steps. The result will be several VLR clones identified as FVIII binders. The next steps would then be to determine the domain of the FVIII molecule that these VLRs bound. This would provide information on whether these selected VLRs can provide any additional benefit over that of the current antibodies available.

In the experiments involving the generation of the neuroblastoma specific VLRs, identifying the antigen bound by the VLR will be important in validating the results of the VLR isolation and testing. This would also provide information on whether the VLRs had bound to a unique antigen on the neuroblastoma surface that has not been targeted by immunoglobulin-based antibodies. Additionally, testing this VLR CAR in cytotoxic immune cells would provide additional evidence of the directed function of the VLR.

### **5.4 Conclusions**

Collectively, the data presented herein provide several methods to enhance research in several fields. The evidence indicating successful generation of antigen specific VLRs through lamprey immunization has been shown with both a soluble protein and a tumor cell line. Furthermore, VLRs generated through this process have been shown to be functional as the antigen recognition region of a CAR construct. Finally, as a means to improve transduction of effector cells, two methods have been investigated that have shown promising results. Improvements in lentiviral

transduction efficiency have been obtained using a microfluidics device and transduction of innate immune cells with AAV6 has shown increases in efficiency over that obtained with lentivirus.

The results relating to the production of antigen-specific VLRs are important as they provide a validated method by which VLRs may be raised against either soluble proteins or cancer cell lines. The relevance of this development is that the VLR may offer a method for either increasing the number of targetable antigens or provide a means to target antigen epitopes that are unavailable to traditional antibodies. As availability of cancer cell epitopes has delayed progress in the development of CAR technology, the ability of the VLR to potentially recognize novel antigens or antigen epitopes shows promise in improving the application of this technology to an increasing number of cancer types. The results indicating the VLR can function to effectively direct CAR effector cell cytotoxicity have further validated the use of the VLR as an effective alternative to antibodies.

A significant limitation in the application of gene therapy to disease treatment is the efficiency of target cell transduction. Several recent studies have indicated a reduced ability of lentivirus to effectively transduce several effector cell types [125, 137]. Overall, methods that improve gene transfer to the target cells would improve the status of gene therapy as an approach to treatment of genetic diseases. The microfluidics method described herein provides another approach that has been shown to improve the efficacy of lentiviral transduction. As lentivirus is one of the most common viral vectors for gene therapy, this method of increasing transduction is valuable in increasing the success of this vector in disease treatment. Although lentivirus has proven successful in many applications, several studies indicate a reduced ability to effectively transduce many innate cell types. Transduction with AAV6 has overcome these limitations and proven to be an effective vector for delivery of a transgene to gamma delta T-cells, primary NK cells, and NK-

92 cells. The implications of this being that this method of transduction might position these innate cell types as effective mediators of CAR action and increase the influence of this technology as a cancer treatment.

1. Wirth, T., N. Parker, and S. Yla-Herttuala, *History of gene therapy*. *Gene*, 2013. **525**(2): p. 162-9.
2. Beltran, W.A., et al., *Gene augmentation for X-linked retinitis pigmentosa caused by mutations in RPGR*. *Cold Spring Harb Perspect Med*, 2014. **5**(2): p. a017392.
3. Szybalska, E.H. and W. Szybalski, *Genetics of human cell line. IV. DNA-mediated heritable transformation of a biochemical trait*. *Proc Natl Acad Sci U S A*, 1962. **48**: p. 2026-34.
4. Temin, H.M., *Mixed infection with two types of Rous sarcoma virus*. *Virology*, 1961. **13**: p. 158-63.
5. Rogers, S., et al., *Induction of arginase activity with the Shope papilloma virus in tissue culture cells from an argininemic patient*. *J Exp Med*, 1973. **137**(4): p. 1091-6.
6. Rosenberg, S.A., et al., *Gene transfer into humans--immunotherapy of patients with advanced melanoma, using tumor-infiltrating lymphocytes modified by retroviral gene transduction*. *N Engl J Med*, 1990. **323**(9): p. 570-8.
7. Rosenberg, S.A., *Gene therapy for cancer*. *Jama*, 1992. **268**(17): p. 2416-9.
8. Rosenberg, S.A., et al., *The development of gene therapy for the treatment of cancer*. *Ann Surg*, 1993. **218**(4): p. 455-63; discussion 463-4.
9. Blaese, R.M., et al., *T lymphocyte-directed gene therapy for ADA- SCID: initial trial results after 4 years*. *Science*, 1995. **270**(5235): p. 475-80.
10. Bordignon, C., et al., *Gene therapy in peripheral blood lymphocytes and bone marrow for ADA- immunodeficient patients*. *Science*, 1995. **270**(5235): p. 470-5.
11. Wilson, R.F., *The death of Jesse Gelsinger: new evidence of the influence of money and prestige in human research*. *Am J Law Med*, 2010. **36**(2-3): p. 295-325.

12. David, R.M. and A.T. Doherty, *Viral Vectors: The Road to Reducing Genotoxicity*. Toxicol Sci, 2017. **155**(2): p. 315-325.
13. Wu, C. and C.E. Dunbar, *Stem cell gene therapy: the risks of insertional mutagenesis and approaches to minimize genotoxicity*. Front Med, 2011. **5**(4): p. 356-71.
14. Peng, Z., *Current status of gene therapy in China: recombinant human Ad-p53 agent for treatment of cancers*. Hum Gene Ther, 2005. **16**(9): p. 1016-27.
15. Wirth, T., et al., *Clinical trials for glioblastoma multiforme using adenoviral vectors*. Curr Opin Mol Ther, 2009. **11**(5): p. 485-92.
16. Regalado, A., *The World's Most Expensive Medicine Is a Bust*. MIT Technology Review, 2016.
17. Escors, D. and K. Breckpot, *Lentiviral vectors in gene therapy: their current status and future potential*. Arch Immunol Ther Exp (Warsz), 2010. **58**(2): p. 107-19.
18. Coffin JM, H.S., Varmus HE, *Retroviral "Lifestyles": Simple versus Complex*. 1997, Cold Spring Harbor Laboratory Press.
19. Lalonde, M.S. and W.I. Sundquist, *How HIV finds the door*. Proc Natl Acad Sci U S A, 2012. **109**(46): p. 18631-2.
20. Menendez-Arias, L., A. Sebastian-Martin, and M. Alvarez, *Viral reverse transcriptases*. Virus Res, 2017. **234**: p. 153-176.
21. Craigie, R., *The molecular biology of HIV integrase*. Future virology, 2012. **7**(7): p. 679-686.
22. Behrens, A.J. and M. Crispin, *Structural principles controlling HIV envelope glycosylation*. Curr Opin Struct Biol, 2017. **44**: p. 125-133.
23. Richard Wyatt, P.D.K., Wayne A. Hendrickson, Joseph G. Sodroski. *Structure of the Core of the HIV-1 gp120 Exterior Envelope Glycoprotein*. 2013.

24. Karn, J. *Tat, a novel regulator of HIV transcription and latency*. 2013; Available from: [www.hiv.lanl.gov/content/sequence/HIV/REVIEWS/KARN2000/Karn.html](http://www.hiv.lanl.gov/content/sequence/HIV/REVIEWS/KARN2000/Karn.html).
25. Yu, Q.L., R; Konig R, *Vif and the Role of Antiviral Cytidine Deaminases in HIV-1 Replication*. 2010: HIV sequence database.
26. *HIV-1 Gene Map*. 2017 [cited 2017; Available from: <https://www.hiv.lanl.gov/content/sequence/HIV/MAP/landmark.html>.
27. Yee, J.K., T. Friedmann, and J.C. Burns, *Generation of high-titer pseudotyped retroviral vectors with very broad host range*. *Methods Cell Biol*, 1994. **43 Pt A**: p. 99-112.
28. Finkelshtein, D., et al., *LDL receptor and its family members serve as the cellular receptors for vesicular stomatitis virus*. *Proc Natl Acad Sci U S A*, 2013. **110**(18): p. 7306-11.
29. Cronin, J., X.-Y. Zhang, and J. Reiser, *Altering the Tropism of Lentiviral Vectors through Pseudotyping*. *Current gene therapy*, 2005. **5**(4): p. 387-398.
30. Zufferey, R., et al., *Self-inactivating lentivirus vector for safe and efficient in vivo gene delivery*. *J Virol*, 1998. **72**(12): p. 9873-80.
31. Miyoshi, H., et al., *Development of a Self-Inactivating Lentivirus Vector*. *Journal of Virology*, 1998. **72**(10): p. 8150-8157.
32. Van Maele, B., et al., *Impact of the central polypurine tract on the kinetics of human immunodeficiency virus type 1 vector transduction*. *J Virol*, 2003. **77**(8): p. 4685-94.
33. Naso, M.F., et al., *Adeno-Associated Virus (AAV) as a Vector for Gene Therapy*. *BioDrugs*, 2017.
34. Calcedo, R., et al., *Adeno-Associated Virus Antibody Profiles in Newborns, Children, and Adolescents*. *Clinical and Vaccine Immunology : CVI*, 2011. **18**(9): p. 1586-1588.

35. Hastie, E. and R.J. Samulski, *Adeno-associated virus at 50: a golden anniversary of discovery, research, and gene therapy success--a personal perspective*. Hum Gene Ther, 2015. **26**(5): p. 257-65.
36. Samulski, R.J. and N. Muzyczka, *AAV-Mediated Gene Therapy for Research and Therapeutic Purposes*. Annu Rev Virol, 2014. **1**(1): p. 427-51.
37. Naumer, M., et al., *Properties of the adeno-associated virus assembly-activating protein*. J Virol, 2012. **86**(23): p. 13038-48.
38. Straus, S.E., E.D. Sebring, and J.A. Rose, *Concatemers of alternating plus and minus strands are intermediates in adenovirus-associated virus DNA synthesis*. Proc Natl Acad Sci U S A, 1976. **73**(3): p. 742-6.
39. Ling, C., et al., *High-Efficiency Transduction of Primary Human Hematopoietic Stem/Progenitor Cells by AAV6 Vectors: Strategies for Overcoming Donor-Variation and Implications in Genome Editing*. Sci Rep, 2016. **6**: p. 35495.
40. McLaughlin, S.K., et al., *Adeno-associated virus general transduction vectors: analysis of proviral structures*. J Virol, 1988. **62**(6): p. 1963-73.
41. Wiemann, B. and C.O. Starnes, *Coley's toxins, tumor necrosis factor and cancer research: a historical perspective*. Pharmacol Ther, 1994. **64**(3): p. 529-64.
42. Parish, C.R., *Cancer immunotherapy: the past, the present and the future*. Immunol Cell Biol, 2003. **81**(2): p. 106-13.
43. Hanahan, D. and R.A. Weinberg, *The hallmarks of cancer*. Cell, 2000. **100**(1): p. 57-70.
44. Wang, J., et al., *PD-1, PD-L1 (B7-H1) and Tumor-Site Immune Modulation Therapy: The Historical Perspective*. J Hematol Oncol, 2017. **10**(1): p. 34.
45. Old LJ, B.E., Stockert E. , *Typing of mouse leukemias by serological methods*. Nature, 1964. **22**: p. 777-779.

46. Kute, T., et al., *Development of Herceptin resistance in breast cancer cells*. Cytometry A, 2004. **57**(2): p. 86-93.
47. Granier, C., et al., *Mechanisms of action and rationale for the use of checkpoint inhibitors in cancer*. ESMO Open, 2017. **2**(2): p. e000213.
48. Eshhar, Z., et al., *Specific activation and targeting of cytotoxic lymphocytes through chimeric single chains consisting of antibody-binding domains and the gamma or zeta subunits of the immunoglobulin and T-cell receptors*. Proc Natl Acad Sci U S A, 1993. **90**(2): p. 720-4.
49. Gross, G., T. Waks, and Z. Eshhar, *Expression of immunoglobulin-T-cell receptor chimeric molecules as functional receptors with antibody-type specificity*. Proc Natl Acad Sci U S A, 1989. **86**(24): p. 10024-8.
50. Romeo, C. and B. Seed, *Cellular immunity to HIV activated by CD4 fused to T cell or Fc receptor polypeptides*. Cell, 1991. **64**(5): p. 1037-46.
51. Irving, B.A. and A. Weiss, *The cytoplasmic domain of the T cell receptor zeta chain is sufficient to couple to receptor-associated signal transduction pathways*. Cell, 1991. **64**(5): p. 891-901.
52. Letourneur, F. and R.D. Klausner, *T-cell and basophil activation through the cytoplasmic tail of T-cell-receptor zeta family proteins*. Proc Natl Acad Sci U S A, 1991. **88**(20): p. 8905-9.
53. Sadelain, M., R. Brentjens, and I. Riviere, *The basic principles of chimeric antigen receptor design*. Cancer Discov, 2013. **3**(4): p. 388-98.
54. Jackson, H.J., S. Rafiq, and R.J. Brentjens, *Driving CAR T-cells forward*. Nat Rev Clin Oncol, 2016. **13**(6): p. 370-83.

55. Gross, G. and Z. Eshhar, *Therapeutic Potential of T Cell Chimeric Antigen Receptors (CARs) in Cancer Treatment: Counteracting Off-Tumor Toxicities for Safe CAR T Cell Therapy*. *Annu Rev Pharmacol Toxicol*, 2016. **56**: p. 59-83.
56. Curran, K.J., H.J. Pegram, and R.J. Brentjens, *Chimeric antigen receptors for T cell immunotherapy: current understanding and future directions*. *J Gene Med*, 2012. **14**(6): p. 405-15.
57. Marcus, A. and Z. Eshhar, *Allogeneic chimeric antigen receptor-modified cells for adoptive cell therapy of cancer*. *Expert Opin Biol Ther*, 2014.
58. Jensen, M.C. and S.R. Riddell, *Designing chimeric antigen receptors to effectively and safely target tumors*. *Curr Opin Immunol*, 2015. **33**: p. 9-15.
59. Gill, S., M.V. Maus, and D.L. Porter, *Chimeric antigen receptor T cell therapy: 25years in the making*. *Blood Rev*, 2015.
60. Heslop, H.E., *Safer CARs*. *Mol Ther*, 2010. **18**(4): p. 661-2.
61. Morgan, R.A., et al., *Case report of a serious adverse event following the administration of T cells transduced with a chimeric antigen receptor recognizing ERBB2*. *Mol Ther*, 2010. **18**(4): p. 843-51.
62. Lamers, C.H., et al., *Treatment of metastatic renal cell carcinoma with CAIX CAR-engineered T cells: clinical evaluation and management of on-target toxicity*. *Mol Ther*, 2013. **21**(4): p. 904-12.
63. Davila, M.L., et al., *Efficacy and toxicity management of 19-28z CAR T cell therapy in B cell acute lymphoblastic leukemia*. *Sci Transl Med*, 2014. **6**(224): p. 224ra25.
64. Maude, S.L., et al., *Chimeric antigen receptor T cells for sustained remissions in leukemia*. *N Engl J Med*, 2014. **371**(16): p. 1507-17.

65. Casucci, M., et al., *Overcoming the toxicity hurdles of genetically targeted T cells*. *Cancer Immunol Immunother*, 2015. **64**(1): p. 123-30.
66. Lee, D.W., et al., *T cells expressing CD19 chimeric antigen receptors for acute lymphoblastic leukaemia in children and young adults: a phase 1 dose-escalation trial*. *Lancet*, 2015. **385**(9967): p. 517-528.
67. Herrin, B.R. and M.D. Cooper, *Alternative adaptive immunity in jawless vertebrates*. *J Immunol*, 2010. **185**(3): p. 1367-74.
68. Mariuzza, R.A., et al., *Structural insights into the evolution of the adaptive immune system: the variable lymphocyte receptors of jawless vertebrates*. *Biol Chem*, 2010. **391**(7): p. 753-60.
69. Boehm, T., et al., *VLR-based adaptive immunity*. *Annu Rev Immunol*, 2012. **30**: p. 203-20.
70. Kasahara, M. and Y. Sutoh, *Two forms of adaptive immunity in vertebrates: similarities and differences*. *Adv Immunol*, 2014. **122**: p. 59-90.
71. Tasumi, S., et al., *High-affinity lamprey VLRA and VLRB monoclonal antibodies*. *Proc Natl Acad Sci U S A*, 2009. **106**(31): p. 12891-6.
72. Xu, G., S. Tasumi, and Z. Pancer, *Yeast surface display of lamprey variable lymphocyte receptors*. *Methods Mol Biol*, 2011. **748**: p. 21-33.
73. Velikovskiy, C.A., et al., *Structure of a lamprey variable lymphocyte receptor in complex with a protein antigen*. *Nat Struct Mol Biol*, 2009. **16**(7): p. 725-30.
74. Herrin, B.R., et al., *Structure and specificity of lamprey monoclonal antibodies*. *Proc Natl Acad Sci U S A*, 2008. **105**(6): p. 2040-5.
75. Kirchdoerfer, R.N., et al., *Variable lymphocyte receptor recognition of the immunodominant glycoprotein of *Bacillus anthracis* spores*. *Structure*, 2012. **20**(3): p. 479-86.

76. Luo, M., et al., *Recognition of the Thomsen-Friedenreich pancarcinoma carbohydrate antigen by a lamprey variable lymphocyte receptor*. J Biol Chem, 2013. **288**(32): p. 23597-606.
77. Yu, C., et al., *Purification and identification of cell surface antigens using lamprey monoclonal antibodies*. J Immunol Methods, 2012. **386**(1-2): p. 43-9.
78. Hirano, M., et al., *Evolutionary implications of a third lymphocyte lineage in lampreys*. Nature, 2013. **501**(7467): p. 435-8.
79. Kishishita, N. and F. Nagawa, *Evolution of adaptive immunity: implications of a third lymphocyte lineage in lampreys*. Bioessays, 2014. **36**(3): p. 244-50.
80. Porada, C.D., et al., *Phenotypic Correction of Hemophilia A in Sheep by Postnatal Intraperitoneal Transplantation of FVIII-Expressing MSC*. Experimental hematology, 2011. **39**(12): p. 1124-1135.e4.
81. Biedler, J.L. and B.A. Spengler, *A novel chromosome abnormality in human neuroblastoma and antifolate-resistant Chinese hamster cell lines in culture*. J Natl Cancer Inst, 1976. **57**(3): p. 683-95.
82. Riley, R.D., et al., *A systematic review of molecular and biological tumor markers in neuroblastoma*. Clin Cancer Res, 2004. **10**(1 Pt 1): p. 4-12.
83. Brodeur, G.M., *Neuroblastoma: biological insights into a clinical enigma*. Nat Rev Cancer, 2003. **3**(3): p. 203-16.
84. Hara, J., *Development of treatment strategies for advanced neuroblastoma*. Int J Clin Oncol, 2012. **17**(3): p. 196-203.
85. Velásquez, A.C., et al., *Leucine-rich-repeat-containing variable lymphocyte receptors as modules to target plant-expressed proteins*. Plant Methods, 2017. **13**: p. 29.

86. Alder, M.N., et al., *Antibody responses of variable lymphocyte receptors in the lamprey*. Nat Immunol, 2008. **9**(3): p. 319-27.
87. Curran, K.A., et al., *Use of High Capacity Terminators in Saccharomyces cerevisiae to Increase mRNA half-life and Improve Gene Expression Control for Metabolic Engineering Applications*. Metabolic engineering, 2013. **19**: p. 88-97.
88. Cottarel, G., et al., *A 125-base-pair CEN6 DNA fragment is sufficient for complete meiotic and mitotic centromere functions in Saccharomyces cerevisiae*. Molecular and Cellular Biology, 1989. **9**(8): p. 3342-3349.
89. Schwarzhaus, J.-P., et al., *Integration event induced changes in recombinant protein productivity in Pichia pastoris discovered by whole genome sequencing and derived vector optimization*. Microbial Cell Factories, 2016. **15**: p. 84.
90. Yu, S., et al., *Chimeric antigen receptor T cells: a novel therapy for solid tumors*. J Hematol Oncol, 2017. **10**(1): p. 78.
91. Marcus, A. and Z. Eshhar, *Allogeneic chimeric antigen receptor-modified cells for adoptive cell therapy of cancer*. Expert Opin Biol Ther, 2014. **14**(7): p. 947-54.
92. Gill, S., M.V. Maus, and D.L. Porter, *Chimeric antigen receptor T cell therapy: 25years in the making*. Blood Rev, 2016. **30**(3): p. 157-67.
93. Porter, D.L., et al., *Chimeric antigen receptor-modified T cells in chronic lymphoid leukemia*. N Engl J Med, 2011. **365**(8): p. 725-33.
94. Baker, A.H., *Development and use of gene transfer for treatment of cardiovascular disease*. J Card Surg, 2002. **17**(6): p. 543-8.
95. Moot, R., et al., *Genetic engineering of chimeric antigen receptors using lamprey derived variable lymphocyte receptors*. Mol Ther Oncolytics, 2016. **3**: p. 16026.

96. Shaw, G., et al., *Preferential transformation of human neuronal cells by human adenoviruses and the origin of HEK 293 cells*. *Faseb j*, 2002. **16**(8): p. 869-71.
97. Gong, J.H., G. Maki, and H.G. Klingemann, *Characterization of a human cell line (NK-92) with phenotypical and functional characteristics of activated natural killer cells*. *Leukemia*, 1994. **8**(4): p. 652-8.
98. Suck, G., et al., *NK-92: an 'off-the-shelf therapeutic' for adoptive natural killer cell-based cancer immunotherapy*. *Cancer Immunol Immunother*, 2016. **65**(4): p. 485-92.
99. Alkins, R., et al., *Early treatment of HER2-amplified brain tumors with targeted NK-92 cells and focused ultrasound improves survival*. *Neuro Oncol*, 2016. **18**(7): p. 974-81.
100. Lee-MacAry, A.E., et al., *Development of a novel flow cytometric cell-mediated cytotoxicity assay using the fluorophores PKH-26 and TO-PRO-3 iodide*. *J Immunol Methods*, 2001. **252**(1-2): p. 83-92.
101. Bundle, D.R., et al., *Molecular recognition of a Salmonella trisaccharide epitope by monoclonal antibody Se155-4*. *Biochemistry*, 1994. **33**(17): p. 5172-82.
102. Vyas, N.K., et al., *Molecular recognition of oligosaccharide epitopes by a monoclonal Fab specific for Shigella flexneri Y lipopolysaccharide: X-ray structures and thermodynamics*. *Biochemistry*, 2002. **41**(46): p. 13575-86.
103. Takeda, K. and S. Akira, *Toll-like receptors in innate immunity*. *Int Immunol*, 2005. **17**(1): p. 1-14.
104. Bell, J.K., et al., *Leucine-rich repeats and pathogen recognition in Toll-like receptors*. *Trends Immunol*, 2003. **24**(10): p. 528-33.
105. Stahelin, R.V., et al., *The origin of C1A-C2 interdomain interactions in protein kinase Calpha*. *J Biol Chem*, 2005. **280**(43): p. 36452-63.

106. Steinberg, S.F., *Structural basis of protein kinase C isoform function*. *Physiol Rev*, 2008. **88**(4): p. 1341-78.
107. Wang, C.X., et al., *Rapamycin relieves lentiviral vector transduction resistance in human and mouse hematopoietic stem cells*. *Blood*, 2014. **124**(6): p. 913-23.
108. Chuck, A.S. and B.O. Palsson, *Consistent and high rates of gene transfer can be obtained using flow-through transduction over a wide range of retroviral titers*. *Hum Gene Ther*, 1996. **7**(6): p. 743-50.
109. Aiuti, A., et al., *Lentiviral hematopoietic stem cell gene therapy in patients with Wiskott-Aldrich syndrome*. *Science*, 2013. **341**(6148): p. 1233151.
110. Spencer, H.T., et al., *Lentiviral vector platform for production of bioengineered recombinant coagulation factor VIII*. *Mol Ther*, 2011. **19**(2): p. 302-9.
111. Cao, F., et al., *Comparison of gene-transfer efficiency in human embryonic stem cells*. *Mol Imaging Biol*, 2010. **12**(1): p. 15-24.
112. Tran, R., et al., *Simplified prototyping of perfusable polystyrene microfluidics*. *Biomicrofluidics*, 2014. **8**(4): p. 046501.
113. Earley, L.F., et al., *Adeno-associated Virus (AAV) Assembly-Activating Protein Is Not an Essential Requirement for Capsid Assembly of AAV Serotypes 4, 5, and 11*. *J Virol*, 2017. **91**(3).
114. Recchia, A. and F. Mavilio, *Site-specific integration by the adeno-associated virus replication protein*. *Curr Gene Ther*, 2011. **11**(5): p. 399-405.
115. Ward, P., N. Clement, and R.M. Linden, *cis effects in adeno-associated virus type 2 replication*. *J Virol*, 2007. **81**(18): p. 9976-89.
116. Agbandje-McKenna, M. and J. Kleinschmidt, *AAV capsid structure and cell interactions*. *Methods Mol Biol*, 2011. **807**: p. 47-92.

117. Mietzsch, M., et al., *Differential Adeno-Associated Virus Serotype-Specific Interaction Patterns with Synthetic Heparins and Other Glycans*. Journal of Virology, 2014. **88**(5): p. 2991-3003.
118. Sands, M.S., *AAV-mediated liver-directed gene therapy*. Methods Mol Biol, 2011. **807**: p. 141-57.
119. Zincarelli, C., et al., *Analysis of AAV serotypes 1-9 mediated gene expression and tropism in mice after systemic injection*. Mol Ther, 2008. **16**(6): p. 1073-80.
120. Vandendriessche, T., et al., *Efficacy and safety of adeno-associated viral vectors based on serotype 8 and 9 vs. lentiviral vectors for hemophilia B gene therapy*. J Thromb Haemost, 2007. **5**(1): p. 16-24.
121. Legut, M., D.K. Cole, and A.K. Sewell, *The promise of gammadelta T cells and the gammadelta T cell receptor for cancer immunotherapy*. Cell Mol Immunol, 2015. **12**(6): p. 656-68.
122. Locke, F.L., et al., *Phase 1 Results of ZUMA-1: A Multicenter Study of KTE-C19 Anti-CD19 CAR T Cell Therapy in Refractory Aggressive Lymphoma*. Mol Ther, 2017. **25**(1): p. 285-295.
123. Re, F., et al., *Circulating gammadelta T cells in young/adult and old patients with cutaneous primary melanoma*. Immun Ageing, 2005. **2**(1): p. 2.
124. Restifo, N.P., M.E. Dudley, and S.A. Rosenberg, *Adoptive immunotherapy for cancer: harnessing the T cell response*. Nat Rev Immunol, 2012. **12**(4): p. 269-81.
125. Rischer, M., et al., *Human gammadelta T cells as mediators of chimaeric-receptor redirected anti-tumour immunity*. Br J Haematol, 2004. **126**(4): p. 583-92.
126. Savan, R., T. Chan, and H.A. Young, *Lentiviral gene transduction in human and mouse NK cell lines*. Methods Mol Biol, 2010. **612**: p. 209-21.

127. Carlsten, M. and R.W. Childs, *Genetic Manipulation of NK Cells for Cancer Immunotherapy: Techniques and Clinical Implications*. *Frontiers in Immunology*, 2015. **6**: p. 266.
128. Boissel, L., et al., *Comparison of mRNA and lentiviral based transfection of natural killer cells with chimeric antigen receptors recognizing lymphoid antigens*. *Leuk Lymphoma*, 2012. **53**(5): p. 958-65.
129. Sutlu, T., et al., *Inhibition of intracellular antiviral defense mechanisms augments lentiviral transduction of human natural killer cells: implications for gene therapy*. *Hum Gene Ther*, 2012. **23**(10): p. 1090-100.
130. Brown, B.D., et al., *In vivo administration of lentiviral vectors triggers a type I interferon response that restricts hepatocyte gene transfer and promotes vector clearance*. *Blood*, 2007. **109**(7): p. 2797-805.
131. Boye, S.E., et al., *Highly Efficient Delivery of Adeno-Associated Viral Vectors to the Primate Retina*. *Hum Gene Ther*, 2016. **27**(8): p. 580-97.
132. Thomas, S., H.J. Stauss, and E.C. Morris, *Molecular immunology lessons from therapeutic T-cell receptor gene transfer*. *Immunology*, 2010. **129**(2): p. 170-7.
133. Minagawa, K., et al., *In Vitro Pre-Clinical Validation of Suicide Gene Modified Anti-CD33 Redirected Chimeric Antigen Receptor T-Cells for Acute Myeloid Leukemia*. *PLoS ONE*, 2016. **11**(12): p. e0166891.
134. Schambach, A. and M. Morgan, *Retroviral Vectors for Cancer Gene Therapy*. *Recent Results Cancer Res*, 2016. **209**: p. 17-35.
135. Dodo, K., et al., *An efficient large-scale retroviral transduction method involving preloading the vector into a RetroNectin-coated bag with low-temperature shaking*. *PLoS One*, 2014. **9**(1): p. e86275.

136. Johnston, J.M., et al., *Generation of an Optimized Lentiviral Vector Encoding a High-Expression Factor VIII Transgene for Gene Therapy of Hemophilia A*. *Gene therapy*, 2013. **20**(6): p. 607-615.
137. Sutton, K.S., et al., *Bioengineering and serum free expansion of blood-derived gammadelta T cells*. *Cytotherapy*, 2016. **18**(7): p. 881-92.
138. Doering, C.B., et al., *Directed engineering of a high-expression chimeric transgene as a strategy for gene therapy of hemophilia A*. *Mol Ther*, 2009. **17**(7): p. 1145-54.
139. Luni, C., et al., *Stochastic model-assisted development of efficient low-dose viral transduction in microfluidics*. *Biophys J*, 2013. **104**(4): p. 934-42.
140. Tran, R., et al., *Microfluidic Transduction Harnesses Mass Transport Principles to Enhance Gene Transfer Efficiency*. *Mol Ther*, 2017.
141. Oelsner, S., et al., *Continuously expanding CAR NK-92 cells display selective cytotoxicity against B-cell leukemia and lymphoma*. *Cytotherapy*, 2017. **19**(2): p. 235-249.
142. Song, L., et al., *Optimizing the transduction efficiency of capsid-modified AAV6 serotype vectors in primary human hematopoietic stem cells in vitro and in a xenograft mouse model in vivo*. *Cytotherapy*, 2013. **15**(8): p. 986-98.
143. Ellis, B.L., et al., *A survey of ex vivo/in vitro transduction efficiency of mammalian primary cells and cell lines with Nine natural adeno-associated virus (AAV1-9) and one engineered adeno-associated virus serotype*. *Virology Journal*, 2013. **10**: p. 74-74.
144. Mirzaei, H.R., et al., *Prospects for chimeric antigen receptor (CAR) gammadelta T cells: A potential game changer for adoptive T cell cancer immunotherapy*. *Cancer Lett*, 2016. **380**(2): p. 413-23.
145. Miller, J.S., et al., *Successful adoptive transfer and in vivo expansion of human haploidentical NK cells in patients with cancer*. *Blood*, 2005. **105**(8): p. 3051-7.

146. Ruggeri, L., et al., *Effectiveness of donor natural killer cell alloreactivity in mismatched hematopoietic transplants*. Science, 2002. **295**(5562): p. 2097-100.
147. Romanski, A., et al., *CD19-CAR engineered NK-92 cells are sufficient to overcome NK cell resistance in B-cell malignancies*. Journal of Cellular and Molecular Medicine, 2016. **20**(7): p. 1287-1294.
148. Resetca, D., A. Neschadim, and J.A. Medin, *Engineering Hematopoietic Cells for Cancer Immunotherapy: Strategies to Address Safety and Toxicity Concerns*. J Immunother, 2016. **39**(7): p. 249-59.
149. Liu, E., et al., *Cord blood NK cells engineered to express IL-15 and a CD19-targeted CAR show long-term persistence and potent anti-tumor activity*. Leukemia, 2017.
150. Klingemann, H., *Are natural killer cells superior CAR drivers?* Oncoimmunology, 2014. **3**: p. e28147.
151. Nakahara, H., et al., *Chronic lymphocytic leukemia monitoring with a Lamprey idiotope-specific antibody*. Cancer Immunol Res, 2013. **1**(4): p. 223-8.
152. Cannon, L., *Humanization of VLR antibodies for therapeutic applications 2015*, National Institute of Health.
153. Harding, T.C., et al., *Intravenous administration of an AAV-2 vector for the expression of factor IX in mice and a dog model of hemophilia B*. Gene Ther, 2004. **11**(2): p. 204-13.
154. Choi, J.-H., et al., *Optimization of AAV expression cassettes to improve packaging capacity and transgene expression in neurons*. Molecular Brain, 2014. **7**: p. 17-17.